2014

Bio-imprinted hydro-gels (BIGS) for protein and virus detection

Wei Bai
Louisiana State University and Agricultural and Mechanical College, baiwei81@gmail.com

BIO-IMPRINTED HYDRO-GELS (BIGS) FOR PROTEIN AND VIRUS DETECTION.

A Dissertation

Submitted to the Graduate Faculty of the
Louisiana State University and
Agricultural and Mechanical College
in partial fulfillment of the
requirements for the degree of
Doctor of Philosophy

in

The Department of Chemistry

by
Wei Bai
M.S., University of Science and Technology of China, 2007
B.S., Anhui University of Technology, 2003
May 2014

ACKNOWLEDGEMENTS

First of all, I'd like to give my most sincere thankfulness to my advisor, Prof. David A. Spivak. It would be impossible for me to overcome the difficulties in my research and life without either his talented and creative advices or his understanding, kindness and patience.

My labmates also supported and encouraged me a lot in the past years. The goodtime we worked together is definitely one of the most beautiful memories in my career. Here, I'd like to express my special thankfulness to Nicolas A, Gariano who I have worked with for 4 years. He has given me lots of valuable help in both research and life.

Additionally, my family is always my most important source of motivation. I would not be in this position if it weren't for their influence and the support of education they have instilled in me.

TABLE OF CONTENTS

ABSTRACT

Detection of bio-markers at low concentration is becoming a more and more important topic in scientific research due to its importance in applications crucially related to people's life like medical diagnosis, environment protection and national security.

In the past decades, as the improvement of the modern analytical technologies progressed, plenty of methodologies have been developed to realize the fast and accurate detection of bio-markers in liquid media. However, some drawbacks still remain like the expensive cost, high requirement of operational environment, and need for skilled operators.

Here, a new kind of aptamer-based bio-imprinted hydrogel sensor (BIG) with specific macroscopic volume response to certain biomarkers like proteins and virus at low concentration is reported.

These super-aptamer hydrogels exhibit macroscopic volume change that can be detected by naked eyes when being treated with bio-marker solutions at extremely low concentration. This extraordinary macromolecular amplification is attributed to a complex interplay between biomarker-aptamer crosslinks and the structure of the hydrogel network surrounding it.

Additionally, based on the work mentioned above, a new kind of bio-imprinted grating hydrogel film which can show visible change of the laser diffraction pattern when treated with biomarker solutions was also designed and fabricated based on the super-aptamer bioimprinted hydrogels. These films have also been proved to be able to detect both proteins and virus at low concentration in solutions.

CHAPTER 1. INTRODUCTION: SENSORS FOR BIOMARKER DETECTION

1. 1 General

Since the very beginning of the human species, the demand to observe and realize our world better has never died away. In fact, the desire to acquire more knowledge continues to flourish while more powerful tools for acquiring knowledge are continuously being invented. Among all the frontiers in science and technology related to humans' ability to explore the world and satisfy people's thirst for knowledge, the invention of an array of different sensors is definitely one of the most important. Generally, a sensor is a device which can respond to certain targets (stimuli) by generating detectable output signals. From a macroscopic view, there are two directions in the development of sensors. In one, the improvements in techniques like the telescope, radar and remote sensing allow exploration of the macroscopic world. In the second, the development of sensors for detection of microscopic targets like chemical compounds or other relative small bio-molecules which can't be directly observed or perceived by humans organs such as the eye.

Due to rapid modernization in today's world, management of health problems has become an important public focus. As a result, the development of bio-sensors is receiving top public attention because they are extremely crucial for medical diagnosis and monitoring. Some examples of biosensor applications in human health care include disease diagnosis, tissue engineering, controlled release and many other medical practices.[1]

1.2. Important factors in biosensor fabrication.

As shown in Figure 1.1, a biosensor is generally composed of three parts: bioreceptor, transducer and detector. The proper integration of these three parts can take advantage of the individual properties of the three and create links between them to work together as a whole. The bio-receptor has specific affinity to the target, and it can recognize and selectively bind to the target. Next, the recognition event will be received by the transducer which creates a detectable signal. Last the signal sent from the transducer is received by the detector and translated to readable results for the observers.

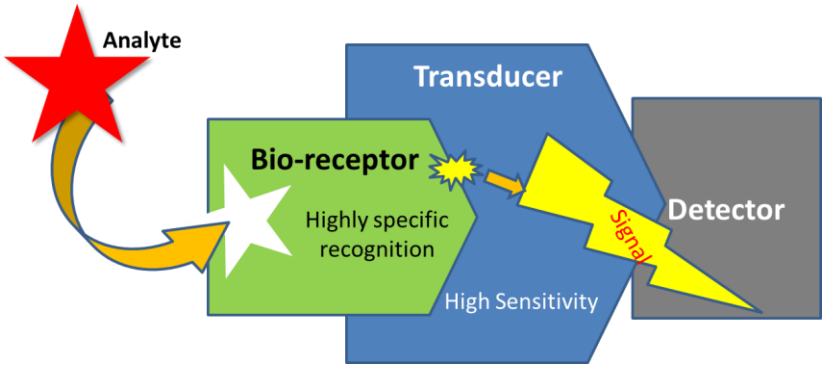

Figure 1.1 Schematic representation of a biosensor.

To fabricate an effective biosensor for the detection of certain targets, there are several factors should be taken into account. First, a suitable bioreceptor should be selected in order to give the sensor the ability to recognize specific target. Second, the proper immobilization of the bioreceptors to the matrix is also an important requirement. Third, reasonable selection and design of the transducer should also be carefully considered in order to successfully transduce the binding event between the target and the bioreceptor to the detectable output signals. [2]

1.3 The components of a biosensor

After decades of research and exploration, researchers have discovered variety of components that can be used as bioreceptors and transducers, some of which are shown in Figure 1.2. In the following sections, a brief introduction of these components will be performed respectively.

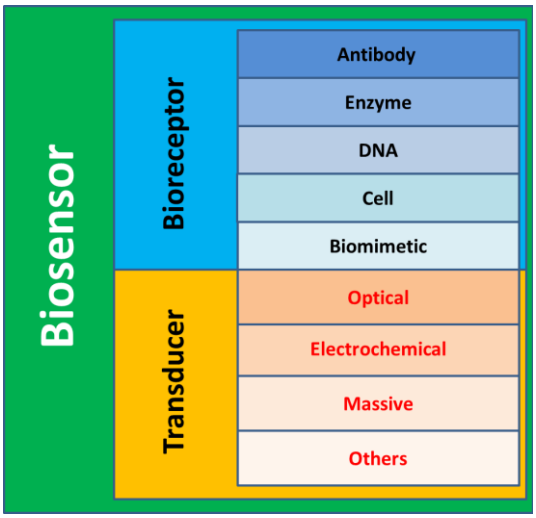

Figure 1.2 Scheme of biosensor classification.

1.3.1 Bioreceptors

Bioreceptors are biological macromolecules or bio-mimetic molecules and polymers that can selectively bind the analyte of interest. It is obvious that bioreceptors are the key factor in the generation of the sensor's specificity to the target. Typically, antibody/antigen systems, enzyme, nucleic acid/DNA, cell and other biomimetic materials are commonly used as bioreceptors in fabrication of biosensors.[3]

1.3.1.1 Antibodies

Antibodies are large, complex Y-shaped biological molecules made of hundreds of amino acids in an ordered sequence (Figure 1.3). They can exhibit very specific binding capabilities to certain structures referred to as antigens.

Figure 1.3 Schematic diagram of antibody

Antibodies were first employed as bioreceptors for in-situ detection of the chemical carcinogen benzopyrene;[4] after this precedent antibodies have become one of the most frequently used bioreceptors for molecular recognition in biosensors to date. Biosensors fabricated using antibodies can be divided into two types. The first use of antibodies to act as connectors between spectroscopic indicators (such as dyes or fluorescent molecules) and the target to enable the indicators to selectively bind and highlight the target. The other way is to immobilize the antibody to a solid-state transducer or through covalent or non-covalent interactions. Then, after the target is captured by the antibody, the transducer can generate the signal to be detected. [5]

1.3.1.2 Enzymes

Enzymes are usually globular proteins composed of dozens to thousands of highly ordered amino acids. Similar to the antibodies, enzymes are candidates for bioreceptors due to their ability to specifically bind to certain target. In addition to excellent selectivity, enzymes are also catalytically active, which can lead to outstanding sensitivity due to amplification of one binding event by thousands of catalytic events.

Generally, this catalytic ability makes the detection limit of the methods employing enzymes much lower than most of the conventional methodologies. However, the catalytic activity of enzymes relies on a static conformation; if an enzyme is denatured, the catalytic ability will be lost. Additionally, some enzymes require no other additives to exhibit catalytic activity while others need the addition of cofactors (usually ions like Fe^{2+}, Mg^{2+}, Mn^{2+}, Zn^{2+} or some other organic or metallo-organic molecules).[6]

1.3.1.3 Nucleic acid receptors (excluding aptamers)

Nucleic acids/ deoxyribonucleic acids (DNAs) are another kind of frequently used bioreceptors to fabricate biosensors. The complementarity of adenine: thymine (A:T) and cytosine: guanosine (C:G) pairing in DNA gives the sensors highly specific recognition ability. The applications of this kind have growing rapidly in the last decades. [7]

1.3.1.4 Cellular structures/cells

Entire cells or a specific cellular component have various capabilities of specific binding to certain molecules and bio-interfaces, and can also be used as bioreceptors in the development of biosensors and biochips. [8]

1.3.1.5 Biomimetic receptors

Biomimetic receptors are artificial receptors designed and fabricated to mimic natural bioreceptors. These methods include: genetically engineered molecules, artificial membrane fabrication, composites, nanoparticles (NPs), nanostructured materials and quantum dots (QDs) and molecular imprinting using artificial bio-receptors (plastic antibody, aptamer). [9] For example, aptamers can form folded stable secondary and tertiary structures when associated with the surface of a specific bio-target which leads to selective binding of the biotarget. Figure 1.4 shows the binding of the two Thrombin aptamers to the surface of Thrombin.

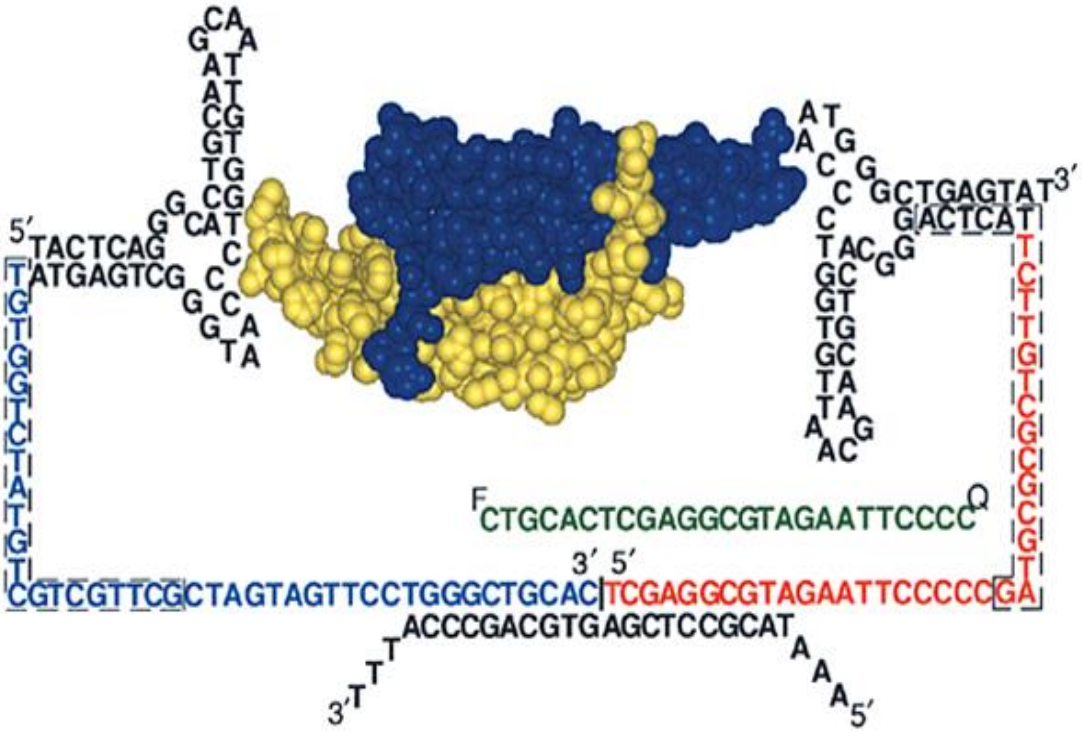

Figure 1.4 Proximity Ligation of PDGF-ββ using ligated homodimeric aptamers for recognition

1.3.2 Transducer

A transducer is a device that can convert one kind of signal into another. Specifically in the area of biosensors, transducers convert the binding event into a detectable signal for the detector. The main transducer designs and techniques used in biosensors is overviewed in the following sections.

1.3.2.1 Optical techniques

An optical transducer is the most commonly used technique in design and fabrication of biosensors. This is because there are many different kinds optical techniques that can be employed in the making of the sensors, allowing researchers to the most suitable method to meet specific requirements. Widely used spectroscopic methods like absorption, fluorescence, phosphorescence, Raman, refraction, Energy dispersion spectrometry etc. are all possible candidates. As a result, change of properties like amplitude, energy, polarization, decay time and/or phase can be generated, detected and recorded to illustrate the occurrence of the target. [10]

1.3.2.2 Electrochemical techniques

Bio-recognition reactions often generate or consume ions or electrons, which can cause a change in the electrical properties of the solution that can be measured by electrochemical methods. Therefore, electrochemical detection is another possible choice for a transducer that has been used in biosensors. Since many analytes of interests are not strongly fluorescent, and tagging a molecule with a fluorescent label can be time consuming and costly, electrochemical transduction can be a competitive alternative. By combining the sensitivity of electrochemical measurements with the selectivity provided by bioreceptor, good selectivity and detection limits comparable to fluorescence biosensors are often achievable. [11]

1.3.2.3 Mass detection techniques

Another option that can be used as a transducer in biosensor systems is mass detection techniques. Compared to optical and electrochemical methods, the concept of mass detection has been applied long time ago but dramatically improving and growing in past decade. The biosensors fabricated by this method are very sensitive to a very small amount of the change in mass. This is achieved using a piezoelectric crystal which can be made to vibrate at a specific frequency with the application of an electrical signal of a specific frequency. The frequency of oscillation is therefore dependent on the electrical frequency applied to the crystal as well as the crystal's mass. Therefore, when the mass increases due to binding of target compounds, the oscillation frequency of the crystal changes, and the resulting change can be measured electrically and used to determine the additional mass of the crystal. [12]

1.3.2.4 Others

Calorimetric measurements are also used to evaluate the biochemical reactions at the sensing element. Isoperibol calorimeter, Isothermal calorimeters and heat conduction calorimeters are the most commonly used kinds. The most important advantage of these methods is they can be easily coupled to flow injection analysis systems.

Polymer materials that can change their size and dimensions are now more and more used as biosensors. The change of the volume is usually caused by the making and breaking of the crosslinks which is triggered by the presence of the target molecules. For example, Peng and et al. reported hydrogels can show macroscopic volume change by reversible DNA hybridization. [13]

1.4 Techniques for making biosensors

1.4.1 Smart materials

Commercialized instruments are now the main force of today's medical diagnostic system. The achievement of modern analytical methodologies greatly enhanced the recognition, transduction, amplification and detection ability of modern instrumental sensors. As a result, this route can generate very accurate and precise quantified results and the detection limit can reach a considerably low level. Although we claim that the development in all kinds of existing instrumental sensors is one of the greatest achievements in human history, some disadvantages should still be mentioned. One of the biggest issues is that the great sensitivity usually comes with high requirements with respect to sophisticated instruments, obtaining reliable data, comparing with pure standard reagents, needing highly trained personnel and ultra-clean operation space.

The high standards are widely adopted in not only the instruments' technical level of but also in operational environment and personnel. This seriously limits the availability of these advanced techniques. Therefore, there is still a huge demand to explore novel routes to realize ultra-sensitive, highly specific, low cost and easy-to-use methodologies with strong adaptability. Developments in this direction can significantly enhance the coverage and decrease the cost of modern medical diagnosis system.

Besides the widely used instrumental methods, materials that can change their chemical or physical properties in response to external stimuli provide an alternative way to fabricate biosensors. Generally, these kinds of materials with environment-dependent properties are called "Smart Material". The ability of "smart materials" to exhibit macroscopic detectable property

changes upon the stimuli can facilitate the fabrication of relatively simple sensors in which the signal can be easily detected without any complicated auxiliary aid (ie. pH paper etc.). [14]

The concept "Smart Material" stands for the kind of designed functional materials which can both selectively recognize certain kinds of external stimuli like pH, temperature, light, magnetic field, electrical field and etc. while transducing a detectable output signal by changing its chemical or physical properties which is illustrated by Figure 1.5. As one of the most important branches in modern material science from the moment the concept was first announced in late 1980s, smart materials have been widely accepted and introduced into many areas due to its outstanding potential. After decades of development, the family of "Smart Materials" now is encompasses a huge number of materials used in fields ranging from lab science to factories and medical to aerospace. Figure 1.4 shows some examples of different kinds of smart materials that can be used to make biosensors for different purposes.

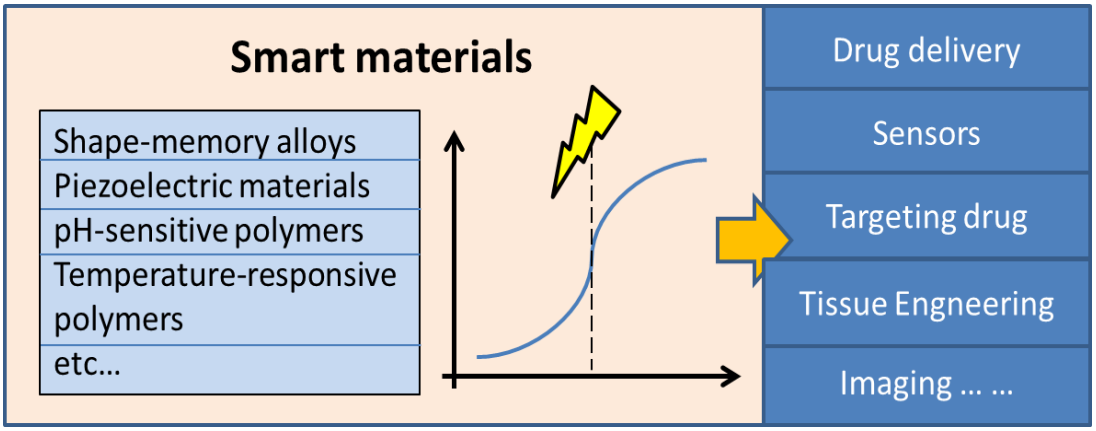

Figure 1.5 Schematic representation of categories and applications of smart materials.

Today, the family of smart materials is still growing fast, including piezoelectric materials, shape-memory materials, pH-sensitive polymers, temperature-responsive polymers,

chromogenic materials, photomechanical materials, self-healing materials, molecular target-sensitive polymers and many others. Currently these materials are widely used in applications like targeting therapy, drug delivery etc. [15]

Modern research is heavily focused on smart materials because compared to traditional instrumental methods; these materials have several important advantages. First, they are relatively easy to use: in most of the cases users can see the readout results easily without the help of complicated devices. The sensors that can perform naked-eye detection are also a hot spot in the field. Second, they are relatively cheap because little or no complicated instrumental parts are required. Third, they are easy to be transported and stored due to their simple build-up and stable properties. All these merits can vastly enlarge the coverage of the technique and the number of the people it can benefit.

1.4.2 Hydrogel

Hydrogels are hydrophilic 3-dimensional polymeric networks that can absorb a large amount of water. Varieties of hydrogels widely exist in nature, typically as organs of plants or animals. Since researchers have already realized that hydrogels play an important role in bio-systems and have outstanding potential for bio-related applications, artificial hydrogels were first developed for biomedical applications.[16] Among all the possible candidates in smart material family, hydrogels are known as one of the most suitable of these candidates to fabricate bio-sensors due to their good biocompatibility, flexibility in synthesis and tunable physical/chemical properties.

The synthesis of biosensors in many cases uses hydrogels as a polymeric immobilization matrix to provide support for immobilized bio-receptors or other functional groups. In fact, hydrogels can act not only in a passive way as immobilization matrix but also as responsive (smart) material, which makes hydrogels very attractive for biomedical or bioanalytical purpose.

In the past decades, stimuli-responsive hydrogel is a hot topic in material science and engineering, especially in bio-related areas. For example, hydrogels as scaffold material in tissue engineering which contain human cells in order to repair tissue;[17] Hydrogels sensitive to environmental changes (pH, temperature, metabolite concentration) responding with swelling and eventually release of their payload drug [18]. Bio-smart hydrogels that are responsive to specific molecules (e.g. glucose, antigens) can be used as biosensors as well as in smart drug release [19]; diffusion barriers: analytes and the reaction products are transported while diffusion of interferents to the microtransducer is prevented [20].

Advantages of hydrogels in biosensors are usually their inherent actuating properties; e.g. stimuli-responsive hydrogels can change their volume or diffusion properties when exposed to an external physical or chemical stimulus. The changes in volume due to molecular recognition or chemical reactions lead to a completely new class of biosensors using micro-mechanical and micro-optical output.

1.4.3 The molecular imprinting technique

1.4.3.1 Traditional molecular imprinting technique

The molecular imprinting technique is an interdisciplinary subject in science. Figure 1.6 shows how the MIP technique works. It has been widely accepted as an effective and practical

method to provide good selective recognition and strong binding to the targets in polymer networks.

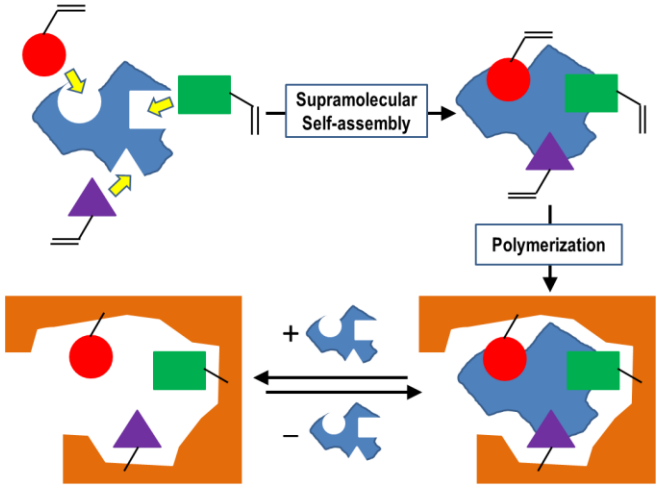

Figure 1.6 Scheme of Molecular imprinting

The significant recognition capability is the result of using target molecules as templates in synthesis. The templates can be removed after polymer synthesis which leads to binding cavities and functionalities which can exhibit specific affinity to the template molecules.

Traditionally, during the imprinting process, the template is included into the polymer network by formation of covalent bonds. After polymerization, the template is removed by chemical methods to regenerate the recognition sites. Although it has been proven to be an effective method to produce good recognition or separation materials for various template molecules, some disadvantages have also been identified. First, the method usually requires chemical methods to break the covalent bond between the target molecules and the polymer matrices in order to remove the template. Chemical treatment always means contamination and a harsh chemical environment which can degrade the polymer, especially the applications related

to environment-sensitive bio-molecules. Second, traditional imprinting generally requires small molecules with molecular weights less than 1000 g/mol, in addition to template interactive functionalities, which also limited the practical utility of the traditional MIPs.

1.4.3.2 Bio-MIPs

In recent years, the molecular imprinting technique employing superamolecular interactions to form the polymerizable target-ligand complexes has attracted more and more attention. Because this method using non-covalent template-functional monomer interactions can provide an easy and effective route to creating recognition of biomolecules such as proteins which can easily form complexes with ligands via interactions like hydrogen bonding, hydrophobic interactions, ionic interactions,etc. Since Hjerten's group first developed protein imprinted polyacrylamide MIP material which can selectively recognize template protein,[21] many successful examples of imprinting biological targets like epitope, proteins, virus and etc. have already been published and the numbers are still growing rapidly.[22] For example, Miyata's group biomolecularly imprinted the protein APF pre-complexed to a polymerizable lectin and antibody, which gave a shrinking response when both the lectin and antibody simultaneously bound AFP.[23]

As a result, improving bio-imprinting techniques for developing bio-sensors to detect bio-molecules like proteins, viruses and bacteria are one of the top interests. It is considered to be important not only in the field of chemistry but also biology, medical, environmental and etc. because of its potential in applications like disease diagnosis, environment monitoring, national security inspection and etc.[24]

1.4.4 Aptamer

One of the newer classes of bio-receptors are aptamers which are believed to be a promising option for creating or enhancing the recognition ability of hydrogels. Aptamers are oligonucleotides (DNA or RNA molecules) that can bind with high affinity and specificity to a wide range of target molecules (proteins, peptides, drugs, vitamins and other organic or inorganic compounds).

Aptamers were first developed in the early 1990s by the development of an in vitro selection and amplification technique,[25] known as SELEX (Systematic Evolution of Ligands by Exponential enrichment) which is shown in Figure 1.7. Later, they soon became popular because of their potential to form specific binding agent (RNA sequences) to any molecule target (ions, small bio-molecules, peptides, proteins, etc.). In fact, for the same reason, aptamers are also considered as an "artificial antibodies" and have been the focus of research toward applications in therapeutics; however they have not found use in biomedical treatment. Due to their effective binding properties to certain target molecules, they have recently been extensively applied in bio-related chemistry research, especially analytical chemistry, as effective means for sensor development.

The outstanding selectively binding ability of aptamers stem from the stable structure formed between the aptamers and the target. The specific interactions between amino acids are facilitated by the sequence-specific, 3-D structure of the aptamer ligand, which provides a rigid scaffold for the arrangement of functionalities of the ligand. Figure 1.8 shows the rigid and energy favored structure formed by the aptamers for HIV and Thrombin.

Compared to other bio-receptors like antibodies and cells, aptamers are artificially synthesized, and which has several advantages. First, the production of aptamers doesn't request animal processing, which mean they are relatively easy and cheap to obtain. Second, compared to antibodies, they're usually more stable. Third, they can be easily modified to add required functions to satisfy different purpose. [25]

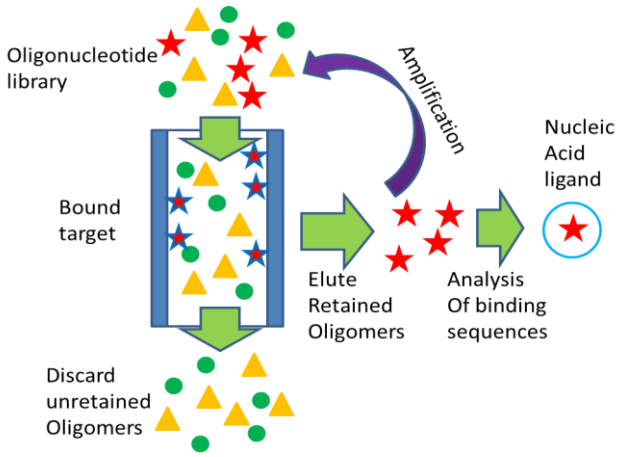

Figure 1.7 Scheme of nucleic acid ligand selection

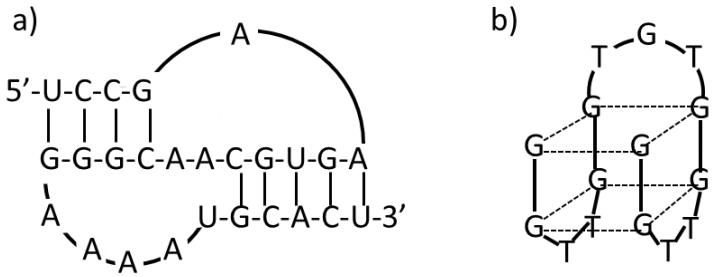

Figure 1.8 Aptamers for HIV (a) and Thrombin (b).

In the past few decades, a lot of work has been done to "discover" new and better aptamers for various types of bio-targets. Fortunately, the two proteins we were interested in had corresponding aptamers proven to be effective, which we will discuss later (*vide infra*).

1.4.5 Amplification

In the design and fabrication of biosensors, once the method for recognition of the target has been determined, the intensity of the output signal generated by the sensor is another vital factor to be developed. In practical detection of biomarkers in real applications like disease diagnosis, the ability to detect low concentration targets is always required. Figure 1.9 shows the concentration level required for detection of the biomarkers for some diseases and the methods can be used. Generally, low concentration levels lead to low signal output, so methods of detection of low levels of analytes rely heavily on signal amplification.

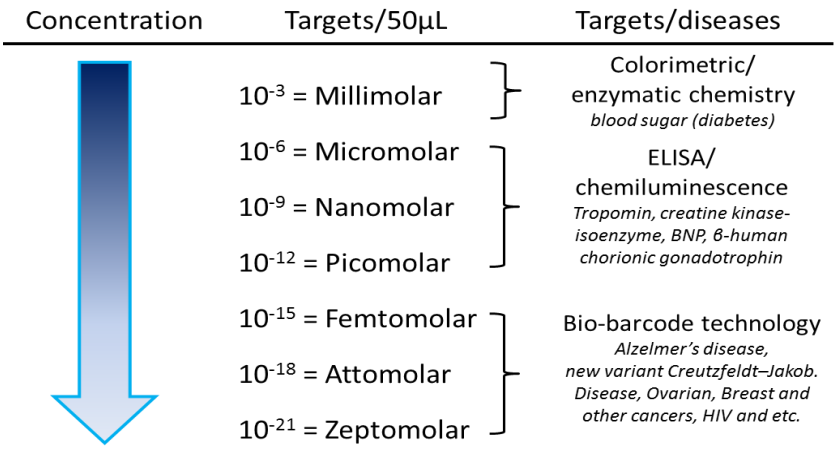

Figure 1.9 Biomolecule detection technologies.

Fortunately, by taking advantage of the development of the modern instrumental analysis technologies these problems can be partially solved by employing ultra-sensitive detectors to the detection instruments. However, as mentioned above, the utilization of sophisticated instruments as well as the required accompaniment of high-standard operational environment and professionally trained personnel also means significantly increased cost and limited locations that the bioanalysis can be undertaken.

Therefore it is a very important task to discover methods that can afford easy, inexpensive but effective detection method for low or ultra-low level concentration analytes in solutions. Furthermore, if the signal is strong enough to be easily caught by simple or even no instruments, this has exceptional merit. Thus, naked eye detection without any sophisticated auxiliary can be a targeted goal for the development of the detection methods.

Research in the past has revealed that the detection of low concentrations of analytes cannot easily be achieved directly, but requires signal amplification by employing catalysts, macromolecules, metal surfaces or supramolecular aggregates. [26] The rapidly progressing field of macromolecular signal amplification has been demonstrated primarily using catalysts, macromolecules, metal surfaces and superamolecular aggregates in the strategies illustrated in Figure 1.10.

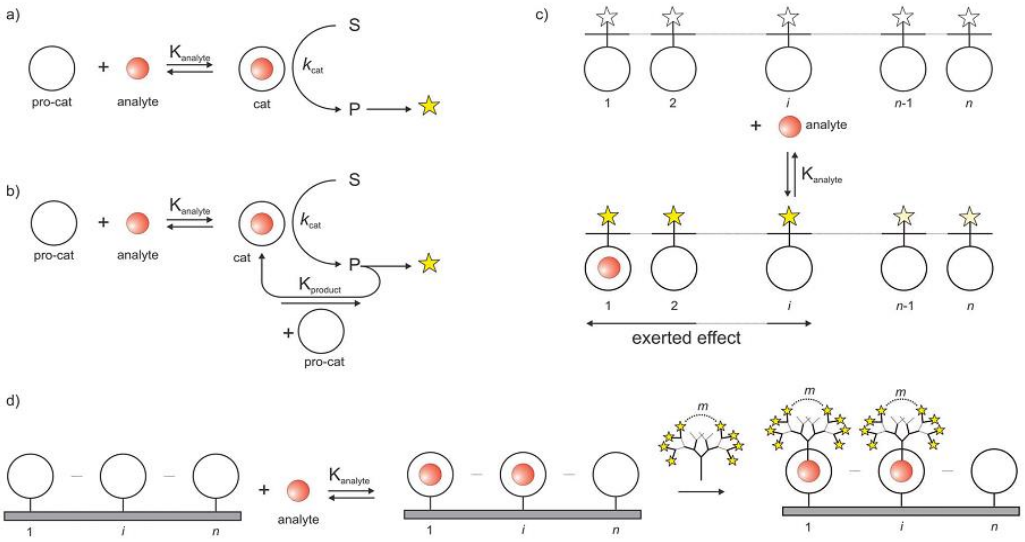

Figure 1.10 Scheme of amplification strategies. **(**Chem. Soc. Rev., 2011,40, 4488–4505**)**

Although researchers have already presented several working methods, the exploration for new pathways is still beneficial and necessary. In the following chapters new bio-imprinted

hydrogels have been synthesized for detection of ultra-low concentration of bio-targets with newly discovered molecular amplification effects. Details and advantages of these materials will be discussed (vide infra).

CHAPTER 2. BIO-IMPRINTED CAPILLARY HYDROGELS (BIG) FOR PROTEINS

2.1. Protein imprinting

2.1.1 General

As one of the most successful methodologies for the preparation of materials applied to the detection and separation of specific molecules, the molecular imprinting technique has been dramatically improved over the past three decades. At present, the traditional MIP technique has become a mature methodology for preparation of sensors and separation media, [28] and some practical products have been marketed and are even commercially available at this time. However, as mentioned in the previous chapter, the traditional MIP technique has several drawbacks; for example, target compounds for imprinting are generally restricted to small molecules which remarkably limits the applications of the MIP technique. This is especially true for extending the advantages of high recognition ability by MIPs to enhance the effect and efficiency of current medical or biological diagnostic or separation methodologies which often target large biomolecules such as proteins, viruses and cells.[29]

Protein detection is an important issue in modern medical/biological technology for monitoring human health status and is attracting increasingly more attention as evaluation targets. To date a large effort has been dedicated to this area resulting in a number of methods that have been developed to realize the accurate, specific and sensitive detection of target proteins. However， current protein detection strategies are dominated by heterogeneous immunological (or separation) assay methods such as enzyme-linked immunosorbent assay (ELISA), Western blot (WB), immunohistochemistry (IHC), flow cytometry etc., Although

these currently well-developed methods can characterize qualitatively and quantitatively target proteins, some apparent shortcomings still exist. For example, many of these methods frequently require multiple steps including multiple incubation and careful washing of a surface onto which the labeled reagent has been immobilized. Also, some of the current methodologies like Flow Cytometry require expensive equipment; and to achieve accurate results, most of these methods need a high-tech operating environment with professionally trained personnel.

Furthermore, even though the availability of cutting-edge medical facilities in the developed world allows outstanding services like timely diagnosis to a large number of individuals in localized medical facilities, there is still need for improvement of delivering these services in field application, or medical services in developing or remote areas. Therefore, the development of sensors that can be easily operated and perform high-specific detection for certain kinds of proteins with high sensitivity is an important and meaningful task. An important development for these applications would be visual detection of signal output to eliminate the high-tech equipment and personnel that is usually required.

For both high-tech and low-tech environments, MIP methodology continues to be an important tool in the fabrication of biosensors for specific detection of bio-targets. In this chapter, we will focus on making, and application of, bio-molecular imprinting polymer (BIMP) sensors for detection of two kinds of important proteins----Thrombin and Platelet Derived Growth Factor- ββ (PDGF- ββ) which are important diagnostics related with human health.

Thrombin is an allosteric serine protease present in human and animal blood (Scheme 2.1a) for normal physiological operation. It is a key protein in thrombrogenesis, which is the process by which blood is coagulated to limit bleeding. Although Thrombin is well-known for

itseffect in helping blood coagulation, Thrombin is also found in other parts of the body in some cases. For example, in the lungs of asthma and pneumonia patients, a large amount of Thrombin is often detected. [30]

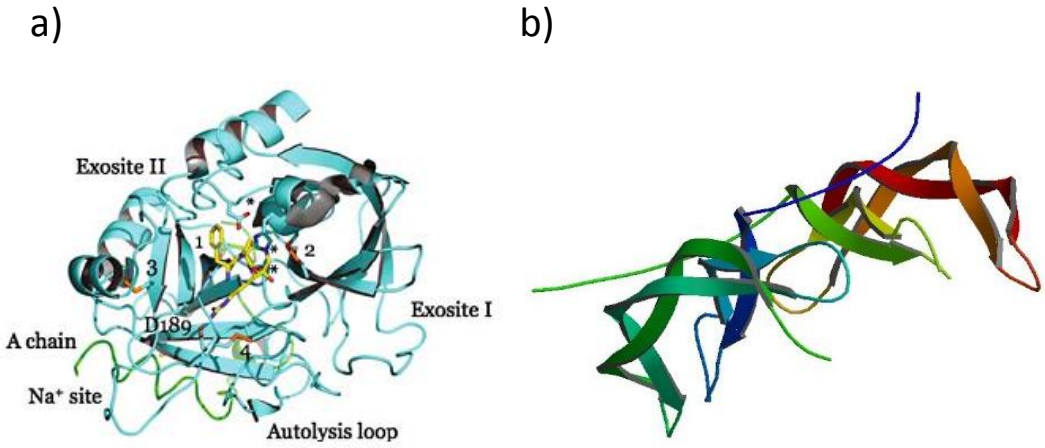

Scheme 2.1 Structure of Thrombin (a) and PDGF-ββ (b).

*adopted from: a) Thrombin: Physiology and Disease (Springer, 2009)***;** *b) http://www.creative-biolabs.com/catalogueprotein/PDGF-BB.htm.*

2.1.2 Thrombin

Since Thrombin plays an important role in human health, its detection in solution is also becoming a focus in analytical chemistry. In recent decades, a large amount of progress on Thrombin detection has been made. Generally, the detection was achieved by using Fluorescent, Electrochemical or Nanoparticle-assisted methods with the help of aptamers [31]. These methods can usually perform the detection of Thrombin at nM level or even lower. However, to monitor the result of the detection, all methods currently in use still need high-tech instrumentation. In addition, the preparation of the sensor materials is generally laborious and expensive.

2.1.3 PDGF-ββ

Platelet-Derived Growth Factor (PDGF) is one of the many growth factors, or proteins that regulate cell growth and division (Scheme 2.1b). It plays a significant role in blood vessel formation (angiogenesis), the growth of blood vessels from already-existing blood vessel tissue. Uncontrolled angiogenesis is a characteristic of cancer. In chemical terms, platelet-derived growth factor is a dimeric glycoprotein composed of two α (-αα) or two β (-ββ) chains or a combination of the two (-αβ). The platelet-derived growth factor (PDGF) family of disulfide-linked dimeric proteins consists of four homodimeric proteins, PDGF-αα, PDGF-ββ, PDGF-CC and PDGF-DD, and one heterodimeric protein, PDGF-αβ.

2.1.4 Current progress in protein imprinted hydrogels

Protein detection has been a topic of high interest and there are a few dozen reports of molecular imprinting to fabricate bio-sensors or separatory materials for detection or separation of proteins.[32] Of recent, hydrogels have proven to be promising candidates to make bio-sensors or separatory materials for bio-mass because of its bio-friendly nature. A handful of examples combining these two promising techniques together to prepare bio-molecular imprinted hydrogels for purposes such as sensors and separation materials for certain bio-markers, drug delivery or other bio-related purposes have been reported and has attracted a large share of attention. [33] For example, Miyata et. al. designed and synthesized biomolecularly imprinted hydrogels for recognition of the protein APF. The bioimprinted hydrogel was formed by polymerization of a complex of APF to a polymerizable lectin and antibody, and the signal output was a shrinking response when both the lectin and antibody simultaneously bound AFP.[39]

Tan and coworkers have also developed hydrogels for detection of certain DNA sequences with macroscopic volume change.[40]

2.1.5 Strategy for fabrication of new protein BIGs

As previously mentioned, aptamers are an exciting new class of synthetic bioreceptors evolved in-vitro by the SELEX method to give artificial receptors that can often rival the binding of antibodies.[34] Using aptamers, the idea for the new strategy of bioimprinting hydrogels is shown in Scheme 2.2 and Scheme 2.3, which takes advantage of the aptamers' highly specific selectivity to enhance the hydrogel sensor's selectivity and transduction of the shrinking signal output.

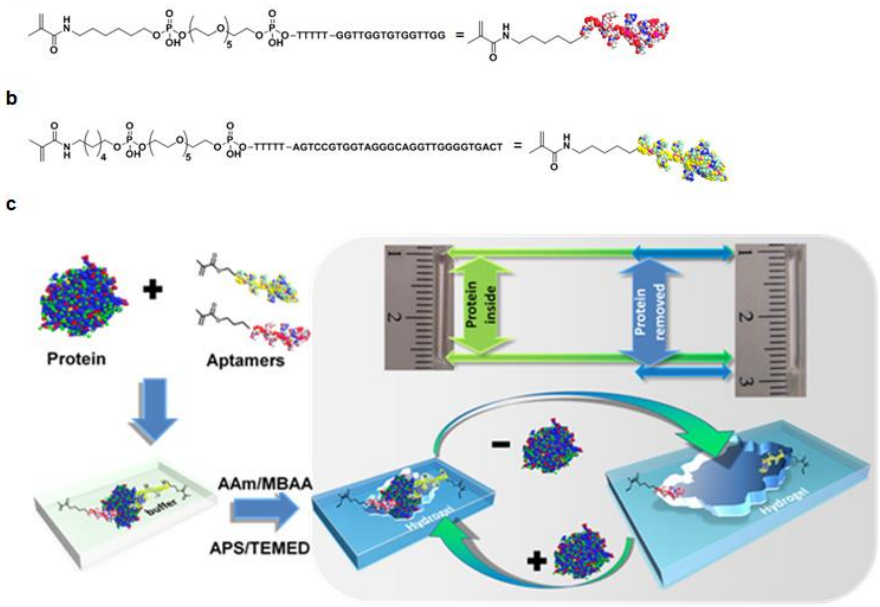

Scheme 2.2 a&b) Sequences of Thrombin aptamers; c） Outline of the Biomolecular Imprinting Scheme used to Create "Super-Aptamer" Thrombin Responsive Hydrogels.

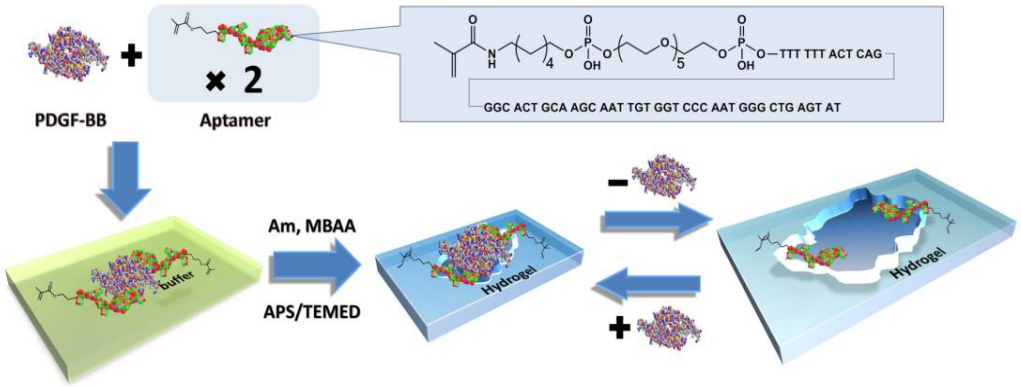

Scheme 2.3 Outline of the Biomolecular Imprinting Scheme used to Create "Super-Aptamer" PDGF-ββ Responsive Hydrogels.

The aptamers were first functionalized with polymerizable groups, followed by formation of a protein-aptamer complex with the target protein, which is polymerized to form the bioimprinted hydrogel. By removal and rebinding of the target proteins it was anticipated that naked-eye detectable macroscopic volume response would be observed.

2.2 Preparation and optimization of the protein BIGs

2.2.1 Materials

Human Thrombin was purchased from Haematologic Technologies, Inc. Human PDGF-ββ, PDGF-αβ were purchased from PeproTech Inc., Thrombin aptamers (A1 & A2) and PDGF Aptamer (A3) were purchased from Integrated DNA Technologies, Inc., AM (Acrylamide), N,N'-Methylenebisacrylamide (MBAM), Ammonium Persulfate (APS), Tetramethylethylene-diamine (TEMED) and all other reagents that used to prepare corresponding buffer and solutions are all analytical reagents purchased from Sigma-Aldrich Co. LLC. or Fisher Scientific Inc. .

2.2.2 Preparation of Thrombin BIG

2.2.2.1 Formulas

To determine the most suitable formulation for the hydrogel sensors, preliminary studies by Nicolas A. Gariano in the Spivak research group developed a formulation for Thrombin bioimprinted polymers that can produce the hydrogels with the best response listed below. All the Thrombin imprinted hydrogels in this study were prepared using the same formula. Table 2.1 below shows the stoichiometry of components used to prepare the Thrombin bio-imprinted hydrogels. From this formulation it is seen that compared to the monomer and crosslinker, the template protein and aptamer only occupied a considerably small stoichiometric portion (template protein: crosslinker = 1:483) of the overall formulation. so it is quite interesting how such a large macroscopic change can be made by this minimal amount of the template and the little change in crosslinking density caused by it.

Table 2.1 Formula of thrombin bioimprinted aptamer hydrogels.

Reagent	**MW (Da)**	**Mass of reagent (mg)**	**Reagent concentration (M)**	**Molar equivalents of reagents**
thrombin	36700	6.07×10^{-2}	1.65×10^{-5}	1
aptamer 1 (A1)	6838	1.13×10^{-2}	1.65×10^{-5}	1
aptamer 2 (A2)	11198	1.86×10^{-2}	1.65×10^{-5}	1
Acrylamide (AM)	71	11.3	1.59	9.64×10^{4}
methylene bis-acrylamide (MBAA)	154	0.123	7.97×10^{-3}	4.83×10^{2}

2.2.2.2 Details of the protein-aptamer complex

Aptamers are short, single-stranded nucleic acid sequences selected *in vitro* from large oligonucleotide libraries to bind a broad range of target molecules specifically on the basis of their high affinity to certain target molecules. The high specific affinity of the aptamers to the target molecules make them ideal for bioimprinting because they can form a stoichiometric complex to the protein, leaving no excess aptamer that would cause the serious problem of making non-specific binding sites. Thanks to the development of very powerful and relatively cheap methods for nucleic acid synthesis on solid support, obtaining aptamers for this project was a straightforward process. The sequences for aptamers with high selectivity as well as high affinity the two proteins studied in this project were previously reported[35]. Two different Thrombin binding aptamers, A1 (GGT TGG TGT GGT TGG) and A2 (AGT CCG TGG TAG GGC AGG TTG GGG TGA CT) used in this case the innate binding affinities of both are on the order of 10^{-9}. Thus, negligible amounts of free aptamers exist in the Thrombin-aptamers complex solution for the bioimprinted hydrogels. And for PDGF-ββ the aptamer (A3) has a sequence of : ACT CAG GGC ACT GCA AGC AAT TGT GGT CCC AAT GGG CTG AGT AT (Shown by Scheme 2.1 and Scheme 2.2, respectively).

There are two different types of aptamers for Thrombin that was needed for the bioimprinting processs, but only one type was needed for PDGF-ββ. This is because although both proteins have two binding sites on the surface that can selectively bind the aptamers, for Thrombin the two sites are different, which can bind to A1 or A2 respectively;. In the case PDGF-ββ, since it's a dimer of two identical PDGF-β chains, the two binding sites are the same and both bind to the same aptamer A3.

The synthetic approaches of the desired aptamers-protein complex for Thrombin and PDGF-ββ are similar in some ways, but different in the sequence of the addition of the aptamers. For Thrombin, the aptamer A2 needs to be added first to the 100mM PBS solution of Thrombin because A1 can crossreact with the binding site that normally binds A2; while the A2 doesn't have this problem (i.e. it does not have any crossreactive binding with the site intended for A1). After the addition of the A2, the mixture is vortexed for half an hour, followed by addition of aptamer A1. The resulting mixture was again vortexed for another 30 minutes and the obtained aptamers-protein complex solution was carried on to the next step.

2.2.2.3 Pre-treatment of the capillaries

The transparent glass capillary (1.7mm in internal diameter) was cut into short pieces (approx. 5cm in length) from 1.2 meter long. The resulted short capillaries were then washed by de-ionized and sonicated for 15 minutes before immersed into the Piranha solution (H_2SO_4:H_2O_2=1:1) and leave them there for overnight. Then the capillaries were washed by de-ionized water, acetone and dried completely in the oven.

2.2.2.4 Making of the BIG

To prepare the polymerization solution for the synthesis of Thrombin BIG, a Phosphate Buffered Saline (PBS, pH=7.4) containing corresponding amount of acrylamide (AM), N,N'-methylenebisacrylamide (MBAM), and ammonium persulfate (APS) (See Table 2.1) was prepared. Then, the aptamer-protein complex solution obtained from previous step was added to the polymerization solution and the final volume of the mixture was adjusted to 100 µL by adding

variable amount of 100mM PBS. The resulting mixture was allowed to vortex for several seconds to get completely mixed before purging with Nitrogen for 10 minutes. Afterward the solution was capped for further use. For preparation of PDGF-ββ imprinted hydrogels, a similar procedure was applied except 2mM PBS (pH=7.4) was used instead 100mM and a 50% concentration (compared to the concentration used in preparation of Thrombin imprinted hydrogels) was used for all components. The total final volume was also adjusted to 100 μL. Afterward, the solution was also treated with same purge process as for Thrombin.

For the bioimprinting polymerization reaction, 0.5 μL of Tetramethylethylenediamine (TEMED) was added and the solution was quickly vortexed; subsequently, a capillary with 1.7mm inner diameter and approximately 10cm in length was dipped into the solution. The capillary was allowed to stay in the solution for a couple of seconds until enough amount of the polymerizing solution (approx. 5-15mm in length) was transferred into it by capillary action. Then both sides of the capillary were quickly sealed with parafilm, and the capillary was allowed to sit at room temperature (21.5℃) for 12 hours to complete the polymerization. After the polymerization, the capillary was unsealed, cut to a suitable length to fit the culture dish, injected with 100mM (2mM for PDGF) PBS and immersed into the PBS in the culture dish. The PBS was changed every several hours until the length of the hydrogel became constant.

2.2.3 Preparation of PDGF-ββ BIG

2.2.3.1 Formula of components

Although the thrombin bio-imprinted hydrogels were successful examples, PDGF-ββ is relatively expensive compared to Thrombin, and can be overly expensive if we directly copy the

formula for Thrombin. If similar properties can be achieved by using a lower protein concentration, the cost can be significantly reduced. To verify if a formula with lower protein-template concentration can still maintain the same level of binding response of the bioimprinted polymer, two Thrombin imprinted hydrogels with 100% and 50% concentration of all components were prepared and their volume response compared under the same binding conditions. The results show that the sample with 50% concentration produced a volume change of $5.25 \pm 1.45\%$ while the original formulation gave a volume change of $5.46 \pm 0.95\%$. Overall the results indicated that the 50% protein concentration formulation can generate hydrogels with approximately the same level of volume response as the 100% while significantly lowering the cost. Thus, the preparation of PDGF-ββ imprinted hydrogels employed the 50% formulation which is also listed below in Table 2.2.

Table 2.2 Formula of thrombin bioimprinted aptamer hydrogels.

Reagent	**MW (Da)**	**Mass of reagent (mg)**	**Reagent concentration (M)**	**Molar equivalents of reagents**
PDGF-ββ	24300		0.83×10^{-5}	1
Aptamer (A3)			1.65×10^{-5}	2
Acrylamide (AM)	71	5.7	0.803	9.64×10^{4}
methylene bis-acrylamide (MBAA)	154	0.0613	3.98×10^{-3}	4.83×10^{2}

2.2.3.2 Making of the PDGF-ββ BIG

In general, the synthesis of the PDGF-ββ BIGs follows the same procedure used in the preparation of the Thrombin BIGs. In the formulation PDGF-ββ bio-imprinted hydrogels only

one kind of PDGF aptamer bound 2 sites on the PDGF-ββ protein, whereas Thrombin hydrogels needed 2 different kinds of aptamers to prepare the protein-aptamer complex. The reason for this is because PDGF-ββ is a dimer, and has two identical copies of the binding epitope on each half, whereas Thrombin is monomeric, but has two different epitopes that bind two different aptamers. The following discussion gives the details of these systems.

2.2.3.3 Polymerization of the Protein-Aptamer Complex

To verify the efficiency of incorporation of the PDGF aptamer-based monomers into the hydrogels during polymerization, a blank sample hydrogel containing just aptamer, monomer and crosslinker was prepared in large scale (50 fold more material than typical polymerizations) in a 20mL glass vial following the procedure described in section 2.3.2.. The resulting hydrogel was then transferred to a vial and immersed into 2mM PBS for washing. The washing procedure that follows was carried out to isolate any unpolymerized aptamer that remain free in the hydrogel. The solution was changed every a few hours and the eluate was collected and dialyzed using a dialysis membrane with a cutoff molecular weight of 3600 against 2mM PBS for 1 week during which the solution was changed every day. The resulting solution collected from dialysis membrane was adjusted to 20mL and subsequently used for UV-Vis study. A set of standard solutions with different aptamer concentrations in 2mM PBS was also prepared to provide a calibration curve for the UV study. The results of UV study are illustrated in Figure 2.1 below.

In Figure 2.1, the peak at approximately 260nm is the absorbance peak corresponding to the aptamer. The result indicates that about 93% of the aptamer-based monomers were successfully polymerized into the hydrogel.

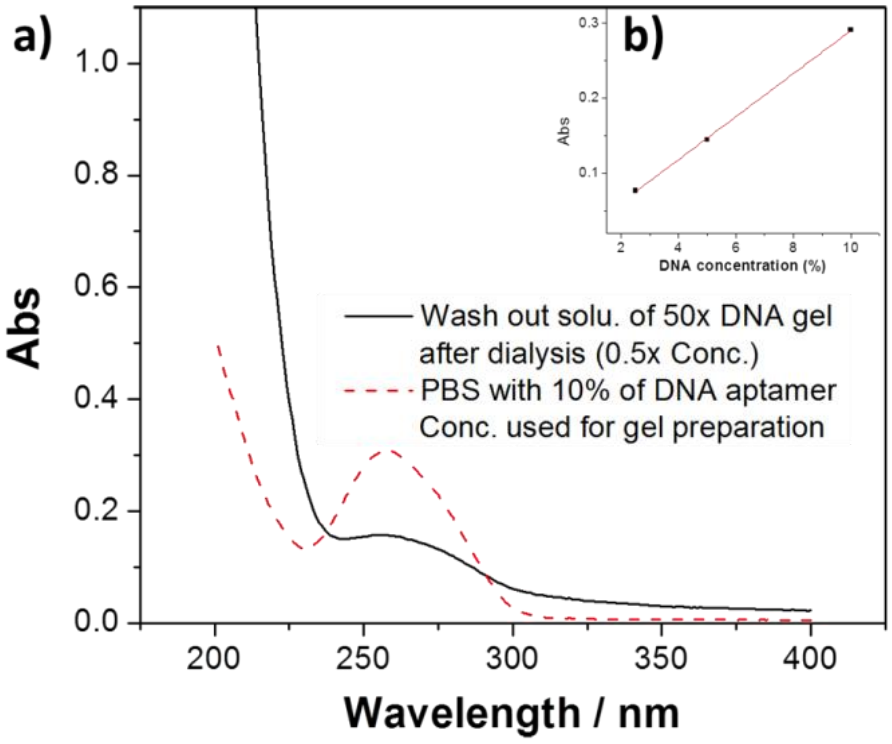

Figure 2.1 UV study of the immobilization of the PDGF-ββ aptamer to the hydrogel matrix. a) comparison of the UV curve of the wash out solution and the 10% DNA solution; b) standard calibration line.

2.3. Optimization of the BIGs

In theory, the extent of response of the hydrogels is related to the distance between two binding groups that is tailored to fit the template geometry. A distance too far away or too close can both lead to low responses. This is due to improper distance between recognition that decreases the ability of these sites to bind simultaneously on the same target protein.

Proximity effects on these bioimprinted hydrogels toward optimizing the response of the Thrombin imprinted hydrogels was explored. For PDGF imprinted hydrogels it was important to

investigate the influence of the crosslinker to the behavior of the hydrogels. For one study a series of bio-imprinted hydrogels containing different amounts of crosslinker were prepared and hydrogel response results are shown in Table 2.3. The results clearly indicate that the original formulation we used for preparation of hydrogels gives the best results.

Table 2.3 The influence of the crosslinker concentration to BIGs' response

Amount of Crosslinker (Equivalents versus the regular concentration mentioned in Table 2.1.)	Volume change %
0.5 ×	4.90±1.65
1.0 ×	8.82±0.88
2.0 ×	5.98±1.08
4.0 ×	3.84±0.59

2.4. Detection of the protein in solution using BIG

2.4.1 General procedure

2.4.1.1 Regeneration

After polymerization, the hydrogel was immersed in PBS (2 mM) to reach equilibrium (constant length) during which, the buffer was changed every several hours. Then regeneration solution was injected into the open sections of the capillary to remove the template protein; the regeneration solution was also changed at 3-4 hour intervals. Details for different regeneration solutions required for the different proteins is provided next,

2.4.1.1.1 Thrombin

For thrombin-bioimprinted hydrogels, a saturated salt solution of 4.3M Guanidine hydrochloride (GuCl) and 1.4M Sodium Chloride (NaCl) was used as regeneration solution to remove the thrombin from the hydrogel. After the first injection, the regeneration solution was changed every few hours until the length of the hydrogel became constant.

Then the hydrogel was put into 100mM PBS and the solution was changed until constant length was reached. The length at this point was used to evaluate the volume change because all the gel lengths used in measuring the extent of the volume response will be the length at full equilibrium in the same buffer.

2.4.1.1.2 PDGF

To break the non-covalent linkage between the PDGF-ββ and its aptamers, 10% (m/m) Sodium dodecyl sulfate (SDS) aqueous solution was used as regeneration solution. The operation was the same as mentioned above for Thrombin imprinted hydrogels.

However, because mixing of the 10% SDS solution and PBS solution with a relative high concentration (> 2mM) can lead the precipitate of the salt in solutions, several different PBS concentrations were tested and the outcome revealed that 2mM PBS will not lead to precipitation while still maintaining the volume shrink response of the hydrogels. As a result, 2mM PBS was used in all the following studies on PDGF-ββ gels.

2.4.1.2 Rebinding

After the regeneration process, the hydrogels were washed with PBS of 100mM for Thrombin imprinted gels and 2mM for PDGF imprinted gels. This was done several times until constant length was reached, and the length was recorded as d_0. For studying the effects of the rebinding step the protein solution was injected into the capillary, and the solution changed every several hours until equilibrium was achieved. The hydrogel was then washed with PBS (no protein) until it reached equilibrium constant length to wash out all unbound protein and let the hydrogels fully relaxed. The length of the hydrogel after rebinding of the protein was recorded as d.

2.4.1.3 Calculation of the hydrogel volume change response

Because the gels are measured in capillaries, the volume change of the gel is limited to only one dimension and the percent change in that dimension is proportional to the overall volume change. Based on the d_0 and d_1 obtained from the section 2.5.3, the volume change of the hydrogel was calculated by the equation:

$$Percent\ Shrinkage = \frac{d_0 - d}{d_0} \times 100$$

2.4.2 Reversibility of BIG volume change

Figure 2.2 shows the experimental results from repeated cycles of washing and rebinding fr both Thrombin and PDGF-ββ bio-imprinted hydrogels, using a concentration of 1×10^{-6}M protein.

a) b)

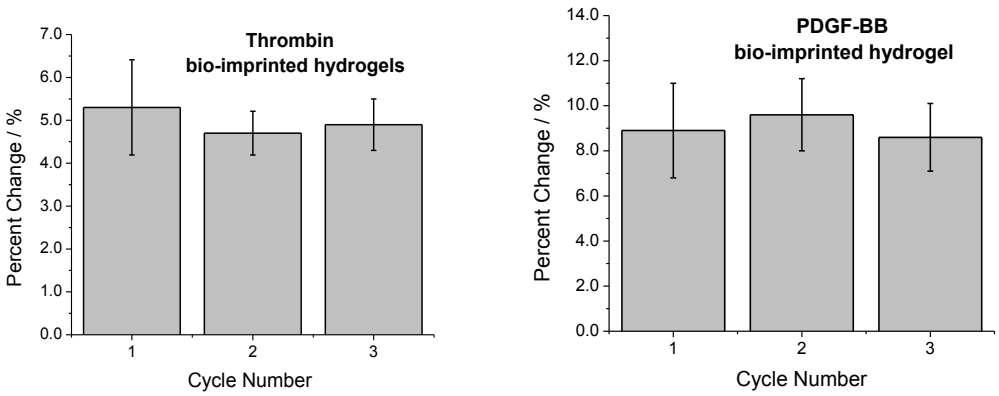

Figure 2.2 Reversible volume change of Thrombin (a) and PDGF-ββ (b) imprinted hydrogels.

It is gratifying to see that both of the hydrogels can exhibit at least 3 cycles of reversible volume changes upon repetition of binding and regeneration of the proteins in the hydrogels. Furthermore, the percentages of the volume changes are relative constant. For Thrombin bio-imprinted hydrogels, the volume changes are approximately 5%, and in the case of PDGF imprinted hydrogels, about 9% of volume change can be achieved. This result initially indicates the success of the application of bio-imprinted hydrogels as analytical sensors.

2.4.3 Picomolar detection limit

Once the bio-imprinted hydrogels were demonstrated capable of being used in protein detection, the next question was how sensitive they were, because for all kinds of sensors, the detection limit is one of the most important indexes among all its properties. So we prepared protein solutions at different concentrations (1×10^{-18}~1×10^{-6}M) by serial dilution of protein stock solutions. The volume change response of our bio-imprinted hydrogels to these different

concentrations was tested from low to high concentrations and recorded. For each concentration, the hydrogel was allowed to experience 3 full "regeneration-rebinding" cycles and And the average volume change recorded. It is important to collect the length data when the hydrogel has reached its maximum extent of volume change. Similar to earlier work by group member Nick Gariano for development of Thrombin binding isotherms, [36] the PDGF- ββ isotherm research is graphed in Figure 2.3.

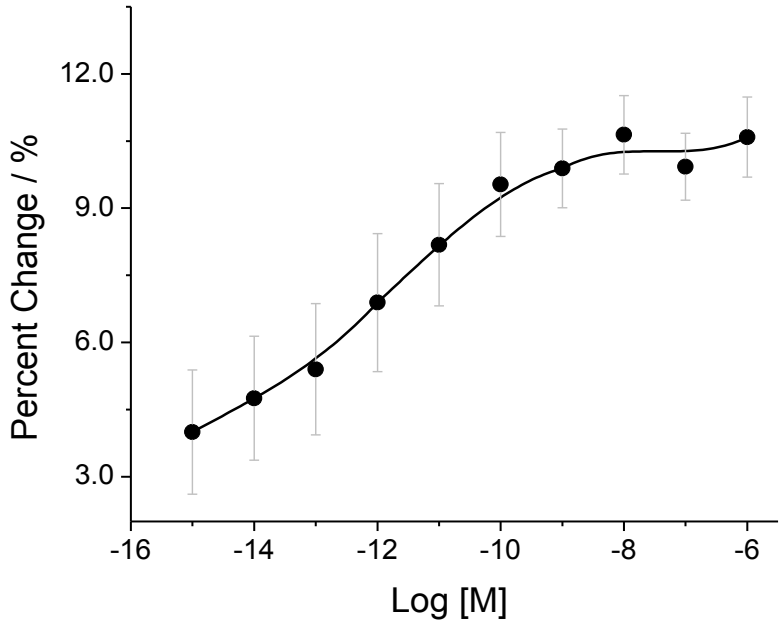

Figure 2.3 Isotherm study of PDGF- ββ imprinted hydrogels

From Figure 3, it is clear that the PDGF BIG can show detectable volume change at a concentration as low as 1×10^{-12}M, and this volume change in the hydrogle length inside the capillary can be caught by our naked-eyes. This phenomenon demonstrated the necessary proof-of-principle that our bio-imprinted hydrogels are sensitive sensors for template proteins. This

level of detection is so good, it compares competitively to the best detection limits of many current instrumental methods; and in some cases, our method is apparently even more sensitive.

2.4.4 Imprinting effect plays a crucial role in the response behavior

To verify the imprinting of the template really plays a key role in the outstanding recognition ability and macroscopic volume change discovered for these bioimprinted hydrogels, two sets of controls samples were prepared. Comparison of the results of bio-imprinted hydrogel and non-imprinted control hydrogels are shown by Figure 2.4 below.

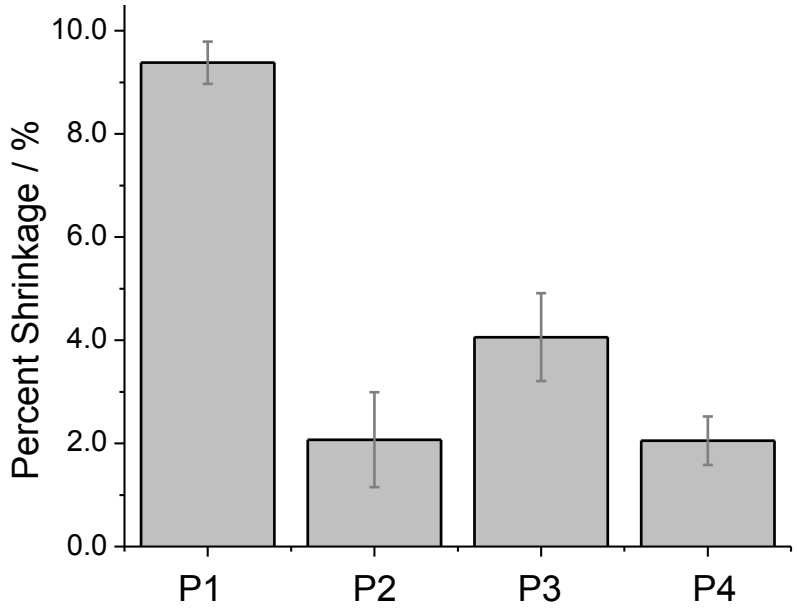

Figure 2.4 Volume Change of BIGs versus non-imprinted control gels. P1: bio-imprinted sample treated with PDGF-solution; P2: sample prepared without aptamer; P3: sample prepared without template; P4: sample prepared without template and aptamer.

The first column (P1) in Figure 2.4 shows the volume response of regular PDGF BIGs; P2 is a control hydrogel synthesized with only template but no aptamer; while P3 is a control

hydrogel made with aptamer but no template; and P4 is a control made without any A3-PDGF-A3 complex. Compared to the non-imprinted control hydrogels, the volume response of imprinted hydrogels is much higher (at least 2 times more than the best control gels).

The effect of the imprinting technique can be further verified by investigating the effects of the aptamer concentration in non-imprinted hydrogels. One purpose of the study is to observe if a proper distance between the aptamers in non-imprinted hydrogels can adventitiously lead to the needed proximity of the two aptamer functional monomers. If this occurs, it can be expected that similar results in volume change would match the results we got from the imprinted hydrogels.

To test this possibility, a set of non-imprinted hydrogels were prepared with 0.25, 0.5, 1.0, 2.0, 4.0 and 8.0 times of concentration of the PDGF aptamer used in the bioimprinted hydrogels, without adding any template protein. Figure 2.5 below graphs the influence of the aptamer concentration on the volume response of the hydrogels. The highest response these non-imprinted hydrogels can reach is about 4.0%, which coincidentally is with the same concentration we used to prepare the regular bio-imprinted hydrogels. Since the regular PDGF imprinted hydrogels can exhibit volume change about 8-9%, the non-imprinted hydrogel only shows less than half of the response to the template protein under the best circumstances.

This undoubtedly proves that imprinting effect plays a crucial role in hydrogels' responsive property, and the correct placement of aptamers is not random for the bioimprinted hydrogels.

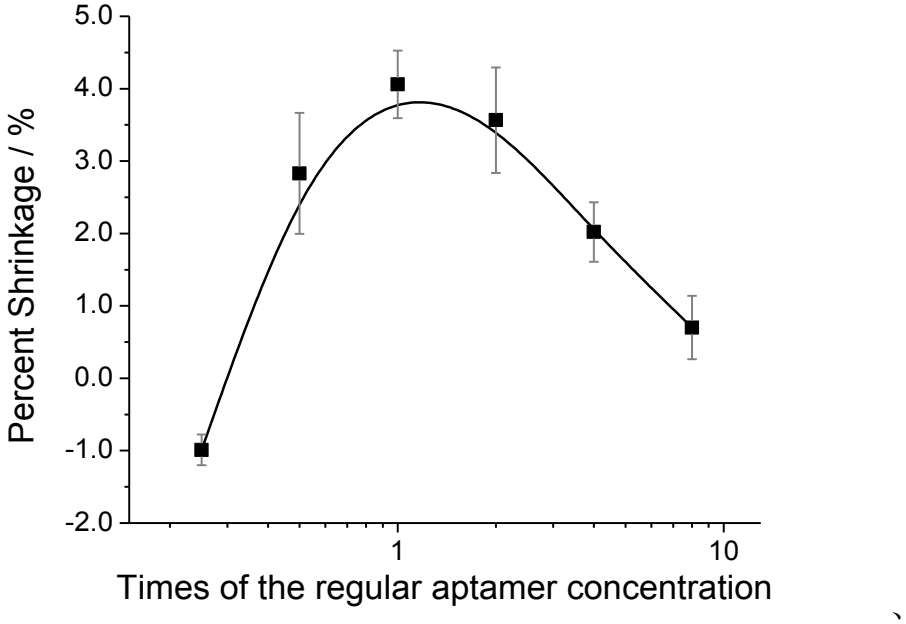

Figure 2.5 Study of the influence of the aptamer concentration to the volume response of BIGs.

2.4.5 The volume response is highly specific to imprinted template

Selectivity is another extremely important index for sensor properties. To verify if the bio-imprinted hydrogels exhibit specific volume response to template protein, we treated the PDGF- ββ imprinted hydrogel with different protein solutions (PDGF-αβ, Thrombin and Bovine serum albumin, all at 1×10^{-6}M) that could be anticipated to be competitive for binding the aptamer binding sites. The results are shown in Figure 2.6 below where P1 is PDGF- ββ imprinted hydrogel treated with PDGF- ββ solution, PC1 is the hydrogel treated with PDGF-αβ solution and PC2 and PC3 are treated with Thrombin and BSA, respectively.

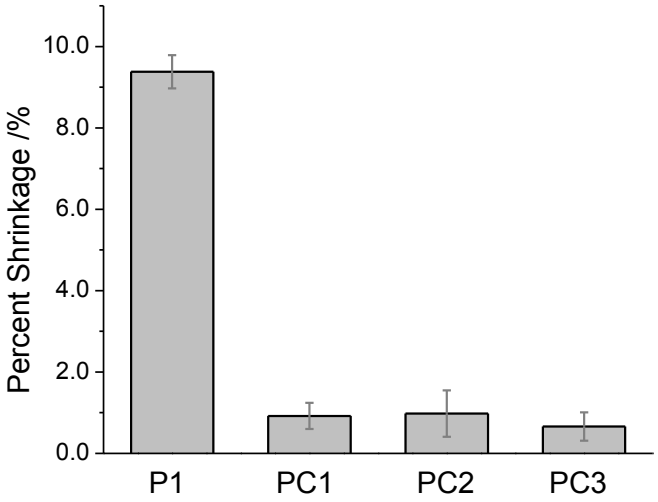

Figure 2.6 Volume response of BIGs to different protein solutions. (Bio-imprinted sample treated with P1: PDGF-solution; PC1: PDGF-αβ; PC2: Thrombin; PC3: BSA.

From the result it can be concluded that none of the PDGF- ββ imprinted hydrogels exposed to proteins other than PDGF- ββ show any kind of a comparable volume response seen with PDGF-solutions, indicating the bio-imprinted hydrogels have very high selectivity.

2.4.6 Dehydration of BIGs maintains or improves binding response.

Considering the hydrogels are 3D polymer networks primarily composed of water, it is not convenient to transport or store them in their wet state which promotes degradation and microbial growth. As a result, for practical applications such field diagnosis or other tasks which may require long-distance transportation or long period storage, it is quite meaningful to investigate the properties of the hydrogels before and after dehydration.

To dehydrate the hydrogels, the unsealed capillaries with hydrogels were allowed to sit in a culture dish left slightly opened to open air until the hydrogels had shrunk to a white or

colorless solid. Next, they were reintroduced to an aqueous environment by immersion in 2mM PBS until the hydrogel swelled to its original size and reached equilibrium. Subsequently, the volume response of these rehydrated hydrogels to the original template protein was tested using the rebinding method described above. The picture of hydrogels at different stages in "dehydration-rehydration" process is shown in Figure 2.7.

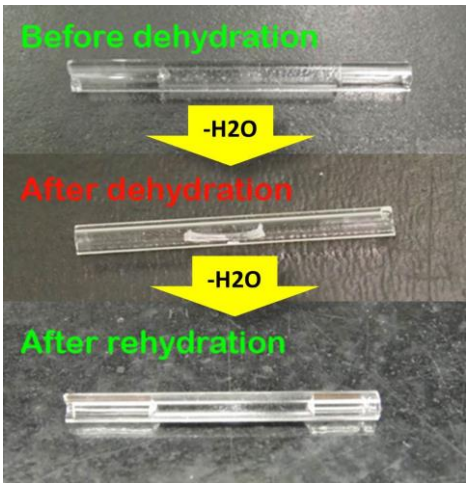

Figure 2.7 Picture of hydrogel at different stages in "dehydration-rehydration" process.

Figure 2.8 shows pictorially the results comparing the PDGF-ββ imprinted hydrogel before and after dehydration. PD0 shows the response of hydrogels before dehydration, PD1 is the volume response after dehydration in the presence of protein which was encapsulated inside and PD2 is the hydrogel dehydrated without protein inside, PD3 is a control blank hydrogel dehydrated with protein in. It is clear in Figure 2.8 that even after dehydration and rehydration process, the imprinted hydrogels still maintains the same volume response when exposed to the template protein solution.

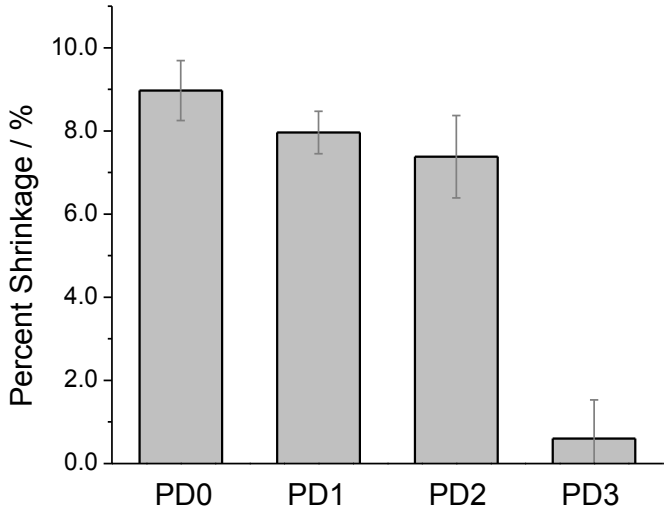

Figure 2.8 The influence of the dehydration process on the behavior of the imprinted hydrogels.

Generally, this result indicates that the dehydration process does affect the responsive behavior of imprinted hydrogels. The stable behavior of reconstituted gels from dehydrated materials reveals the potential advantage in storage and transportation of this kind of hydrogel sensor.

2.4.7 Hydrogel detection of protein in bodily fluids

Up to this point, all research described was conducted in PBS buffer; however, as a bio-sensor for applications like diagnosis and etc., practical applications are usually carried out in real bio-fluids like plasma, urine, tears, etc. To test whether the hydrogels can still detect target proteins in "close-to-real" media and not just in PBS buffer, artificial tear solution was prepared based on the formulation reported in [37]. The exciting result showed that the hydrogel can still exhibit a volume change of 7.16±0.32% in the mimetic body fluid. This outcome clearly

indicates the potential of our methodology in real-life biological or medical applications like disease, diagnosis, etc.

2.4.8 Problems with weight analysis of bioimprinted hydrogels.

The fact that the weight of the hydrogel is proportional to its volume, opened the possibility of analyzing volume changes in the hydrogels using weight changes to characterize the hydrogels. To investigate this possibility, after polymerization the hydrogel was carefully pushed out of the capillary using a suction bulb and immediately immersed into PBS solution in a culture dish. The solution was changed every hour and the weight of the hydrogel was measured by an electronic balance every 30 minutes until the weight became constant. Next, to remove the template protein from the hydrogel, it was transferred to the regeneration solution, which was also changed regularly until constant weight was achieved. Last, the hydrogel was washed again with PBS until constant weight, and the weight at this point was recorded as W_0.

To measure protein rebinding, the hydrogel was then immersed into protein solutions and washed by PBS after constant weight was achieved, which was marked as W_1.Overall, the volume change of the hydrogel can be characterized by the equation:

$$\text{Percent Weight Change} = \frac{W_0 - W_1}{W_0} \times 100\%$$ The results showed that after the removal of the protein, the weight of the hydrogel increased about 15%. However, after immersing the hydrogel in protein solution to reform the crosslink between proteins and aptamers, the weight change was only 0.2%.

There was a problem with this in that although a significant increase of the weight can be observed after the regeneration, it seems there's no change of the weight was observed after the hydrogel was immersed into the protein solution.

The reason for this disparity may be that when taking the hydrogels out of the capillary it is very difficult to control the amount of solution remaining on the surface. Furthermore, the gels were removed from solution for weighing, and the move from solution to air may cause changes due to the change from hydrophilic to hydrophobic surroundings. Thus, the experimental errors may completely conceal the small changes caused by the volume response to the protein. Another fundamental reason may lie in the restricted geometry of the hydrogel when in the capillary that maintains certain hydrogel morphology. It may be that hydrogel relaxes when outside of the capillary, and changes the morphology to one that is not responsive anymore. Perhaps the larger distance between recognition sites caused by non-restricted 3D expansion may also be a reason.

2.5 Underlying mechanism of volume change in BIGs

By using the biomolecular imprinting technique and employing corresponding aptamers as recognition sites, we synthesized bio-imprinted hydrogels. Rebinding experiments revealed that these bio-imprinted hydrogels show macroscopic volume shrinking changes in presence of dilute or even highly diluted protein solutions. The lowest concentration that has produced a detectable volume signal in PDGF bio-imprinted hydrogels is 1×10^{-15}M, at which the resulting volume change was around 3%. However, it is important to point out that at protein concentrations up to 1×10^{-9}M, the volume response is almost the same as the response for

protein solution that are 1000 fold more at concentrated (1×10^{-6}M). Although all literature reports for similar molecular responsive hydrogel in the past attribute the macroscopic volume change to the change of the crosslinking density [37], the negligible changes in overall crosslinking density in this case reveals that the macroscopic volume change is not simply caused by the change of the crosslinking density due to the forming and breaking of the protein-aptamer complex. Moreover, the volume change is also not caused by either the increase of the mass or the osmotic effects, which is demonstrated by the non-imprinted control gels which containing the same target protein.

We believe macromolecular excluded volume effects may be the reason that leads to this unusual molecularly triggered macroscopic volume response. In fact, similar effects have been observed in a recently published paper for change in melting temperature of DNA crosslinked nanoparticles. [38] In addition, research on the influence of the crosslinker mentioned above indicated that increase of the crosslinker can actually lead to a decrease of the volume response also supports the excluded volume concept.

To further prove the excluded volume hypothesis, a temperature study of the bio-imprinted hydrogels was performed. As shown in Figure 2.9 below, the volume change responses of PDGF imprinted hydrogels rebound with protein solutions at different concentrations were measured at various temperatures the results show that the hydrogels expand as temperature is increased at first, then contract, or at least stop expanding, even when the temperature is further increased. The temperature at which the hydrogel stopped expansion is classified as the theta condition where hydrogel insolubility cancels the effects of excluded volume. Additionally, when the hydrogel was rebound with low concentration protein solutions, thermal swelling was counterbalanced and thus leads to a lower volume response.

This can be attributed to the decrease of the volume exclusion caused by restricted polymer chains. Meanwhile, the theta temperature increased, indicating that the restricted polymer chains require more thermal energy to be surrounded by solvent as expected for volume exclusion effects. Furthermore, when the concentration of the protein is increased, the volume response decreased more and the theta temperature continuously increased. Overall, the evidence of theta temperature effects supports the idea that the influence of the excluded volume effects to the macroscopic volume response of the hydrogels should be taken into account rather than simply crosslink density.

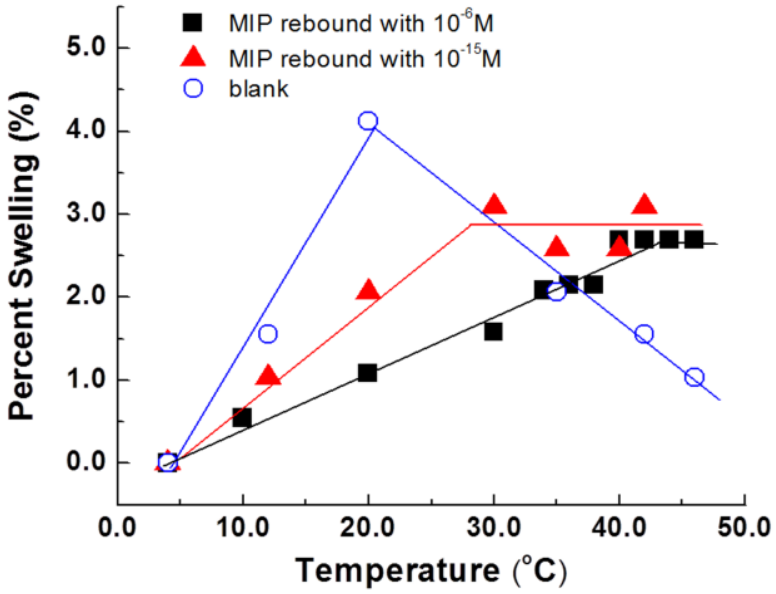

Figure 2.9 Temperature study of PDGF BIGs indicating an excluded volume mechanism.

2.6 Summary

In conclusion, BIG (Bio-Imprinted Hydro-Gel), a novel bio-sensor for specific detection of target proteins (Thrombin and PDGF-ββ) successfully developed based on the bio-macromolecular imprinting technique using aptamer-based functional monomers. The use of

protein-specific aptamers to the hydrogel grants the hydrogel sensors high selectivity. Moreover, the hydrogel sensors exhibit naked-eye volume change at very low concentration, in fact, the detection limit can be as low as femtomolar level. It was determined that the excluded volume effect may be a possible reason for this unusual macroscopic volume response. An important finding was that the hydrogel sensor also works in bio-mimetic bodily fluids, and also that dehydration did not affect the sensor's responsive ability.

CHAPTER 3. AM-NIPAM COPOLYMER BIO-IMPRINTED CAPILLARY HYDROGELS

3.1 Introduction

In the previous chapter we successfully developed a novel type of bio-imprinted hydrogel sensor (BIG) that can generate a naked-eye detectable volume response to targeted proteins. Having established a successful method, we investigated optimization parameters to improve the method such as larger volume change response, faster responsive speed etc. Typically, to enhance the materials' properties, the most common approach is to modify the materials chemical or physical structure, or any other component the material's properties are closely related to.

In polymer chemistry, using two or monomers to form a copolymer instead of changing the single monomer of a homopolymer to endow materials with new properties or enhance their inherent properties is the most frequently applied strategy. This is especially true for bio-related areas including biology or medical science and engineering, where copolymers have been proven to be a very prolific in biospecific molecular recognition. This is due to the potential of copolymers to form arrangements of chemical functions which mimic natural biospecific sites by choosing monomers with different functionality and adjusting the feed ratio. Up until now, there are a few successful examples in fabrication of copolymer materials to generate biosensors for recognition of certain biomolecules.[41] For instance, Molecular imprinted copolymers which are called "plastic antibodies" that can selectively recognize and bind to certain bio-targets have also been developed and proven to be a useful tool in in vivo imaging and therapy [41a].

As a result, synthesis of copolymer bio-imprinted hydrogels and the study of responsive properties using different functional monomers were most often been used to explore improvements to materials that can result in better responses. For example, Prof. Miyata's group developed biomolecularly imprinted protein APF pre-complexed to a polymerizable lectin and antibody, which gave a shrinking response when both the lectin and antibody simultaneously bound AFP.[42] Several other systems have also been developed for detection of glucose and other biomarkers. These methods can usually achieve a relative low detection limit with high specificity and considerably easy operation.[43] For the systems described in this study, in addition to acrylamide as a monomer, candidates of second monomer will be chosen from commercial available water soluble monomer such as acrylic acid (AA), Methyl acrylic acid (MAA) and N-isopropylacrylamide (NIPAM). It is anticipated that the difference in properties like hydrophobicity and charge density can lead to better recognition and/or response.

Previously we reported fabrication of bio-imprinted hydrogels for the visual detection of Thrombin and PDGF in solution which exhibit very high selectivity and sensitivity. It was also determined that the mechanism for the macroscopic volume change may not only be caused by the small amount of the change of the percent of crosslinking but also the change of the material's excluded volume. Here in we present a study of copolymer bio-imprinted hydrogels which exhibit better responses while still maintaining high selectivity and sensitivity, and adds further proof of the excluded volume mechanism we hypothesized in the original paper.

3.2 General synthesis and measurement of the NIPAM-AM Bio-Imprinted Hydro-Gel (BIG)

3.2.1 Materials

Human Thrombin was purchased from Haematologic Technologies, Inc. Human PDGF-ββ, PDGF-αβ were purchased from PeproTech Inc., Thrombin aptamers (A1 & A2) and PDGF Aptamer (A3) were purchased from Integrated DNA Technologies, Inc., Acrylamide, N-isopropylacrylamide, MBAM, APS, TEMED and all other reagents that used to prepare corresponding buffer and solutions are all analytical reagents purchased from Sigma-Aldrich Co. LLC. or Fisher Scientific Inc. .

3.2.2 Formulation and synthesis

Generally, the synthesis follows the example in the previous chapter for preparation of protein imprinted BIGs. The only difference is that a second monomer, NIPAM, will be added to the pre-polymerization solution together with AM at different molar ratios for copolymer optimization. NIPAM was picked as the second monomer because NIPAM is one of the most commonly studied monomers for the fabrication of bio-related polymeric materials, especially those that are thermally responsive. For other applications, the most significant merit of NIPAM is that its polymer can exhibit a LCST at approximately 32^{o}C which is fairly close to human body temperature.[44] Additionally, its hydrophilicity and relatively low toxicity also helps to make it a good choice for making bio-friendly materials for different purposes like tissue engineering, drug delivery, etc. In our research, we were interested in the molecular structure of NIPAM which consists of both hydrophilic and hydrophobic parts.

It is now known that hydrophobicity plays an important role in forming and maintaining the structure and property of bio-macromolecules. Employing hydrophobic effects in molecular self-assembly to fabricate materials for different applications is currently also a hot topic.[45] Since the bio-imprinted hydrogels actually contain the molecular recognition and stimuli response, both of these effects may benefit from increased hydrophobicity inducing hydrophobic effects. Thus the introduction of the NIPAM was anticipated to lead to some interesting changes in the bioimprinted hydrogels' properties.

The detailed formulation for fabrication of these NIPAM-AM copolymer bio-imprinted hydrogels is provided in Table 3.1 below. After synthesis following the procedure in the previous chapter, the obtained hydrogels were incubated with PBS buffer until equilibrium is reached, which was indicated by a constant length of the hydrogel.

Table 3.1 Formulation of thrombin and PDGF copolymer BIGs

Reagent	**MW (Da)**	**Mass of reagent (mg)**	**Reagent concentration (M)**	**Molar equivalents of reagents**
Platelet-derived growth factor-ββ (PDGF)	24300	2.02×10^{-5}	8.30×10^{-8}	1.0
Thrombin	36700	3.03×10^{-5}	8.25×10^{-8}	1.0
aptamer 1 (A1)	16013	2.64×10^{-5}	1.65×10^{-8}	2.0
aptamer 2 (A2)	6838	5.35×10^{-6}	8.25×10^{-8}	1.0
aptamer 3 (A3)	11198	9.30×10^{-6}	8.25×10^{-8}	1.0
Acrylamide (AAm)	71	5.6	7.88×10^{-5}	9.57×10^{4}
N-isopropylacrylamid (NIPAM)	113	8.9	7.88×10^{-5}	9.57×10^{4}
methylene bis-acrylamide (MBAA	154	0.061	3.96×10^{-7}	4.81×10^{2}

3.2.3 Template removal and evaluation of rebinding

The method used for removal and rebinding of the templates from the imprinted hydrogels; the equation used to calculate the percent volume change; as well as the buffer, regeneration solution, and rebinding solution were identical to those described in the previous chapter. Generally, a saturated salt solution of 4.3M Guanidine hydrochloride (GuCl) and 1.4M Sodium Chloride (NaCl) was used to regenerate the binding sites for thrombin bio-imprinted hydrogels and 10% SDS solution was used for PDGF-ββ bio-imprinted hydrogels. After treatment with regeneration solution, the BIGs that reached equilibrium were further washed with plain PBS buffer until constant gel-length was achieved, and the length of the hydrogel was recorded as d_0. Next, the hydrogels were incubated with the desired protein solution of defined concentration until equilibrium, followed by washing against plain buffer. The equilibrium length at this point was recorded as d. The percent volume change was calculated by

$$\text{Percent Shrinkage} = \frac{d_0 - d}{d_0} \times 100$$

The values of percent shrinkage obtained were compared as a function of NIPAM concentration to determine the optimum formulation.

3.3 Results and discussion

3.3.1 Copolymer BIGs exhibit larger volume response

At the very beginning of the study on copolymer bio-imprinted hydrogels, we prepared Thrombin and PDGF-ββ copolymer BIGs using the formula mentioned in section 3.1 to verify if a higher volume response can be achieved. An exciting result was that we discovered that both Thrombin and PDGF-ββ bio-imprinted copolymer hydrogels exhibit an increase in response of

about 50% (Shown in Figure 3.1) versus the acrylamide homopolymer bioimprinted hydrogels discussed in the previous chapter.

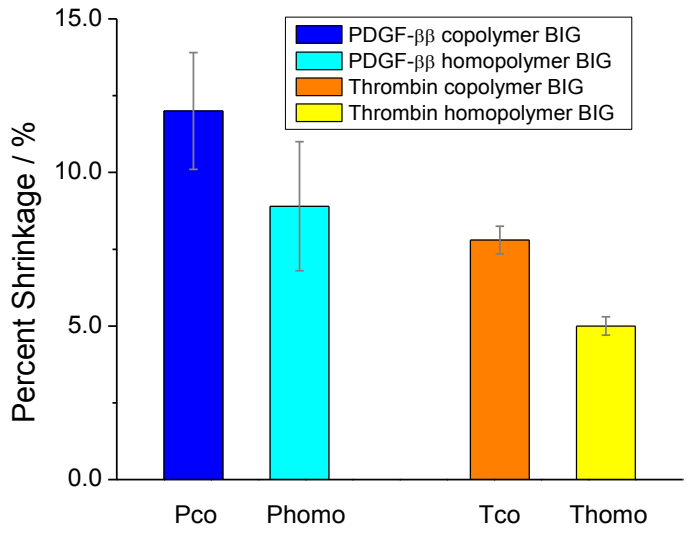

Figure 3.1 Comparison of the volume response between protein bio-imprinted copolymer hydrogels and homopolymer hydrogels.

The results are shown in Figure 3.1, Pco stands for the PDGF-ββ imprinted copolymer BIGs, while Phomo stand for the PDGF-ββ imprinted homopolymer BIGs, Tco stands for the Thrombin imprinted copolymer BIGs, and Thomo stands for the Thrombin imprinted homopolymer BIGs. Compared to the acrylamide hydrogels, the volume response of Thrombin bio-imprinted copolymer BIGs went up from 4-6% for the acrylamide homopolymer, to 6-7% for the acrylamide/NIPAM copolymer. For the PDGF- ββ imprinted hydrogels, the change was from 8-9% for the acrylamide homopolymer to 10-15% for the acrylamide/NIPAM copolymer. These results indicate that the introduction of the NIPAM is successful for improving the shrink responsive behavior of the hydrogel sensors.

3.3.2 Changing monomer ratio for material optimization

To further study the influence of the monomer ratio on the volume changing properties of the BIG for sensor applications, a series of copolymer PDGF-ββ bio-imprinted hydrogels (BIGs) were prepared with different monomer ratios (NIPAM content = 12.5%, 25.0%, 37.5%, 50.0% and 75.0%). After polymerization, all hydrogels were treated with 10% SDS solution which was replaced every 5-6 hours until the hydrogel ceased to show volume changes. The result of this study is shown in Figure 3.2 below.

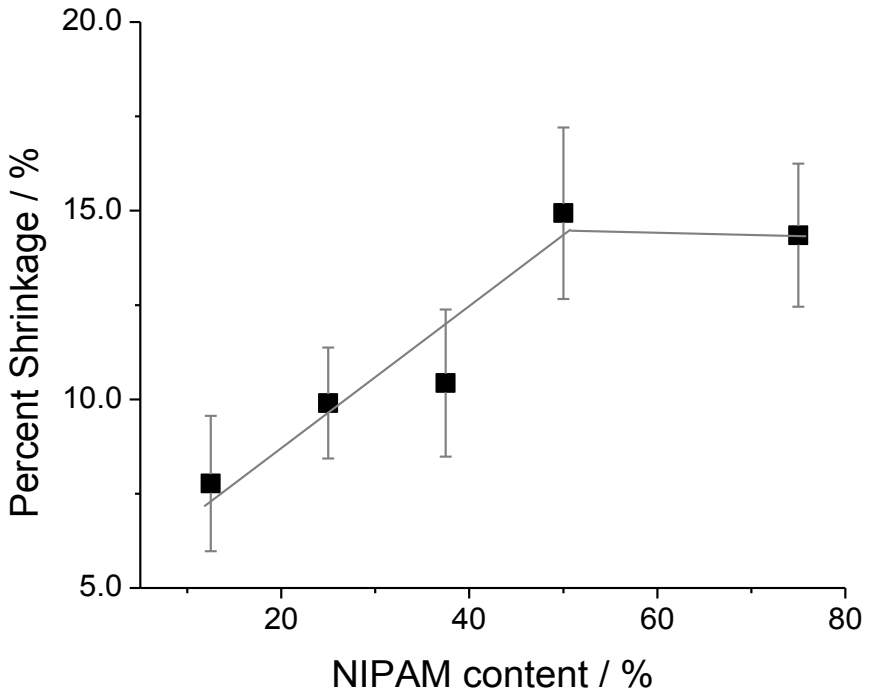

Figure 3.2 Influence of the percentage of NIPAM to volume response of the bio-imprinted copolymer BIGs.

From the graph of Figure 3.2 it can be seen that the volume response of copolymer BIGs increases as the NIPAM concentration increases until a molar percentage of 50% was reached and volume change remained virtually constant even as the NIPAM concentration was further

increased, even when the ratio of NIPAM went up to 75%. The 100% NIPAM hydrogels formed a white precipitate, however, after polymerization instead of transparent hydrogel. The white condensed hydrogels that were obtained showed no volume response was observed. From the results of this study, the 50 mol% NIPAM monomers were chosen as the optimum ratio for BIGs.

3.3.3 BIGs with other second monomers

In addition to NIPAM, two other commonly used water soluble monomers were investigated as co-monomers with acrylamide----acrylic acid (AA) and methyl acrylic acid (MAA). These monomers were copolymerized with either acrylamide or NIPAM at different ratios, in an effort to explore materials with increased volume changing properties. This time all hydrogels were imprinted with thrombin as the template due to its relatively low cost. After preparation, all the hydrogels were treated as described before. The formula combinations that were investigated are listed in table 3.2 below.

It was first observed that all of the hydrogels expanded much larger than our original hydrogels after the removal of the protein template. This might have been caused by the increase of hydrophilicity of the polymer by introducing a much hydrophilic second monomer. However, none of the BIGs showed volume response to the protein solution in rebinding experiment which may due to the distance between aptamers extending too far away. The large distance may have prevented the formation of the subsequent crosslinks between proteins and aptamers.

Table 3.2 Formulas investigated for hydrogel copolymers

Entry	Monomers & ratio		Crosslinker	Aptamer	Template
1a	AM&AA	2:1	MBAM	F1&F2	Thrombin
1b	AM&AA	1:1	MBAM	F1&F2	Thrombin
1c	AM&AA	1:2	MBAM	F1&F2	Thrombin
2a	AM&MAA	2:1	MBAM	F1&F2	Thrombin
2b	AM&MAA	1:1	MBAM	F1&F2	Thrombin
2c	AM&MAA	1:2	MBAM	F1&F2	Thrombin
3a	NIPAM&AA	2:1	MBAM	F1&F2	Thrombin
3b	NIPAM&AA	1:1	MBAM	F1&F2	Thrombin
3c	NIPAM&AA	1:2	MBAM	F1&F2	Thrombin
4	AM&NIPAM&AA	1:1:1	MBAM	F1&F2	Thrombin
5	AM&NIPAM&MAA	1:1:1	MBAM	F1&F2	Thrombin

3.3.4 Repeatability and selectivity

Figure 3.3 below shows the volume response of both PDGF-ββ and Thrombin BIGs (50/50: AM/NIPAM) over 3 cycles of washing and rebinding. From this graph we can see that the volume shrinking response of the hydrogel to the presence of the protein remains stable over several cycles of use. For PDGF-ββ imprinted hydrogels, the volume changes are usually around 16%, and for Thrombin imprinted hydrogels the volume changes are approximately 10%. The result indicates that the volume response of these copolymer hydrogel sensors is reversible and

repeatable over at least 3 cycles. Favorably, the extent of the volume change is also relative stable when compare these cycles.

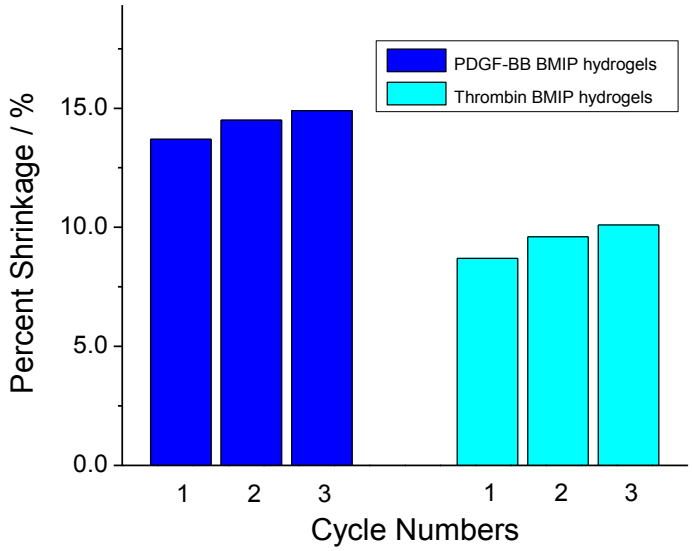

Figure 3.3 The repeatability of the bio-imprinted copolymer hydrogels.

In addition to stability to repeatability, the selectivity of the sensor is also a decisive index that can determine if a sensor is good or not. To test the selectivity of our bio-imprinted hydrogel sensor, we prepared several PDGF-ββ bio-imprinted hydrogels and treated them with different solutions. As shown in Figure 3.4 both PDGF-ββ BIGs and Thrombin BIGs exhibit excellent selectivity against other non-template proteins. In Figure 3.4a, P0 is the volume shrinking response of the PDGF-ββ imprinted hydrogel treated with PDGF-ββ solution (column 1) and P1, P2, P3 are the volume response of same kind of hydrogels to PDGF-αβ, Thrombin and BSA, respectively.

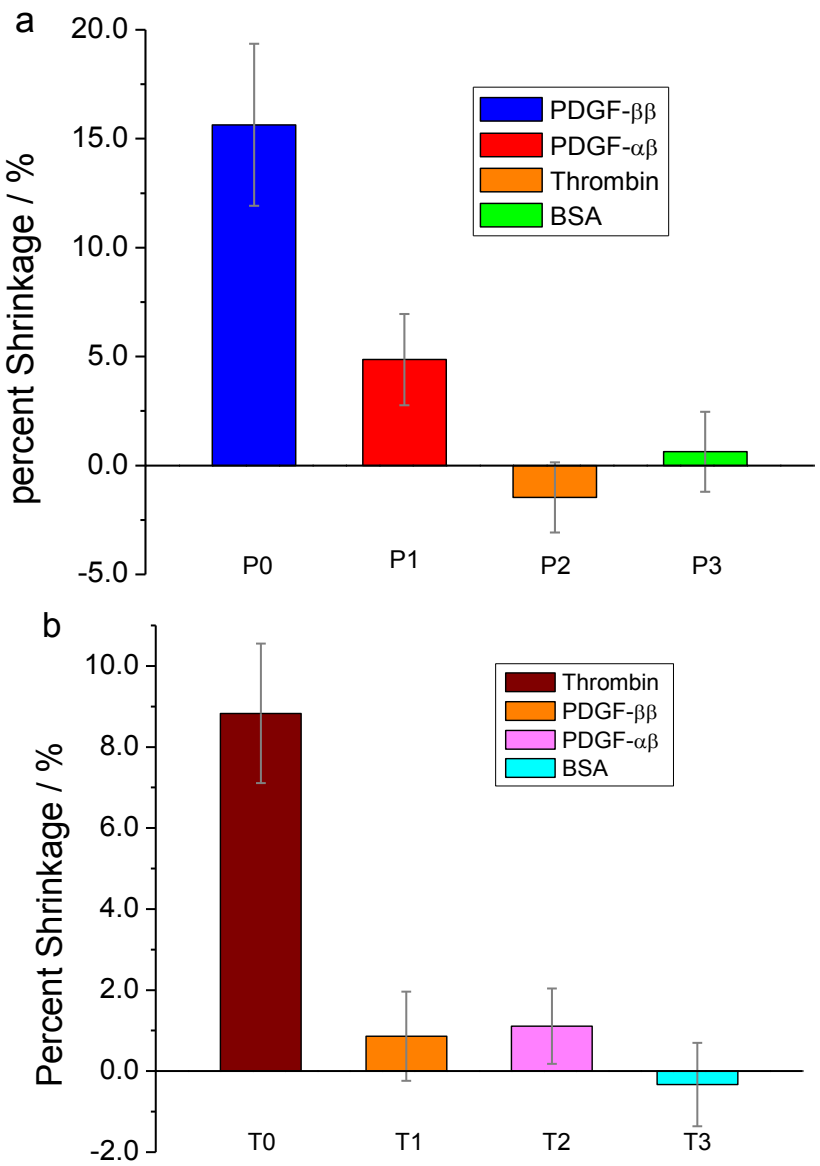

Figure 3.4 Selectivity of the a) PDGF-ββ bio-imprinted hydrogels and b) Thrombin bio-imprinted hydrogels.

Thus, the figure shows the highest volume response was achieved by the hydrogel treated with a solution of the intended template protein giving a high response of approximately 15%. In contrast, proteins other than the template do not lead to a volume response of the magnitude caused by the template protein. This is also the case for the Thrombin imprinted hydrogels,

shown in Figure 3.4 b, where the highest volume response also corresponds to treatment with template solution. The highest volume response of the control gels that measured binding of proteins other than the template was 1.1%, which is also much lower than the 9% volume change to Thrombin solution (T0). Therefore, from the results above, we can claim that the selectivity of the bio-imprinted hydrogel sensors highly specific to the target protein.

3.3.5 Hydrogel response is clearly due to the bioimprinting technique

It is important to verify that the bioimprinting process is responsible for generating the imprinting effect, which is correlated to the macroscopic volume response and great selectivity of the hydrogel sensors. To achieve this goal, several non-imprinted control samples were prepared. These control hydrogels were subjected to the regular regeneration-rebinding procedure and their volume responses were compared with the response of the imprinted hydrogels.

The results are shown in Figure 3.5, where MIP refers to the bio-imprinted hydrogel (BIG), PC1 refers to the non-imprinted hydrogels prepared in the absence of aptamer, PC2 for absence of protein, and PC3 refers to absence both of aptamer and protein respectively. It is not surprising to see that the imprinted hydrogels produce the largest volume response while all the other non-imprinted hydrogels only exhibit a small volume change. Thus it can be concluded that the imprinting effect decisively plays a crucial role in creating the molecular triggered response of these hydrogel sensors.

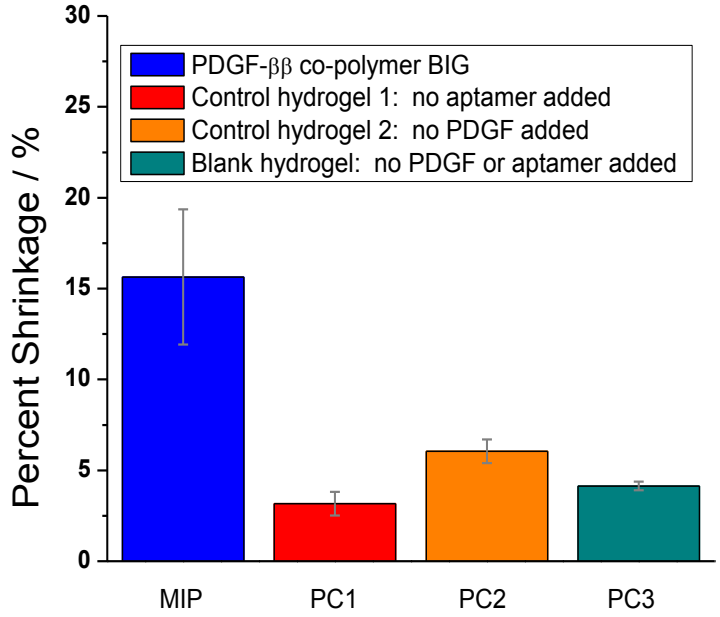

Figure 3.5 Selectivity of the bio-imprinted hydrogels.

3.3.6 Isotherm study

To determine the detection limit of the copolymer BIGs, a concentration versus response isotherm study was performed. A series of PDGF-ββ bio-imprinted hydrogels were prepared and treated with buffered PDGF-ββ solutions with different protein concentrations (from 1×10^{-18}–1×10^{-6}M), prepared by diluting protein stock solutions of1×10^{-6}M concentration.

In Figure 3.6, which shows the influence of the protein concentration on the volume response, the results reveal that the hydrogels have a very low response until the concentration becomes higher than 1×10^{-12}M. It is important to note that a naked-eye detectable volume change was also generated at this concentration. As the template protein concentration was increased further, the volume change continued to increase until a volume change of approximately 12% was achieved at the concentration of 1×10^{-8}M. This result indicated that even at a concentration as low as 1×10^{-12}M, naked-eye detection is still feasible by using this new

copolymer methodology and the detection limit matches that seen previously for the homopolymer hydrogel sensors.

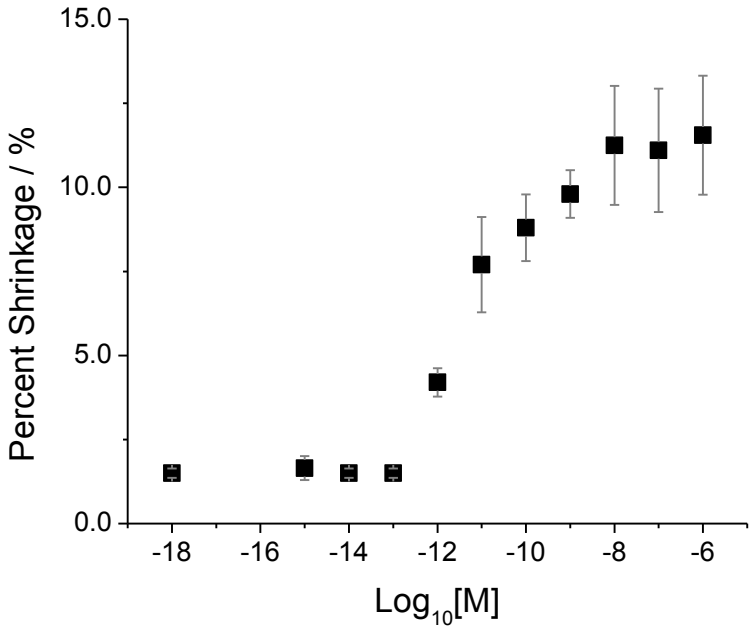

Figure 3.6 Isotherm of volume response versus concentration of PDGF-ββ for the copolymer PDGF-ββ imprinted hydrogels.

3.3.7 Effect of dehydration on bioimprinted copolymer hydrogels

As pointed out in the previous chapter, it is much easier for the hydrogels to be stored and transported in their dry state. This is also true of the new copolymer hydrogel sensors; it is important to determine if the bioimprinted copolymers can maintain their volume response to a certain target even after dehydration. To explore this possibility, Thrombin and PDGF-ββ imprinted hydrogels were first treated with three regeneration-rebinding solution (same as above) cycles, followed by dehydration by exposure to open air for 2-3 days. After the hydrogels were dried to a constant weight, clean PBS buffer was injected into the capillaries to rehydrate the

hydrogels. Once the hydrogels became fully hydrated (i.e. constant length was achieved), three regular cycles were measured again, and the results shown in Figure 3.7 below.

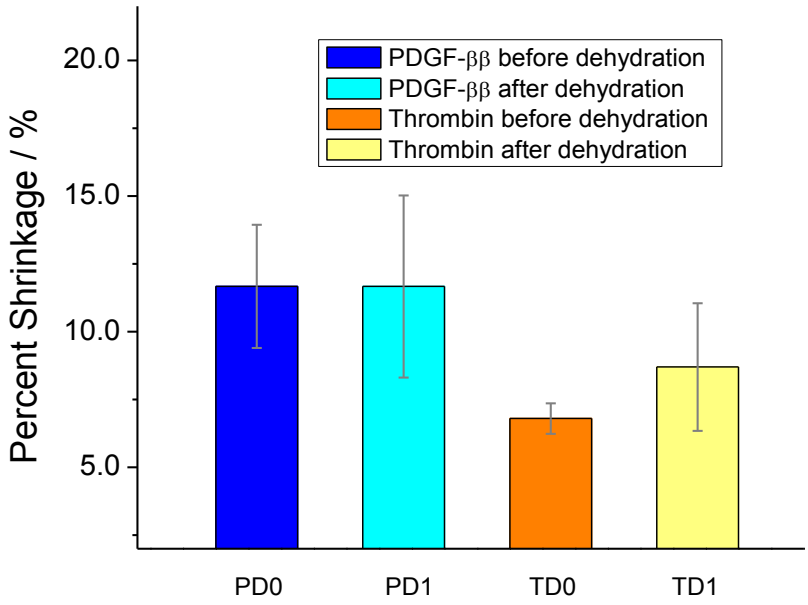

Figure 3.7 Comparison of volume change for dehydrated copolymer PDGF-ββ imprinted hydrogels compared with the initial undried hydrogels.

In this figure, PD0 stands for the volume response of PDGF-ββ imprinted BIGs before dehydration, and PD1 stands for the volume response of the same hydrogel after dehydration and rehydration processes. Similarly, TD0 stands for the volume response of the Thrombin imprinted hydrogel before dehydration and TD1 stand for the volume response after dehydration and rehydration process. From the results we can see that both PDGF-ββ and Thrombin imprinted hydrogels maintained their expected responses well after dehydration and rehydration. In fact, there may have been improvement for the Thrombin hydrogel, although not conclusively with the error range detected. None-the-less, these results indicate that the dehydration process does little harm to the original volume changing properties of the hydrogel sensors.

3.3.8 Volume response in bio-mimetic fluid.

In addition to binding studies in buffer, tests were also performed in artificial tears to determine whether the new copolymer PDGF-ββ imprinted BIG sensors can still be used to detect template bio-markers by visual volume change in bio-mimetic fluids. The same copolymer hydrogels previously run in simple buffer were also immersed in protein solutions made in artificial tears to determine efficiency in this medium. The results revealed a volume change of 14.2±1.5% in the artificial tears solution compared to approximately 12-15% usually obtained from the tests performed in PBS buffer. Thus the results are essentially the same; and this result again verifies that copolymer hydrogel sensors are promising for applications in real biological systems.

3.3.9 Possible mechanism for the enhanced volume response.

In the previous chapter, the possible mechanism for the macroscopic volume change triggered by the presence of a considerably small amount of protein was discussed, and it was pointed out that excluded volume effects may be responsible for this phenomenon. Since the new copolymer imprinted hydrogel sensors were shown to be similar to the homopolymer hydrogels in last chapter, excluded volume remains the most likely reason for the macroscopic change as a whole. However, the enhanced performance must be caused by the addition of the second monomer----NIPAM. It is known that NIPAM is a water soluble monomer; and PolyMIPAM is famous for its ability to collapse into a condensed state when the aqueous solvated hydrogel temperature is in excess of its Lower Critical Solution Temperature (LCST). [47] However, in this study experiments were performed at room temperature, which was far below the LCST. Thus, the thermal response need not be considered as a possible explanation for the enhanced volume

change. Another factor to consider is hydrophobicity; aggregation caused by hydrophobic effects in protein folding and polymer self-assembly is well known and still an active area of research. It has been shown that hydrophobic components in polymer structure influence the structure, and thus the properties, of the polymeric material. [46]

In our case, which is demonstrated by Figure 3.8, NIPAM is more hydrophobic than acrylamide, and it is hypothesized that NIPAM in the polymer chain will promote hydrophobic aggregation in aqueous buffer. It is possible under these conditions to form some relatively condensed hydrophobic domains. These domains can play a role as particles that form physical crosslinks which can pull adjacent area in the hydrogels closer. The amplification of volume change seen in the bioimprinted hydrogels is hypothesized to promote further aggregation when template binding takes place.

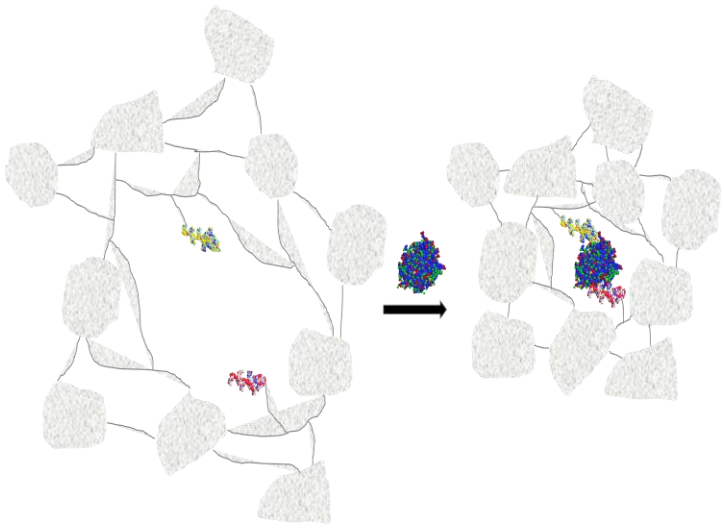

Figure 3.8 Cartoon of hydrogel excluded volume scenario where protein binding to both aptamers pulls together phase-separated aggregates of hydrogel which are multiply crosslinked to other phase separated aggregates.

3.4. Summary

In conclusion, Thrombin and PDGF-ββ copolymer BIG sensors were successfully prepared with enhanced volume response affected by addition of a second monomer----NIPAM. The enhanced macroscopic volume response to the protein molecular trigger is visually easier and improves detection by naked eye. The experiments provided in this chapter have proven that this kind of new bio-imprinted copolymer sensor has good selectivity and stability to multiple uses. Furthermore, these hydrogels can maintain their specific responsive behavior after dehydration or in bio-mimetic fluid. A possible mechanism was put forward to explain the enhanced performance based on hydrophobic aggregation effects.

CHAPTER 4. BIOIMPRINTED COPOLYMER CAPILLARY BIGS FOR DETECTION OF APPLE STEM PITTING VIRUS

4.1 Introduction

Moving beyond proteins, viruses are another attractive biological target that are closely related to animal and plant life. Most of the time, a virus becomes well known when it becomes an formidable source of infective diseases. The appearance of a virus is then associated with existence of corresponding diseases. Although the presence of a virus is not desirable, in the fields like disease diagnosis a virus can be considered to be an important bio-marker for certain diseases. Thus, the direct detection of viruses is an important and interesting topic to research.

Generally, viruses are small intracellular pathogenic particles consisting of DNA/ RNA coated by proteins that protect these genes, and an envelope of lipids surrounding the protein coat. A virus can spread (infect) living organisms in various ways such as the transmission of bio-fluids, faecal–oral contact, etc. Although viruses can be quite useful and beneficial in many aspects of our life, they are usually more well-known as the cause of many diseases. For human beings, influenza is the most widely spread viral disease. Other diseases seriously threaten the world; an example is HIV which is also caused by its corresponding virus. In fact, harmful viruses are not only affecting our lives directly, but also undermining the material foundation of the modern society. For example, Bovine spongiform encephalopathy (BSE) has caused the loss of billions of dollars from the production of cattle in global agriculture. It has also greatly decreased the amount of food that can be used to feed starving populations. Another example exists in the production of the most important commercial food plant ---- wheat. This class of

diseases is generally called Wheat Viral Diseases (including Wheat yellow dwarf, Wheat rosette stunt, Wheat soil-borne mosaic, etc.) which can seriously undermine wheat production. [48]

Since the discovery of viruses in the late 19th century, researchers have become aware of the relationship between these little infective living particles and a number of diseases. As a result, detection of viruses has been a hot topic for biomedical research for quite a long time. In the past several decades, thanks to dramatic improvements in biology, chemistry, instrumental technology and all other related areas; the detection of viruses has experienced a rapid growth and a number of methods have been developed.[49]

In relation to the work presented here, several reports appeared in 2006 with different approaches to fabricating virus imprinted hydrogels. In one, cylindrical shaped tobacco mosaic virus (TMV) was preferably bound in batch experiments versus icosahedral shaped tobacco necrosis virus (TNV). Another report described bioimprinted Semliki Forest Virus (SFV) hydrogels, and used capillary electrophoresis to demonstrate higher binding of SFV to the gel versus a SFV-mutant and BK-4 virus-like particle. The third report used an "epitope" approach where thin films were imprinted with a 15 amino-acid peptide sequence found in the dengue virus coat-protein, and incorporated into a quartz crystal microbalance which successfully detected the virus in actual blood samples. Last, there has been one recent report of a non-imprinted responsive hydrogel for virus detection using a displacement assay; however, signal detection requires the use of expensive and sensitive quartz crystal microbalance (QCM) apparatus.

For research on general approaches to virus detection, it is not necessary to use viruses toxic to humans; therefore, plant viruses are safe targets for study. Specifically, Apple Stem

Pitting Virus (ASPV) is a filamentous virus that is approximately 15nm wide and 800 nm long which has many copies of the MT32 protein forming the coating. It usually causes xylem pitting, epinasty, partial yellowing of leaf veins and red mottling on infection.[50] The worldwide spread of the virus has led to a loss of 30% of whole apple and pear production globally. The research on detection of ASPV is currently an important topic in agriculture; however, it still relies heavily on methods like PCR, ELISA, SPR and other modern instrumental methodologies that are inaccessible to farmers and crop owners.

The following discussion focuses on development of an ASPV bio-imprinted hydrogel sensor in a capillary for naked-eye detection of ASPV in impure extract (directly from ground up leaves of infected apple trees). The use of impure leaf extract has the potential of our method to be used for easy and quick field diagnosis. These virus-responsive super-aptamer hydrogels are envisioned to provide not only a useful assay for low-cost, easy to use, and portable detection of ASPV; but as a proof-of-principle that can be applied to the detection of any virus for which a polymerizable bioreceptor can be made.

4.2 General formula and preparation of ASPV capillary BIGs

4.2.1 Materials

The ASPV leaf extract positive sample, corresponding negative sample, ASCLV infected extract sample and APMV infected extract sample were purchased from Bioreba AG Inc. and diluted with 2.5mL PBS buffer following the direction provided by the company. MT32 aptamer was purchased from IDGT Inc and dissolved in 1mL of pBS buffer. All the other chemicals were purchased from Sigma-Aldrich Co. LLC. or Fisher Scientific Inc.

4.2.2 Formulation of virus-imprinted BIGs

The formula used to prepare an ASPV imprinted capillary hydrogel generally follows the recipe that used for preparation of the protein copolymer imprinted hydrogels, except for the ratio between the number of virus particles concentration and the virus concentration. A detailed discussion of this ratio will be presented later in this chapter (vide infra). Table 4.1 lists the chemicals used in preparation of the ASPV bioimprinted hydrogels.

Table 4.1 Formula of ASPV imprinted capillary hydrogels

	MW (Da)	**Molarity**	**Ratio**
ASPV*	20000000 (approx.)	2.5×10^{-9} mol/L	1
Aptamer MT32	13210.7	7.6×10^{-5} mol/L	3.0×10^{4}
NIPAM	113	0.4mol/L	1.6×10^{9}
AAm	71	0.4 mol/L	1.6×10^{9}
MBAM	154.2	4.0×10^{-3}mol/L	1.6×10^{7}

4.2.3 Synthesis of the ASPV capillary BIGs

4.2.3.1 General procedures

The general procedure used to prepare the virus-imprinted capillary hydrogel is illustrated in scheme 4.1 below. First, the virus-aptamer complex was prepared by mixing virus extract suspended in 2mM PBS buffer and aptamer solution in the same PBS buffer at corresponding concentrations (Table 4.1) for 2 hours. Then the formed virus-aptamer complex was put into a plastic Eppendorf vial together with monomers, crosslinker and oxidant reagent (TEMED) of redox initiator. Afterward, the total volume was adjusted to 100mL.

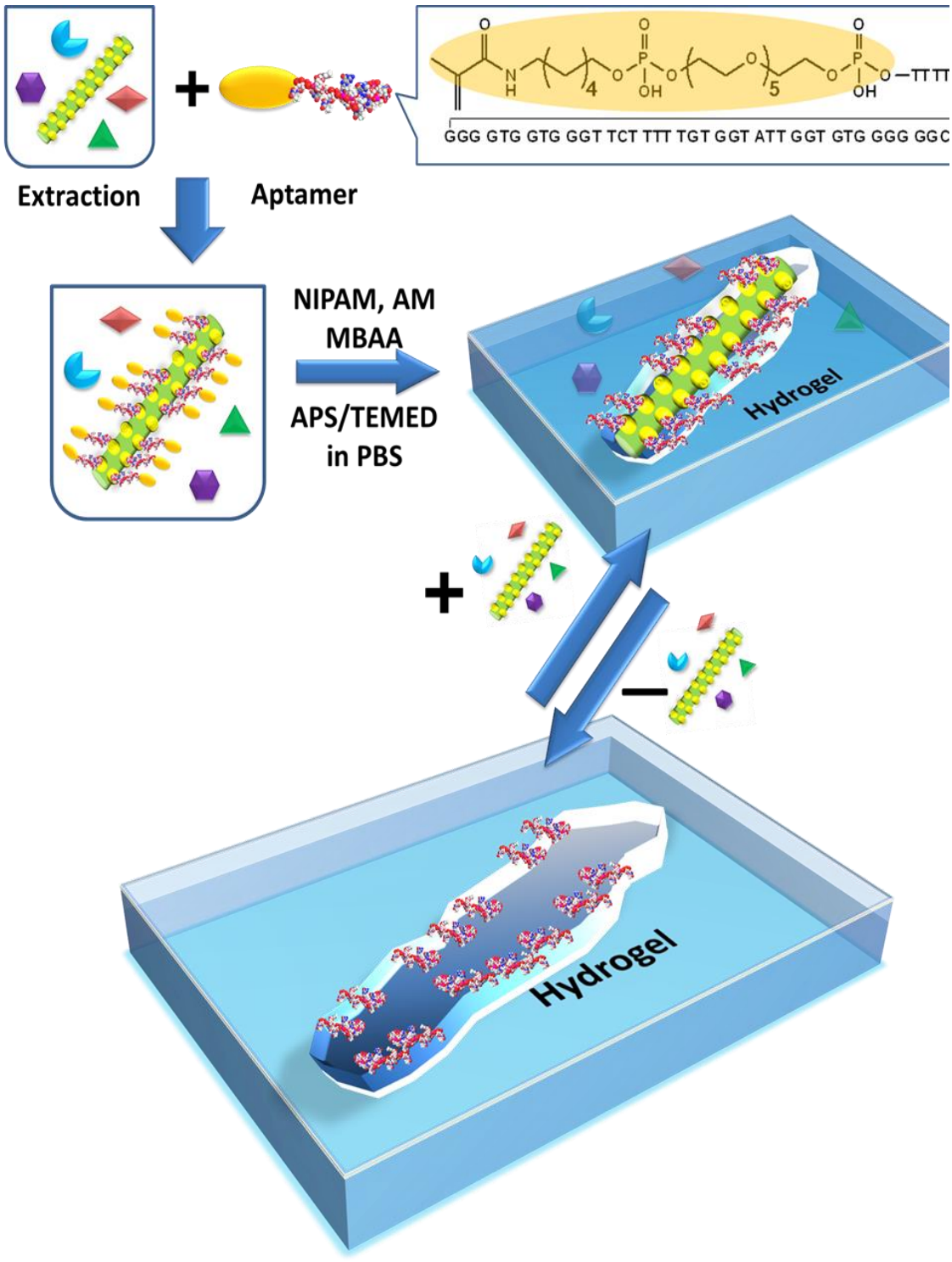

Scheme 4.1 The outline of making of the virus imprinted hydrogel.

Next, the mixture was purged with nitrogen for 5-10 minutes to expel the oxygen dissolved in the mixture. Afterward, reductant was added and the mixture was immediately vortexed for about 1-2 seconds and quickly transferred into a capillary pre-treated by washing with acetone and deionized water for 3 times and dried. The capillary containing polymerizing mixture was immediately sealed and allowed to sit still overnight to allow completion of polymerization.

4.2.3.2 Polymerization of MT32 aptamer

It is not guaranteed that an aptamer-based monomer will actually polymerize into the rest of the hydrogel. Thus, to verify the MT32 aptamer was covalently immobilized in the hydrogels, a big batch of hydrogel with a large quantity of all reagents (20x the original formulation) but no templates was prepared using the same recipe as the bio-imprinted hydrogels. The large batch allowed detection of small amounts of aptamer that may remain unpolymerized. After polymerization, the hydrogel was washed by 2mL of 2mM PBS buffer 5 times with a time interval of 2-3 hours between each. The supernatants from the washings were combined and dialyzed against plain 2mM PBS in dialysis tubing with a 3500 MW cutoff for 4 days, during which the 2mM PBS was also changed every few hours. After dialysis, the volume of the solution was adjusted to 10mL by adding 2mM PBS and the absorbance measured at λ = 260 by UV-Vis. The absorbance curve was shown by the dark spectral line in Figure 4.1.

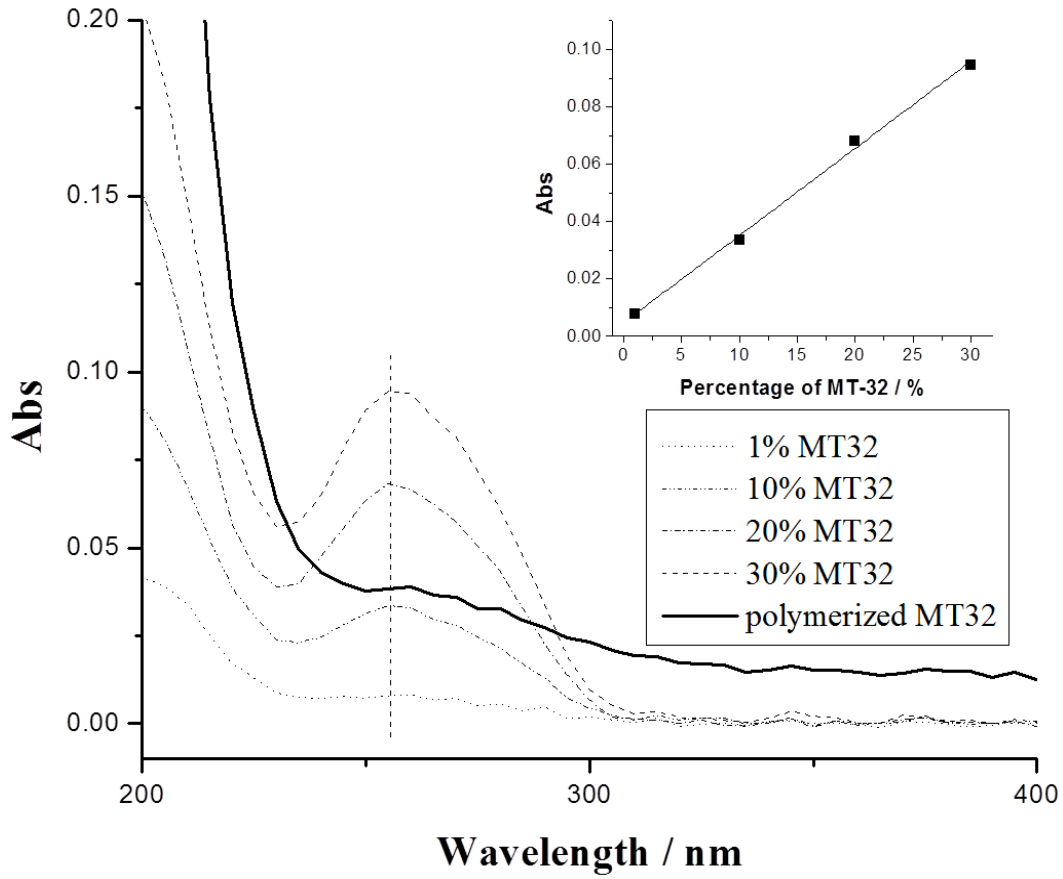

Figure 4.1 UV study of polymerization of MT-32 aptamer in bio-imprinted hydrogel.

The calibration curve was made by measuring aptamer solutions with 1%, 10%, 20% and 30% of the aptamer concentration used in preparation of regular bio-imprinting hydrogels (dash curve in spectra in Figure 4.1), and the absorbances found at $\lambda = 260$ were used to form the calibration plot. From the results presented in Figure 4.1, it can be concluded that the concentration of aptamer from the hydrogel washout was approximately 12% which indicates that about 88% of the aptamers were successfully polymerized into the hydrogel.

4.2.4 Regeneration, rebinding of the virus template and evaluation of the volume change

4.2.4.1 Regeneration of the hydrogel

Removal of the virus was carried out by incubating the capillary in a culture dish containing regeneration solution composed of 12mM NaOH and 1.2% ethanol in deionized water.[51] The regeneration solution was changed every 3-6 hours until the hydrogel volume-changes reach equilibrium. Then the hydrogel was immersed in plain 2mM PBS buffer which was also constantly changed until the hydrogels equilibrated constant length.

4.2.4.2 Rebinding of the virus template

After removal of the template, the hydrogel was incubated in ASPV extract suspension to rebind template virus. The ASPV extract suspension was changed every few hours until equilibrium in hydrogel length was achieved (in about a day). Subsequently, the hydrogel was washed by immersion in 2mM PBS buffer until constant length so that measurement are taken at thermodynamic equilibrium.

4.2.4.3 Evaluation of the volume change.

The method used to evaluate the extent of volume change in the ASPV imprinted capillary BIGs used the equations previously employed to measure the previously discussed protein imprinted capillary hydrogels.

4.2.5. Optimization by changing aptamer concentration

To optimize the volume response of the virus bio-imprinted hydrogels and explore the influence of the aptamer concentration to its responsive behavior, a series of imprinted capillary hydrogels were prepared with different aptamer concentrations. The concentrations used were 0.5×, 1.0×, 2.0×, 4.0× and 8.0× times of the original concentration shown in Table 4.1. After polymerization, all hydrogels were treated with 3 cycles of regeneration-rebinding procedure and the volume change recorded using the same methods described for the protein imprinted hydrogels. The results are graphed in the isotherm presented in Figure 4.2 below.

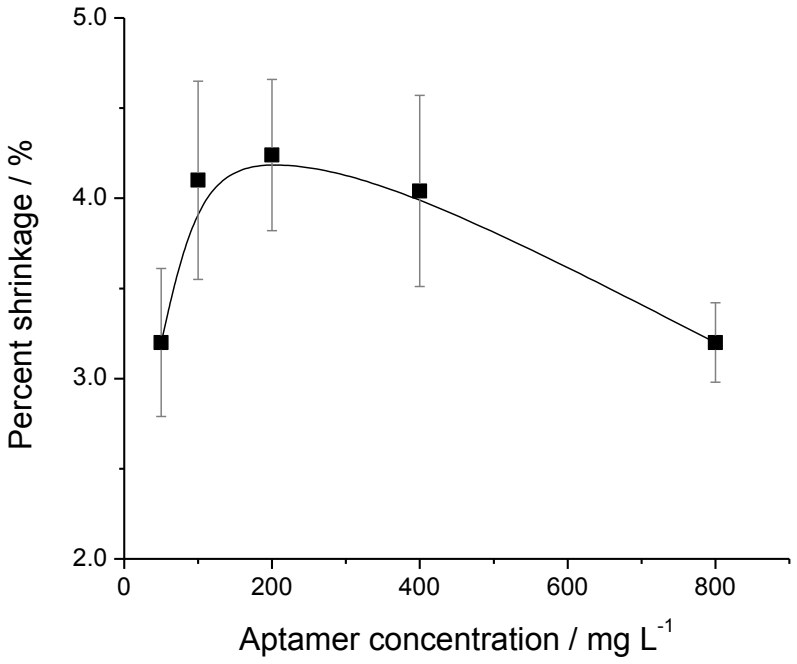

Figure 4.2 Study of the influence of the aptamer concentration to volume response of the ASPV bio-imprinted hydrogels.

In this figure, the highest volume change appears at the original concentration we used in the initial preparation and similar responses are also observed when double or 2-fold of the regular concentration was used. However, the volume response was smaller (about 3.2%) when only half of the aptamer concentration was applied to the preparation. For concentrations up to more than 4 fold of the regular concentration the volume response seems to decrease a little to about 3.3%. As a result, the original concentration appears generate the highest volume effect in our experimental conditions, with the least amount of aptamer, that can maintain the balance between material's property and cost. Meanwhile, a volume change of approximately 4.0% can still be seen by the naked-eye and quantitive measurements can still be performed by simply using a magnifying glass and a ruler.

4.3. Results and discussion

4.3.1 Reversible volume change

In addition to the advantages of naked-eye detection, the virus imprinted hydrogels were also able to show volume response to the target template in a reversible and stable manner. Figure 4.3a photographically depicts the bioimprinted hydrogel during measurement of the length change of the hydrogel in the capillary after both the regeneration and rebinding steps using a ruler with a minimum scale of 1mm. The upper photograph is the hydrogel after removal of the virus template, while the lower one was taken after the hydrogel was exposed to the virus template. The length of the hydrogel changed from 1.96cm to 1.88cm representing a volume change of 4.1%. From these pictures it is clear that the volume change of the hydrogel can be caught by the naked-eye.

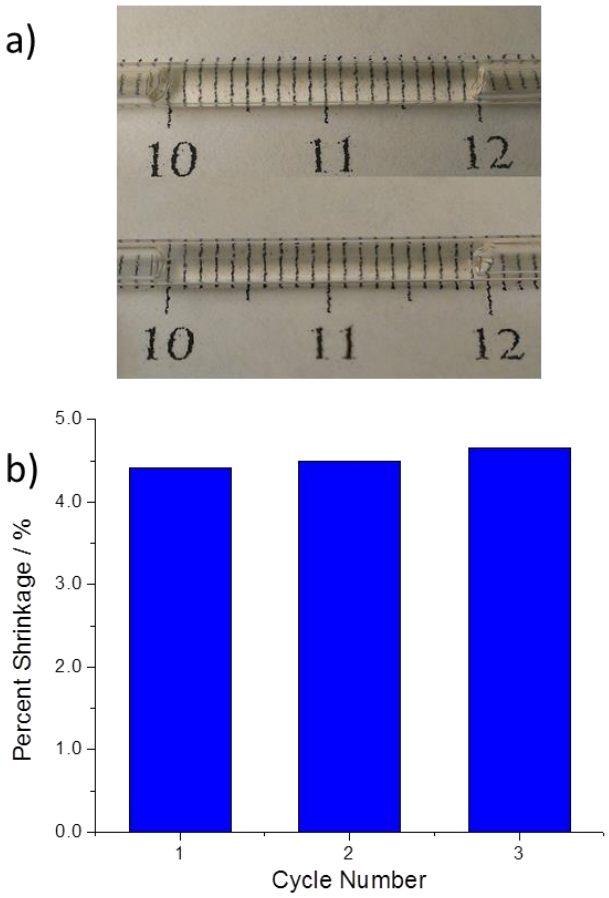

Figure 4.3 a) volume change of the ASPV imprinted BIGs measured by a ruler; b) Reversible volume change of the virus bio-imprinted hydrogels upon the presence of the virus extract in 3 cycles.

Figure 4.3b is the volume response of a virus imprinted hydrogel over 3 regeneration-rebinding cycles. From the graph it is apparent that the volume changes of the hydrogel in each cycle were very close to each other; the average volume change was 4.52 ±0.12%. This phenomenon indicates that the behavior of the hydrogel sensor is stable over multiple runs and thus the data obtained from it is reliable.

4.3.2 Selectivity

Selectivity is a very important index in the determination of whether a sensor is good or not. Thus, verification of the hydrogels' selectivity was investigated and the results obtained are graphed in Figure 4.4 below. In this figure, the blue column on the left gives the response for the ASPV bio-imprinted hydrogel treated with ASPV extract suspension. The volume response was 4.32±0.57% which was clearly the highest on the chart. The second column in light blue is the ASPV bio-imprinted hydrogel treated with negative extract, made from healthy leaves, which didn't contain any virus particles. The green and yellow columns on the right side of the graph stand for the same kind of ASPV bio-imprinted hydrogels incubated with two other kinds of apple virus extracts: apple mosaic virus (APMV) and apple chlorotic leaf spot virus (ACLSV) respectively.

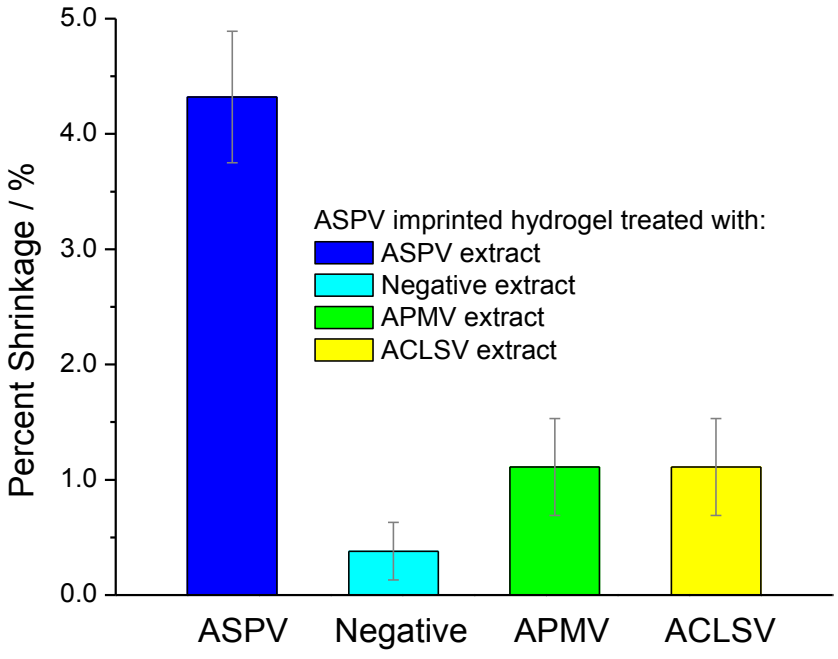

Figure 4.4 Study of the selectivity of the ASPV bio-imprinted hydrogels.

Apparently, only the hydrogel treated with ASPV virus can lead to a volume change detectable by the naked-eye, while all other extract samples only lead to a negligible amount of volume response. This result indicates that the virus-imprinted hydrogel can maintain its high selectivity in the presence of other bio-mass components such as different viruses and proteins. This is a clear evidence that our method is capable to produce bio-sensors with good selectivity.

4.3.3 Important role of the imprinting effect toward hydrogel response

Several non-imprinted control hydrogels were prepared for comparision to the results from the virus bio-imprinted hydrogels, in order to probe the extent of the influence of the imprinting effect on the behavior of the hydrogels. The results in Figure 4.5 show the effects of ASPV exposure to imprinted and non-imprinted hydrogels. The blue column on the left shows the significant volume response by the ASPV bio-imprinted hydrogel gel. The other 3 columns represent the results for the non-imprinted hydrogels prepared without aptamer and template virus, without aptamer and without template virus respectively.

In this study, the highest volume response was expectedly found for the ASPV bio-imprinted hydrogels (blue column) with a volume change of about 4% with is naked-eye detectable. All other non-imprinted hydrogels were not able to show naked-eye discernable volume change responses, which demonstrated that the bio-imprinting technique is a crucial factor in the formation of the hydrogel volume response.

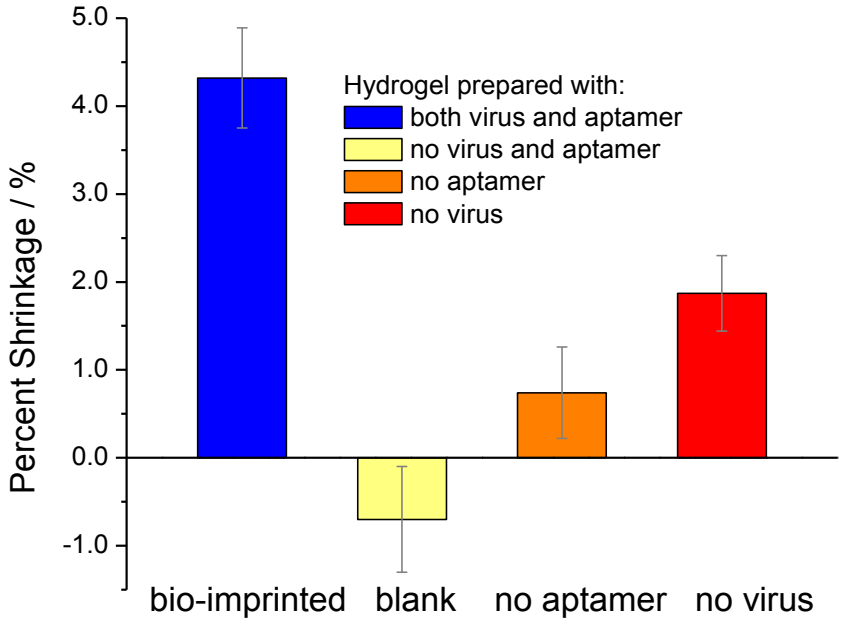

Figure 4.5 Comparison of the volume change of bio-imprinted hydrogels and non-imprinted control hydrogels.

4.3.4 Isotherm research

To investigate the detection limit and dynamic range of our virus bio-imprinted hydrogels, an isotherm was constructed. In this study, virus imprinted hydrogels were treated with virus extracts at different virus concentrations, prepared by diluting a virus extract stock solution containing 10mg virus particles per liter[52]. The measurements were carried out from the lowest concentration to the higher ones (from 1×10^{-6} to 10 mg/L) and for each concentration, the hydrogel was measured during 3 full cycles of regeneration and rebinding.

The results of the isotherm study are shown Figure 4.6 which correlates the influence of the virus concentration in the extract to the volume response of the bio-imprinted hydrogels. When the virus concentration in diluted extract was as low as 1×10^{-6} - 1×10^{-4} mg/L there was

little volume response was observed. However when the concentration increased to 1×10^{-3} mg/L the volume change jumped from about 1% to 4%, then remained at the same level even when treated with extract containing much higher virus concentration. Thus we can conclude that the lowest concentration that can generate naked-eye detectable volume response (detection limit) is 1×10^{-3} mg/L (1.0 μg/L). This detection limit is generally at the same level as the currently used routine methods such as PCR, ELISA, etc., which can reach a detection limit around 1.0 μg/L.

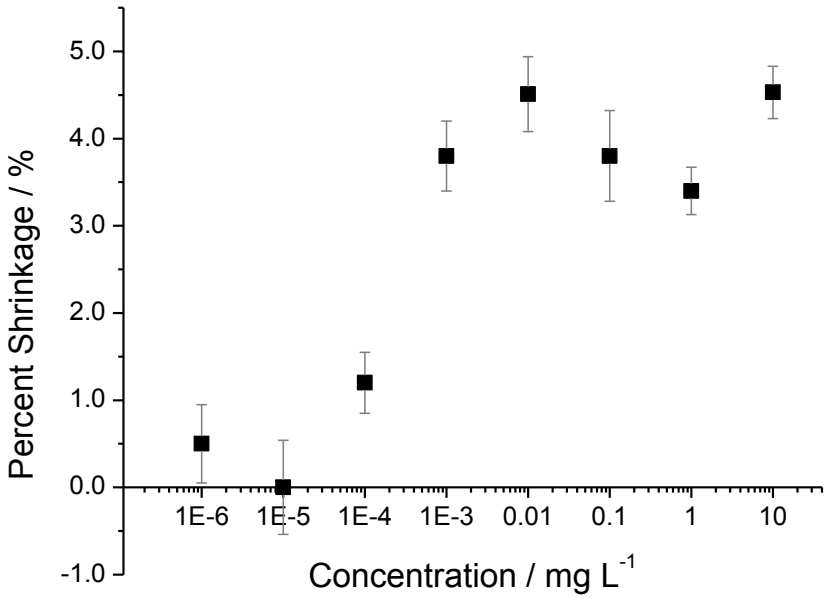

Figure 4.6 Isotherm study of the virus bio-imprinted hydrogels.

The previous chapter pointed out the phenomenon that the bio-imprinted hydrogels can show almost equal amount of the volume response to protein concentrations that were much lower than the one used in the making of the hydrogel sensor. In the case of Thrombin and PDGF-ββ, the ratio difference between the detection limit and imprinting concentration can be as much as 1×10^{6} M. Studies of this phenomenon led to the conclusion that the amplification is caused by excluded volume effects. In the study of virus bio-imprinted hydrogels, a similar effect

has also been noticed. The ASPV imprinted hydrogels show almost the same amount of volume change when being treated with concentrations around 1.0mg/L of virus which was used preparation of the hydrogel, and as low as 1×10^{-4} mg/L. Although the amplification is as high as observed in protein imprinted hydrogels, it is still very likely that it is the excluded volume effect again that plays an important role in the behavior of these materials. The difference in the extent of the amplification could be caused by the much larger size of the virus particle versus the protein. Another factor may be the lower template concentration of virus versus protein; however further research is still needed to provide a deeper understanding of this system.

4.3.5 Dehydration

Following the same reasoning as presented earlier for the protein bio-imprinted hydrogels, dehydration and rehydration studies were also investigated on the virus imprinted hydrogel properties. The dehydration-rehydration procedure was carried out as before on protein bio-imprinted hydrogels which has been described in detail in the previous chapters.

A pictorial log of the process is shown in Figure 4.7a showing the virus bio-imprinted hydrogel before dehydration, after dehydration and after rehydration. During the process, the transparent hydrogel shrank to a little white piece after dehydration. After it was put back to PBS buffer, the little solid hydrogel in the dry state returned to its original transparent wet hydrogel form that filled the capillary again.

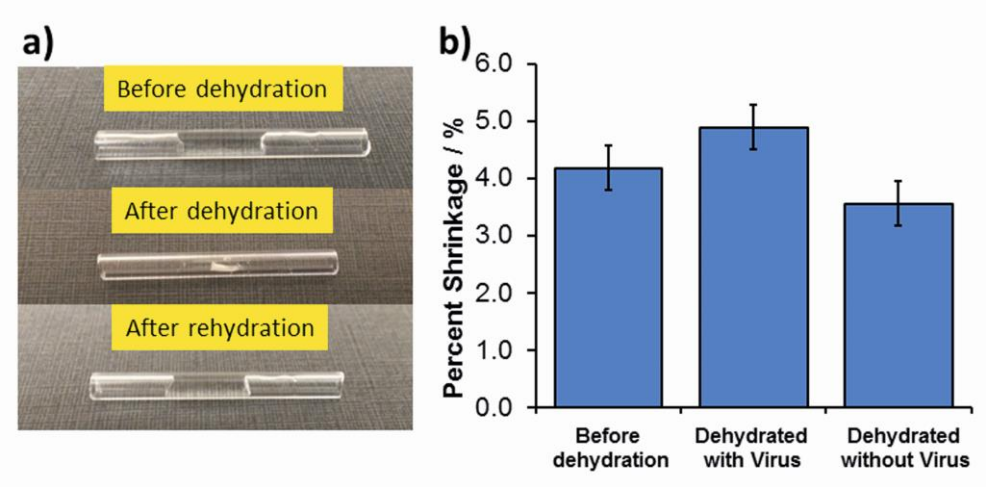

Figure 4.7 a) Picture of dehydration and rehydration of the virus imprinted capillary hydrogel. b) Study of the volume response of the virus bio-imprinted hydrogels before and after dehydration-rehydration process.

Figure 4.7b graphs the volume response of the hydrogel before and after the dehydration-rehydration process. Before dehydration, the hydrogel exhibited a volume response of approximately 4.1%. Column 2 in Figure 4.7b shows an interesting phenomenon; after the gel was dehydrated, followed by rehydration exposure to virus particles, the extent of response was a little higher than the volume change it showed before dehydration (column 1 in Figure 4.7b). However, if the hydrogel is dehydrated in the absence of virus, the volume response appears to decrease. In general, it can be concluded that the hydrogel maintained approximately the same level of volume response before and after both dehydration-rehydration processes. Thus, the dehydration-rehydration process has very little influence to the behavior of our hydrogel. Further experimentation still needs to be done here to better understand the dehydration-rehydration process and its influence on the material's properties.

4.4 Summary

In the previous chapters, success was achieved on design, synthesis and evaluated protein bio-imprinted hydrogel sensors for naked-eye detection of protein in buffer or bio- mimetic fluids. The results indicated that the method developed is successful for easy and low cost detection of biomarkers at ultra-low concentrations. However, although proteins are one of the most frequently researched biomarkers related to many practical applications; it should be considered to be equally important to explore other biomarker targets also suitable for detection.

Building on the fundamental work we have already done in the past our design of virus bio-imprinted capillary hydrogels also proved to be a successful one. Generally, like the protein bio-imprinted hydrogels, the ASPV bio-imprinted hydrogels can undergo reversible volume shrinkage in presence of virus extract and generate a volume change large enough for naked-eye detection. In addition, this hydrogel sensor also has low detection limit and good selectivity. The responsive property can be maintained even after dehydration –rehydration processes which are important for potential storage and transportation. Finally, an amplification effect similar to the protein imprinted hydrogels has also been observed.

CHAPTER 5. BIO-IMPRINTED GRATING FILMS FOR DETECTION OF PROTEINS AND VIRUS

5.1 Introduction

The incredible development of science and technology in the past 2 centuries has granted humanity unprecedented ability to recognize and remold our world, including ourselves. For years, hardworking (not so hard working) explorers have accumulated countless scientific and technological achievements that are now taken advantage of in full or in part. Recently, it seems that scientific research has become slow at times in discovering and developing new and clear fundamental breakthroughs. For many researchers this may present an opportunity to look to past discoveries and make use of existing scientific principles. Specifically, in our research, the molecular imprinting technique has been known for decades and has dramatically developed from initial studies four decades ago. However, although molecular imprinting has been shown to be useful in areas like small molecule separation and detection, improved applications of the MIP technique are yet to be invented for larger molecules and assemblies. Especially developments in novel directions utilizing advanced technical elements for problems that were hard to solve in the past.

One of the most important challenges of our continuing efforts is to reveal simple new methodologies to achieve relatively difficult tasks. For example, volume changing hydrogels such as those we have focused on for biomolecule detection. These materials achieve ultra-sensitive detection of targeted biomass in solutions using simply made, easy to use and low cost bio-imprinted materials with high sensitivity and selectivity. Although we have shown bio-imprinted materials are capable visual macroscopic responses triggered by microscopic stimuli,

we realized in the previous chapters that we directly measure the volume change and use it as the only index to characterize the macroscopic change of the hydrogel properties. Even though the direct length measurement we used before is a facile one, in most circumstances it is still worthwhile to explore new physical parameters that can be used to characterize this micro-triggered macroscopic property change. This expansion of measurement methods is crucial to increase the possibilities of that the technique to be applied in myriad specific conditions.

As in the case of the capillary hydrogels, controlling or monitoring of a material's macroscopic volume change has in fact long been proven to be a practical way to realize molecular detection, controlled release, tuning of mechanical properties, etc. However, there are still shortcomings of the capillary bio-imprinting hydrogel sensors even though this format has shown impressive ability in performing accurate, specific and naked-eye detection. For example, the most serious drawback is that the bio-imprinted hydrogel sensors need to be incubated in protein solutions for at least 12-15 hours before they became fully equilibrated. In addition, even though the volume change of the hydrogel is detectable to the naked-eye; usually a magnifying glass is still needed for a relatively accurate measurement, which is not absolutely "assist-free naked-eye detection".

Continuing advancement of the imprinted hydrogel research was carried out to overcome these two drawbacks.[1] In the previous chapter, we discussed making fast responsive hydrogels by preparing porous bio-imprinting hydrogels using freezing treatment or pore-forming agents. This was because in theory these porous-rich structures can enhance the mass-transfer within the materials and thus lead to a faster response. Alternatively, hydrophobic capillaries were also made to see if it can shorten the response time since the friction between hydrogel and the wall of the glass capillary can be part of the reason that make the volume response of the hydrogel

slower. However, these methods did not lead to a significantly shorter response time. These results redirected our efforts, and we turned to some other possible methods.

Optical response to diffraction grating patterns is an important technique that has been widely used in spectroscopy because of its ability to separate polychromatic light into constituent monochromatic components or split a mono-beam into multi-beams. In chemistry research, diffraction gratings also play an active role in molecular detection and environmental factor monitoring. [54] An important feature of diffraction gratings is that the change of the chemical environment such as specific molecules, change of pH, temperature or other corresponding physical factors can effectively influence grating's physical properties. For example, gratings made of hydrogels can deform the grating structure, which can lead to the changes of a light beam going through the hydrogel grating. The changes in beam light result in changes in either the intensity or the diffraction pattern can be observed, sometimes requiring instrumentation.

In our case, we were interested in diffraction grating hydrogels which would combine the advantages of hydrophilic and bio-friendly hydrogels with optical output of light-splitting gratings. Stimuli-responsive hydrogels are widely used in bio-related areas like tissue engineering, drug delivery etc.; due to the bio-friendly nature of hydrogels and their ability to change properties under certain external stimuli. Having tunable properties allows the hydrogels to be made strong enough to support lithographed gratings. The grating pattern can impart the hydrogels with the ability to diffract the light beam going through and therefore changes light patterns as a result of the presence of certain external signals like pH, temperature, etc. Specifically, based on the previous research for bio-imprinted hydrogels it is possible to make bio-imprinted diffraction grating hydrogels that can exhibit volume change to the presence of specific molecule templates. The molecular trigger causes the hydrogel volume to shrink in

dimension, leading to the change of the light beam pattern that passes through the grating hydrogel. The same process as Scheme 4.1 was also used in the making of the virus imprinted hydrogels.

Fabrication of a grating surface is a technique that has been extensively studied and is generally accomplished by a lithographic process or using a grating mold. [55] In the project presented here, a pre-prepared mold is used with a grating structure on the surface to create grating hydrogels. Theoretically, the proposed grating hydrogels should be able to split the laser beam going through it and generate a 1D diffraction pattern composed of laser spots with certain distance between each other which is illustrated by Scheme 5.1.

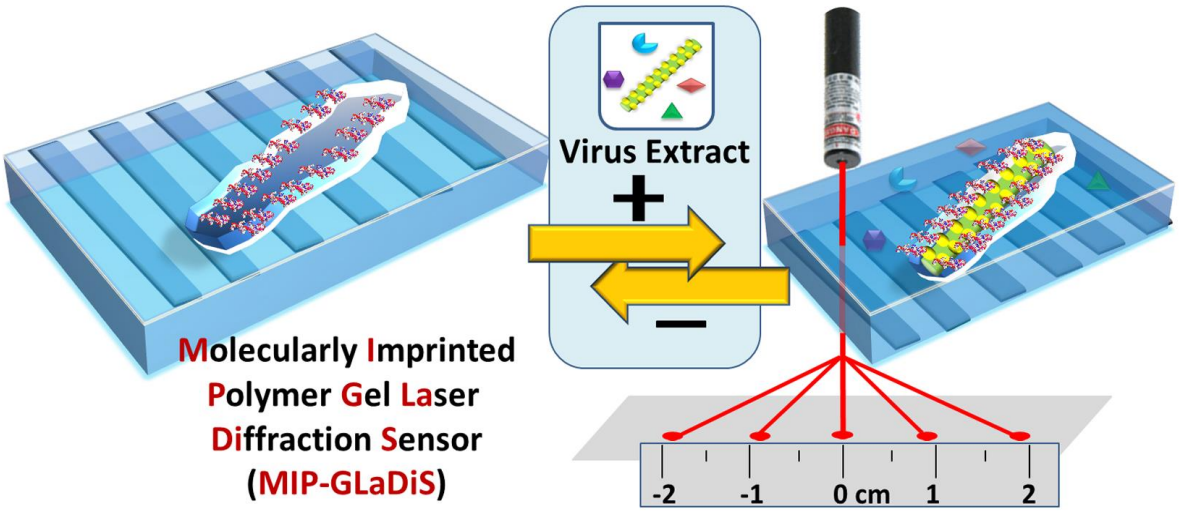

Scheme 5.1 Laser light diffractionfrom transmission through the bio-imprinted diffraction grating hydrogels.

In fact, although our idea of hydrogel polymer grating for detection of bio-target in solution was developed independently, there have been a few examples published very recently

before this work was carried out.[56] However, compared to these recent pioneering achievements, it should be pointed out that there are several advantages in the hydrogel grating sensors presented here that make our system different than others. First, the bioimprinted hydrogels made in our labs use less crosslinker relative to other published procedures,[56] which leads to hydrogels with larger pores for detection of bio-targets with larger dimensions. Second, our grating hydrogels are capable of detecting biological targets at ultra-low concentrations. Third and most important, compared to using light intensity as the index which requires a diode light sensor, our method simply uses the distance change in the regularity of the light pattern caused by the hydrogel shrinking. The direct measurement of the change in diffraction pattern can be performed by the naked-eye and an ordinary ruler without the help of any sort of microscopy.

5.2 Formulas, Preparation and Test methods

5.2.1 Materials

The ASPV, Apple Chlorotic Leaf Spot Virus (ACLSV), Apple Mosaic Virus (APMV), and "negative control" virus solutions were purchased from Bioreba AG, Switzerland. These were all converted to stock solutions of concentrations 10 μg/mL and 1 μg/mL using 2.0 mM PBS, and kept at -4^{o}C while not being used. AAm, MBAA, TEMED, SDS, and APS were all purchased from Sigma-Aldrich; guanidinium hydrochloride was purchased from Amresco; N-isopropylacrylamide (NIPAM) was purchased from TCI Amercia. Sylgard 184 silicone elastomer kit was purchased from Dow corning corporation.

5.2.2 Preparation of the Grating hydrogels

The general procedure for making the grating template replica, grating hydrogels and the subsequent laser diffraction analysis is demonstrated by Scheme 5.2 below. Generally, the whole procedure can be separated into two parts: making of the mold and making of the hydrogel. Both of these steps will be described in detail in the following section.

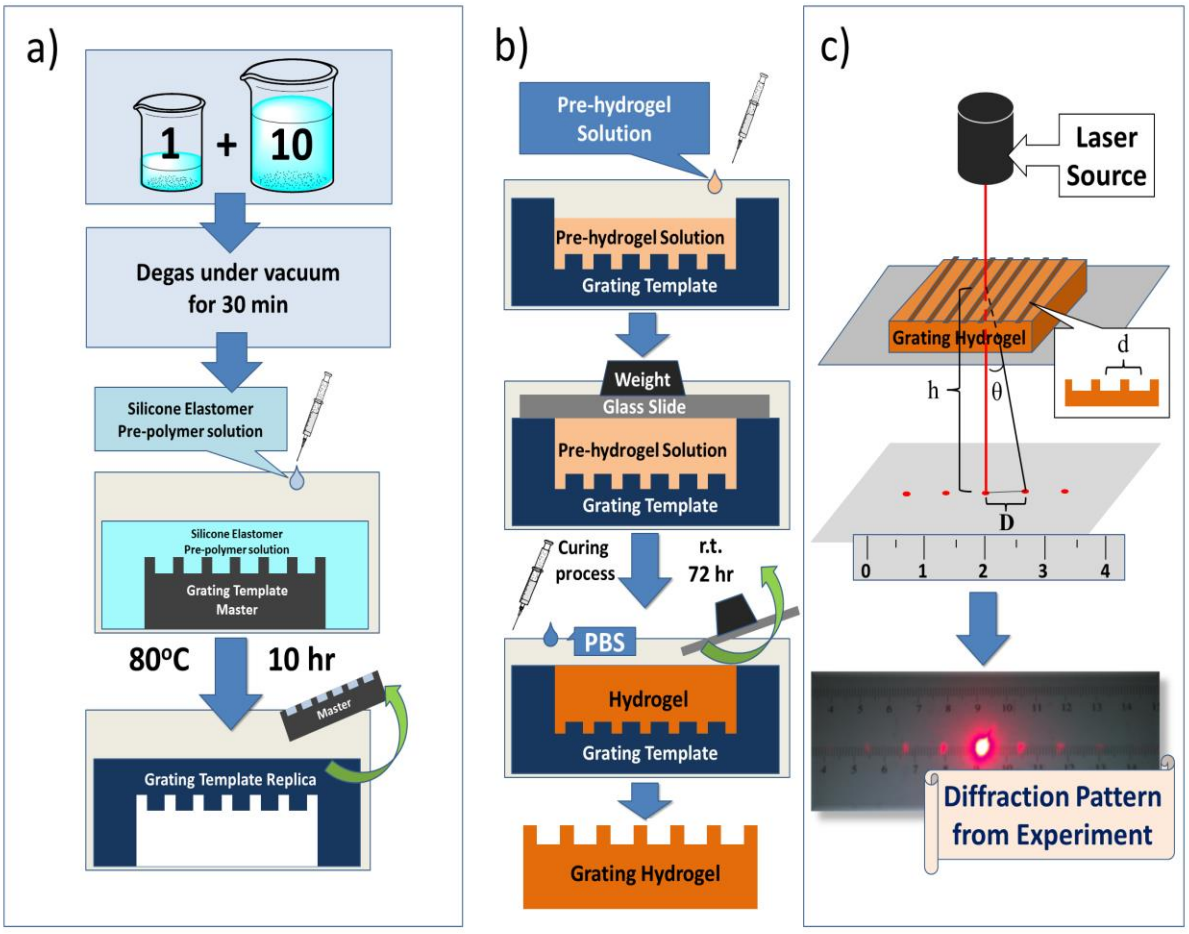

Scheme 5.2 a) Preparation of the elastomer grating template; b) Making of the grating hydro gel; c) Laser test of grating hydrogel.

5.2.2.1 Preparation of the elastomer mold

Master microgratings molds with gratings 5 μm in width and 10 μm in spacing were prepared by spin-coating 5 μm of negative photoresist SU-8 (MicroChem Corp., Newton, MA) onto a pre-cleaned silicon wafer, followed by UV exposure (Quintel Ultraline 7000 series mask aligner, Morgan Hill, CA), then washed and dried by conventional developing and hard-baking processes. The grating master was sized to 1.0 cm^2, and placed face up in a culture dish.

A mixture of Sylgard 184 silicone elastomer base and Sylgard 184 silicone elastomer curing agent (10:1, w:w), was degassed for 15 minutes under vacuum and carefully poured into a culture dish, then covered using the template. The elastomer was cured in an oven at 80^oC and cured for 10 hours. Subsequently the culture dish was removed, and the master was peeled away from the elastomer replica. The SU-8 grating template replica is shown in Figure 5.1, which indicates good replication of the 5 μm width and 10 μm spacing dimensions from the master was achieved.

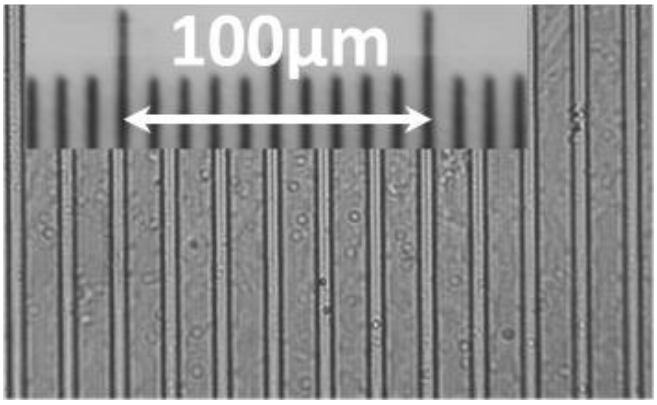

Figure 5.1 Microscope image of the grating template replica.

5.2.2.2 Pre-treatment of the mold

The replicas of the silicone template are pre-treated in order to increase the hydrophilicity to promote wetting of pre-polymer solution. First, the mold was washed by water and acetone several times. Subsequently, 100mM PBS buffer was injected into the mold and the mold was put into a vacuum chamber until no further bubbles appear. The disappearance of the bubble means the residual air within the gaps and on surface of the mold was completely removed so the contact of the polymerization solution and the mold surface can be improved. Last the buffer was removed as much as possible by syringe and the mold was dried in an oven at 45^{o}C overnight.

5.2.2.3 Synthesis of the double imprinted hydrogels

The reagents for synthesis and bioimprinting the aptamer hydrogels are shown in Table 5.1 below.

Table 5.1 Formula for making of the virus imprinted hydrogels.

	MW (Da)	**Mole number**	**Ratio**
ASPV	20000000 (approx.)	2.5×10^{-13}mol	1
Aptamer MT32	13210.7	7.6×10^{-9}mol	3.0×10^{4}
NIPAM	113	4.0×10^{-5}mol	1.6×10^{9}
AAm	71	4.0×10^{-5}mol	1.6×10^{9}
MBAM	154.2	4.0×10^{-7}mol	1.6×10^{7}

The synthesis of the double-imprinted hydrogels was carried out as follows: in a plastic vial, 10.0 μL of ammonium persulfate (APS) solution (10 wt% in PBS buffer) and 30.0 μL of N, N'-Methylenebisacrylamide solution (1 wt% in PBS buffer), were added to 160.0 μL of 2mM

PBS solution containing 0.5μg (2.5×10^{-14}mol) of Apple Stem Pitting Virus (ASPV) extract, 0.01μg (7.6×10^{-9}mol) of ASPV aptamer, 22.0mg of N-isopropylacrylamide and 28.0mg of acrylamide. The solution was then added 1.0μL of N, N, N', N'-Tetramethylethylenediamine (TEMED) to initiate the polymerization, the mixture was vortexed for approximately 2 seconds and transferred into the elastomer replica (mold) and cover with a clean glass slide and put either into a vice clamp, or clamped on opposite sides with .

Preparation of the protein imprinted hydrogels generally follows the same procedure described in previous chapters; the only difference was the amount of the template protein and aptamers used in preparation. When making protein imprinted grating hydrogels, the ratio between protein and monomer was the same as the capillary gels and stoichiometric amount of the aptamers were used. The polymerization was allowed proceed for at least 72 hours, and during the first 90 seconds of polymerization, the temperature within the gel is measured to be 28.3 °C ± 2.1°C. The temperature of the polymer gel remains at room temperature, measured to be 22.5°C ± 2.0°C over the duration of the polymerization. It is important to note that the bioimprinted polymer remained below the LCST of NIPAM during the entire experiment, and thus the LCST effects were not of concern. Next, the mold as well as the glass slide was removed from the clamp. The mold together with the polymer was immersed in a culture dish containing 2mM PBS buffer. The film was allowed to expand in the buffer wash solution, which caused the bio-imprinted grating films to delaminate from the grating replica after several hours. The film was then transferred to another culture dish with PBS for measurement and/or storage at room temperature.

5.2.3 Evaluation of the hydrogels response

5.2.3.1 Laser test of the grating hydrogels

The laser diffraction analysis of the grating hydrogels was performed by using an apparatus shown in Figure 5.2. A commercial hand-held laser pointer shines a laser beam through a polarizing filter and onto the surface the grating hydrogel. Due to the grating on hydrogel surface, the laser beam was split, forming 1D diffraction patterns on the paper ruler positioned below the grating samples (Scheme 5.3(c) and Figure 5.3 below).

In Scheme 5.3 (c), the distance d gives the angle of diffraction (θ) for transmitted laser light determined by

Eq. 1: $$\theta = sin^{-1}(\lambda / d)$$

d = trough to trough distance of the hydrogel grating

λ = wavelength of the incident laser

Thus, θ becomes larger as the distance d becomes smaller. The angle of diffraction determines the distance between two adjacent projected laser points (D), which are in turn a function of the geometrical parameters of the apparatus in Figure 5.2 according to the equation:

Eq. 2: $$\theta = tan^{-1}(D / h)$$

Combining both equations gives dependence of the distance (D) as a function of the hydrogel grating period (d):

Eq. 3: $$D = h \tan\left[Sin^{-1}(\lambda / d) \right]$$

Equation 3 shows how the decrease in d as result of the bio-imprinted grating hydrogel shrinking inversely expands the distance D between two projected laser points. This change in distance D is used to quantify the hydrogel volume change.

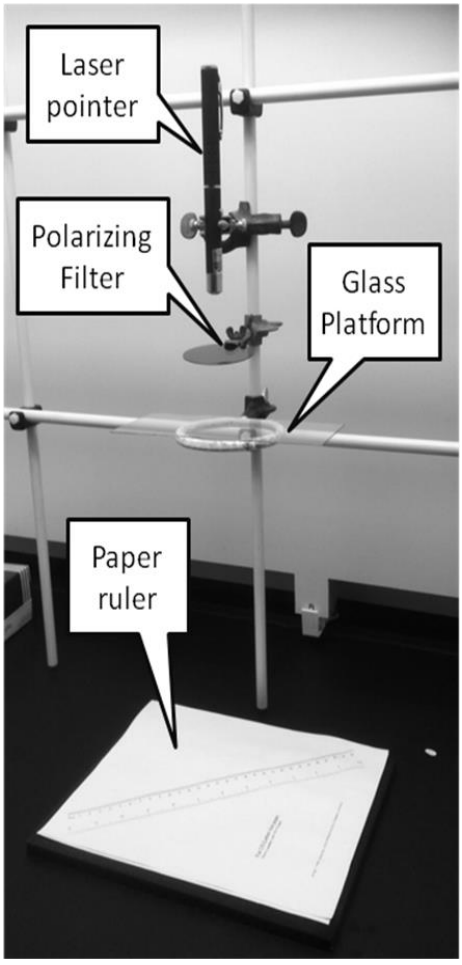

Figure 5.2 Photograph of actual apparatus used to measure diffraction distances of laser light transmitted through hydrogels.

5.2.3.2 General regeneration-rebinding process

The removal of the virus was carried out by incubating the film in a regeneration solution composed of 12mM NaOH and 1.2% ethanol in deionized water. The regeneration solution was changed every 3-6 hours until the hydrogel volume-changes reach equilibrium. Afterward the hydrogel film was washed by 2mM PBS buffer until equilibrium. The hydrogel film was then put on a clean glass slide and covered by another piece of glass slide for laser diffraction evaluation. The distance between -1 and +1 laser spot (demonstrated by Figure 5.3 below) was recorded as d_0.

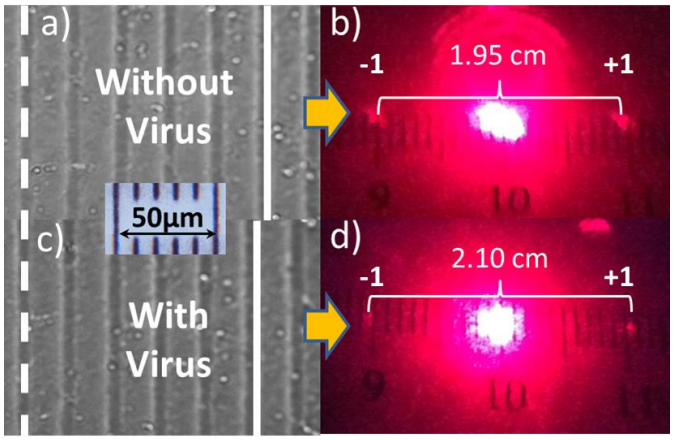

Figure 5.3 Optical microscopy images of ASPV responsive MIP-GLaDiS and the corresponding laser diffraction pattern in 2.0mM phosphate buffer without virus (a & b), and in the presence of the ASPV extract (c & d).

After the test, the hydrogel film was immersed in ASPV extract until equilibrium and then washed by plain buffer. Thereafter, laser diffraction was performed and the distance between -1 and +1 laser spot was again recorded as d_1. The change of the grating size in the presence of or absence of the virus template and the corresponding change of the diffraction pattern is illustrated in Figure 5.3 below. For PDGF-ββ and Thrombin imprinted grating

hydrogel, the same method was applied by using the same regeneration and rebinding solutions that were used for imprinted capillary hydrogels that have been mentioned in previous chapters.

5.2.3.3 Evaluation of the hydrogel response.

First, the hydrogel was taken out of the culture dish and put on a glass micro slide with its top covered by another coverglass. Then the sample was put on the glass platform shown by Figure 5.2. After turning on the laser pointer, the beam goes through the hydrogel vertically. A laser diffraction pattern should be able to be seen on the paper ruler, and the response of the grating film can be evaluated by measuring the value of d_0 and d_1 described above. The value of the percent change of the grating hydrogel gel was calculated by equation 4 below.

Eq. 4
$$Percent\ Change = \frac{d_0 - d_1}{d_0} \times 100$$

5.2.4 Exploration of the Formula

Initial experiments in this research used the the same component formulation as that used to prepare capillary hydrogel sensors were tested to see if it still worked. However, the results indicated that sometimes the hydrogels formed were not solid enough to support a good grating structure on its surface. As a result, to determine the proper formula for our proposed grating hydrogel sensor, several different component formulations were tested. The best grating hydrogel formed when using the least amount of the monomer and crosslinker which is what was used in further research and listed in Table 5.1 previously.

5.3. Results and Discussion

5.3.1 Reversible volume change

The reversibility of virus imprinted grating hydrogel was examined by measuring the change of the diffraction pattern over 4 cycles of regeneration and rebinding. The results shown in Figure 5.4a below illustrate that the change in diffraction pattern is not only reversible but also stable and reproducible. In addition, the changes were all around 4% which means at least 1-2 mm of change in the length between the -1 and +1 spot that can be easily seen by our naked-eyes (Figure 5.3b, 5.3d). Moreover, the results from protein imprinted grating hydrogels revealed that different kinds of templates can produce the same stable and repeatable response in diffraction patterns which are also shown by Figure 5.4b&c.

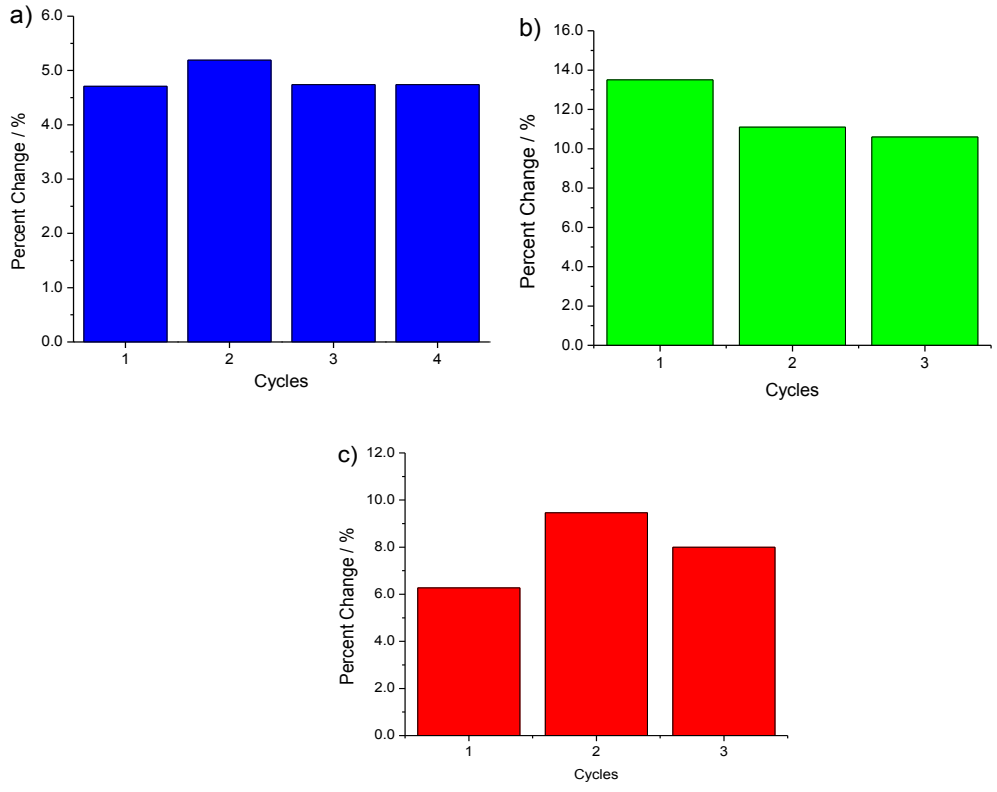

Figure 5.4 Reversible response of bio-imprinted grating hydrogel sensor a) ASPV imprinted grating hydrogel; b) PDGF-ββ imprinted grating hydrogels sensor; c) Thrombin imprinted hydrogel sensor.

5.3.2 Selectivity

The selectivity of bio-imprinted grating hydrogels versus biological targets other than the templates imprinted has also been evaluated as a control. Figure 5.5 below shows the results of the selectivity analysis for both virus and protein bio-imprinted hydrogels. Both of the hydrogel sensors exhibit high selectivity to specific template. This is not surprising, and reflects the selectivity inherent to the aptamer for the ASPV protein coat epitope.

For the virus imprinted grating hydrogel in Figure 5.5a, the largest blue column is the imprinted hydrogel treated with virus extract showing a diffraction pattern change of about 4.5%. The rest of the columns represent the imprinted hydrogels treated with negative extract which was made from grinding up healthy leaves containing no virus (yellow column). After that, different virus extracts were tested; APMV extract and ACLSV extract respectively. None of the imprinted hydrogels showed any change more than 2.0% to stimuli other than template virus extracts, which means the selectivity of the imprinted hydrogels for their specific target is considerably good.

For protein imprinted grating hydrogels, similar results were also observed. In Figure 5.5b, the blue column represents the PDGF-ββ imprinted grating hydrogel treated with PDGF-ββ solution, while the red column represents the Thrombin imprinted grating hydrogel treated with Thrombin solution. The other columns show the control results comparing the PDGF-ββ imprinted grating hydrogels treated with BSA (yellow column), Thrombin (orange column) and Thrombin imprinted grating hydrogel treated with PDGF-ββ (pink column) respectively. From these results it is seen that none of the protein bio-imprinted grating hydrogels show any significant responses to non-template protein control solutions. This result also verifies the outstanding selectivity of our grating hydrogel sensors.

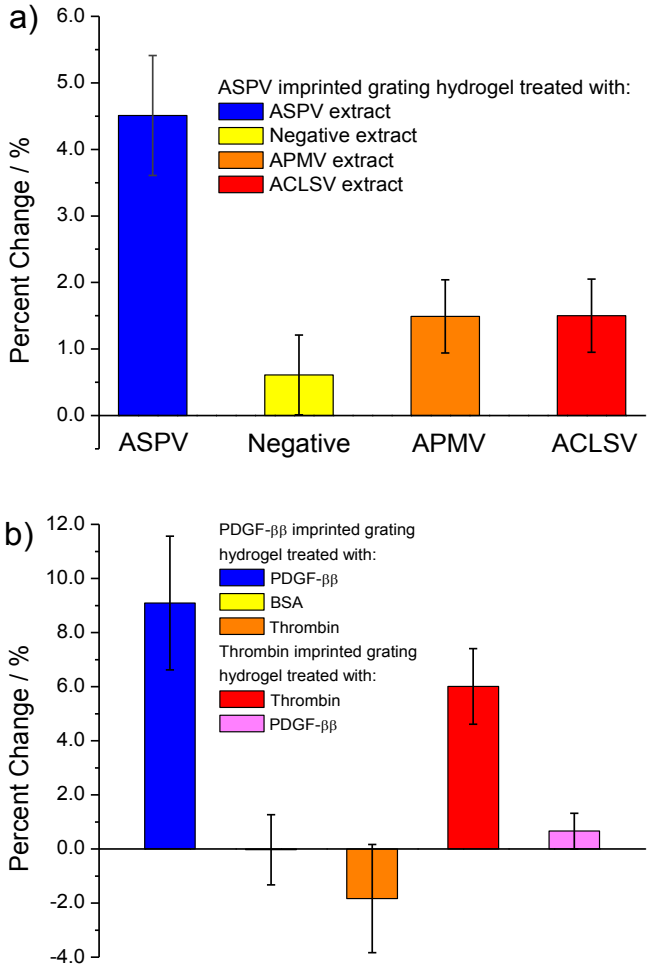

Figure 5.5 Study of the selectivity of the ASPV (a) and protein (b) bio-imprinted grating hydrogels.

5.3.2 Imprinting effect

The comparison between bio-imprinted grating hydrogels and non-imprinted grating hydrogels was performed to test if the bio-imprinting effect still plays an decisive role in the forming of the sensors' highly specific recognition and responsive ability.

Figure 5.6a shows the comparison of ASPV bio-imprinted grating hydrogel and non-imprinted grating hydrogel. The highest blue column represents the response of the ASPV imprinted grating hydrogel which can produce a shrinking change of 4.5%, while the responses of other control non-imprinted hydrogels to the ASPV extract solution were much lower (less than 1%).

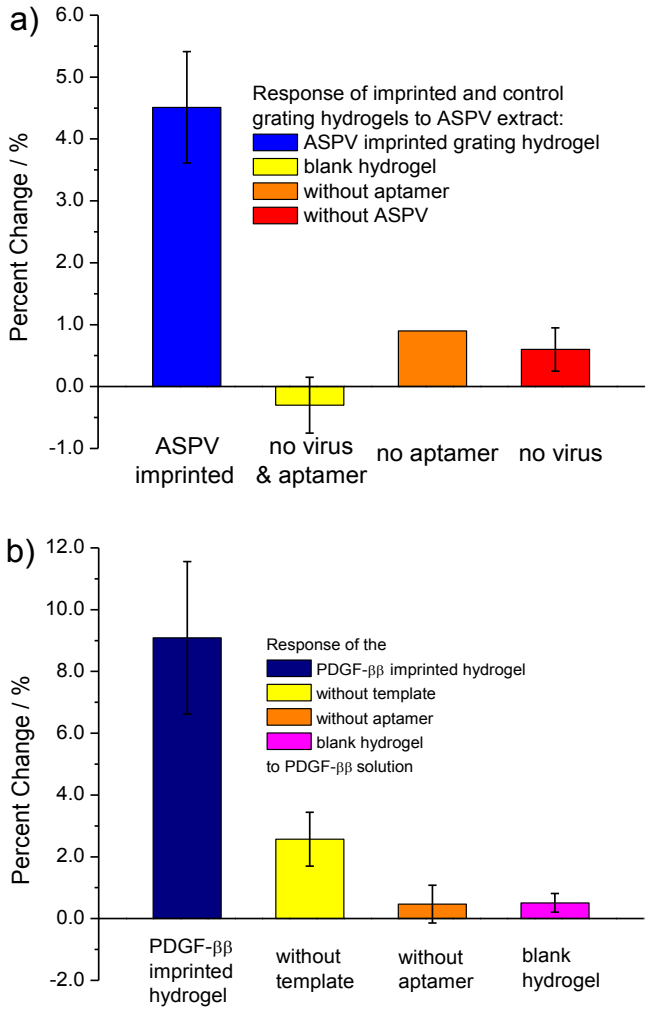

Figure 5.6 Comparisonof the change of the diffraction pattern of ASPV (a) and PDGF-ββ (b) bio-imprinted hydrogels and non-imprinted control hydrogels.

In Figure 5.6b, the PDGF-ββ imprinted grating hydrogel also show an overwhelming advantage over all controls. Compared to about 9.1% of the response generated by imprinted hydrogels, non-imprinted hydrogels can only produce a maximum response of 2.2% in case of control gels without any aptamer immobilized in the hydrogel. These results again demonstrate the fact that only imprinted hydrogels provide a large and specific response, while none of the non-imprinted controls can show any equivalent extent of response. This phenomenon further support the conclusion that the bio-imprinting effect is a crucial factor in the shrink-responsive behavior of the grating hydrogel sensors.

5.3.3 Isotherm research

To determine the detection limit of our bio-imprinted grating hydrogel sensors, the ASPV and PDGF-ββ imprinted grating hydrogels were treated with ASPV extract and PDGF- ββ solution at different concentrations. Figure 5.7 (a & b) show the results of this isotherm research. In Figure 5.7a, the response of the grating hydrogel was almost negligible when the concentration was below 0.1 μg/mL (less than 2%), but then increased dramatically to 4-5% becoming naked-eye detectable at this concentration and higher. This indicates the detection limit of our ASPV imprinted grating hydrogel is approximately 0.1 μg/mL. In the case of the PDGF- ββ imprinted grating hydrogel shown in Figure 5.7b, the response was lower than 1×10^{-12}M, and rises slowly for two orders of magnitude in concentration after that. However, when the concentration of the template protein solution went up to more than 1×10^{-10}M, the response increased significantly to more than 6%, and the change in the diffraction pattern clearly becoming naked-eye detectable. This result indicates that the detection limit of protein-imprinted hydrogels is approximately 1×10^{-10}M.

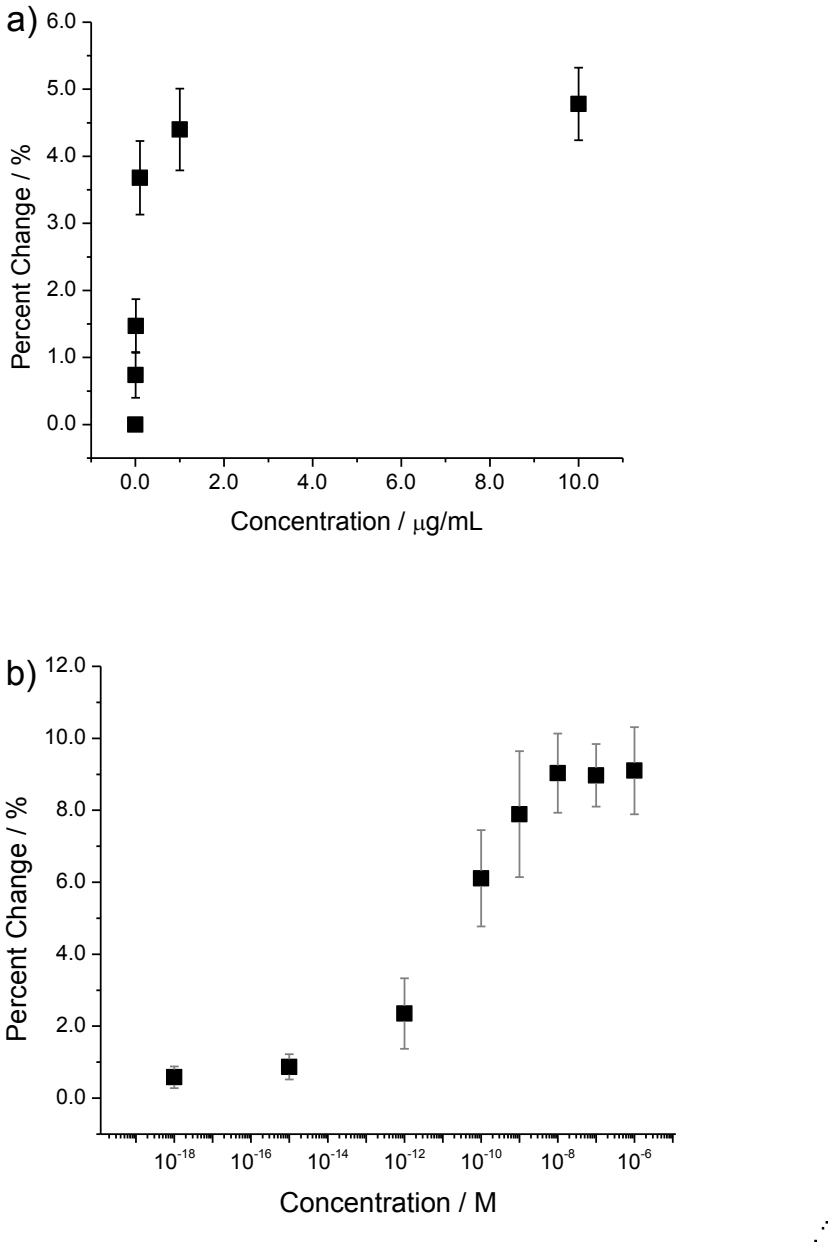

Figure 5.7 Isotherm study of the ASPV (a) and PDGF-ββ (b) bio-imprinted grating hydrogels.

Thus, an amplification of the shrinking response of these virus specific grating hydrogel sensors has also been observed. Compared to the template concentration used to prepare our hydrogel sensor, the concentration of the template as analyte required to shrink the gel is much

lower. In this study the concentration of ASPV used in the bio-imprinted grating hydrogel was 10 μg/mL; however, when incubated with extract having a concentration of 0.01 μg/mL ASPV, an obvious response can be detected; and as the concentration goes up an order of magnitude to 0.1 μg/mL, nearly a full response can be observed. In the case of PDGF-ββ imprinted grating hydrogels, a detectable response was observed at a concentration of 1×10^{-10}M, which is also 10,000 times lower than the concentration we used in making these hydrogels (1×10^{-6}M).This phenomenon showed the reproducibility of the amplification effect we observed and reported for the proteins and now found for the virus imprinted materials, may be a widely existing mechanism in the recognition and response of similar smart materials.

5.3.4 Dehydration

As described in previous chapters, these bio-imprinting grating hydrogels were subjected to a dehydration-rehydration procedure to verify the influence of these processes on their responsive behavior. Figure 5.8a&b shows the grating hydrogel before and after dehydration and rehydration processes. Figure 8c is the response of the PDGF- ββ imprinted grating hydrogels before and after dehydration-rehydration process.

From the result it is clear that the dehydration-rehydration process did not affect the shrink-responsive performance of the hydrogel. The change of the diffraction pattern was maintained at about 8-9% without significant decrease after dehydration and rehydration processing. Looking back at previous chapters, this phenomenon matches the results obtained from the bio-imprinted capillary hydrogels, and also demonstrated that the grating hydrogel films are easy to store and transport until needed as a detection device.

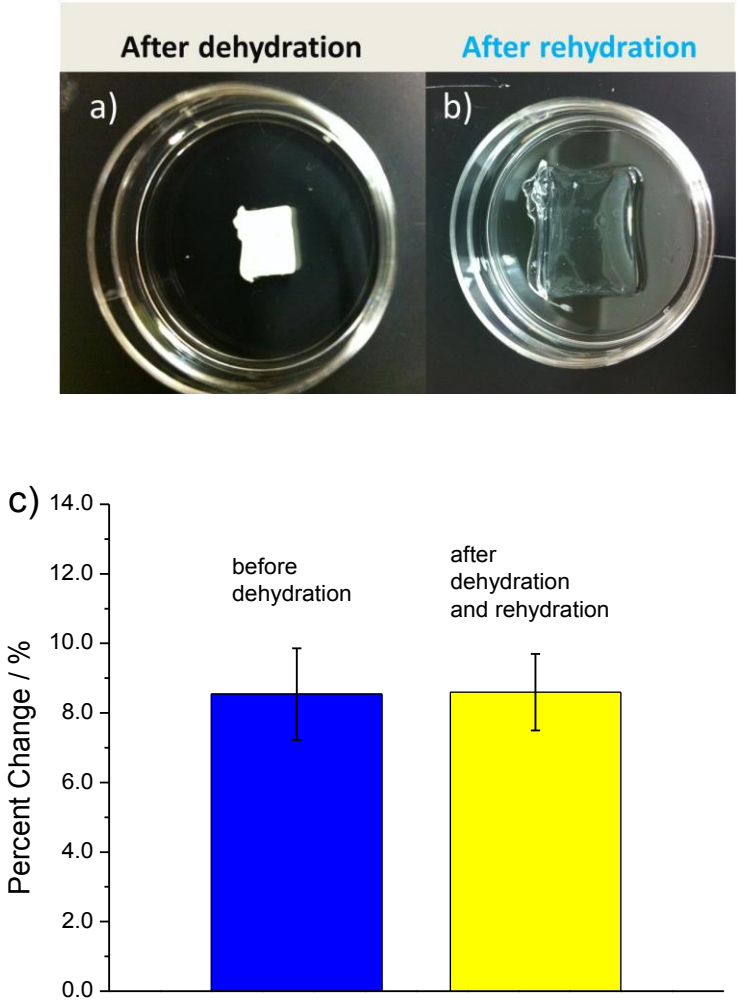

Figure 5.8 Picture of dehydrated (a) and rehydratated (b)of the bio-imprinted grating hydrogel. C) Study of the volume response of the virus bio-imprinted hydrogels before and after dehydration-rehydration process.

5.4. Summary

In this chapter, we successfully designed and synthesized a new kind of bio-imprinted grating sensor for detection of a targeted virus in impure extract, as well as proteins previously only studied in capillaries. Specifically, ultra-low concentrations of ASPV, as well as PDGF- ββ and Thrombin proteins, have been successfully detected by the diffraction grating hydrogel

sensors. Like the capillary hydrogel sensors we reported in previous chapters, these new bio-imprinted grating hydrogels can also undergo reversible volume shrinkage in presence of virus extract or protein solutions, and generate a change of the diffraction pattern large enough to be visible to the naked-eye. In addition, this hydrogel sensor also has a low detection limit into the sub-nanomolar range, and exhibits good selectively. Further study also supported the supposition that the imprinting effect plays a crucial in the formation of these hydrogel's responsive abilities. The responsive ability can be maintained ever after dehydration–rehydration process which is important for potential storage and transportation. Moreover, the amplification effect we noticed in our previous protein-imprinted hydrogel study has also been observed again in these grating hydrogel sensors.

CHAPTER 6. CONCLUSIONS

Detection of ultra-low concentrations of analytes for biomedical, environmental, and national security applications is becoming more and more important these days. Meanwhile, new techniques or technical strategies that that allow inexpensive, portable, simple and (if possible) naked eye detection are always in demand due to the fact that accessibility of current detection techniques can be severely restricted due to their requirements of trained personnel, expensive equipment, or complex detectors and etc..

Novel bioimprinted hydrogel based biosensors (BIGs) have been developed using polymerizable aptamers that can specifically recognize and display a visual response to target biomarkers such as proteins and viruses. The reversible response of these super-aptamer hydrogels provided an equal or larger response (approximately 5-10% volume change) than previously reported biomolecule-responsive hydrogels fabricated with antibodies and proteins. The sensitivity of the hydrogels is very high and the BIG sensors can detect proteins down to femtomolar concentrations. This is competitive with modern methods requiring sophisticated instrumentation and highly trained personnel such as surface Plasmon resonance, electrochemical devices, microscopy, microbalance technologies, fluorescent methods, and sandwich assays.

Subsequently, a new "double imprinting" method was developed by further micromolding a virus-bioimprinted hydrogel into a diffraction grating hydrogel sensor. Very simple and inexpensive laser transmission apparatus can be used to measure diffraction responses to biomarkers like proteins and viruses while maintaining high accuracy. Furthermore, the laser diffraction format can potentially be automated for fast and easy measurements, which

can also be incorporated into a multi-array format. Additionally, this is the first example of using an impure virus extract as the source of template which was facilitated by the use of virus-specific aptamers that can prevent the interference of the other extract components in the sample. Control hydrogels polymerized with random placement of the aptamers (i.e. in the absence of the proteins or virus templates) did not show appreciable response to the bio-imprinted samples, further proving that random incorporation of aptamers cannot compete with the pre-organized aptamers in the bioimprinted hydrogel.

It should also be pointed out that these aptamer-based hydrogels with specific response to target proteins also demonstrates an additional category of macromolecular signal amplification. Usually the detection of low concentration analytes cannot be achieved directly, and require additional strategies employing conjugated polymers, chirality in polymers, solvating polymers and polymerization/depolymerization for signal amplification. However, the macromolecular amplification seen in our research doesn't belong to any of these categories and cannot be attributed simply to a change of crosslink density because the percentage of overall crosslinks formed and broken by addition and removal of analyte is negligible. On the other hand, the volume-shrinking effect cannot be related to changes in osmotic pressure as shown by control experiments. The effects are attributed to an excluded volume effect triggered by the loss of protein crosslinks, providing insight into the large volume amplification that affords the visual detection of biomolecules at concentrations lower than many analytical techniques and instrumentation. The results from study of the origins of macromolecular amplification in these hydrogels can be used to improve the volume change and response time in the next generation of super-aptamer hydrogels.

REFERENCES

1. (a) Clark, L.; Lyons, C., Electrode systems for continuous monitoring in cardiovascular surgery. *Annals of the New York Academy of Sciences* **1962,** *102* (1), 29-45; (b) Cooper, J. C.; Hall, E. A. H., The nature of biosensor technology. *Journal of Biomedical Engineering* **1988,** *10* (3), 210-219; (c) Hall, E. A. H., Recent progress in biosensor development. *International Journal of Biochemistry* **1988,** *20* (4), 357-362; (d) Tess, M.; Cox, J., Chemical and biochemical sensors based on advances in materials chemistry. *Journal of Pharmaceutical and Biomedical Analysis* **1999,** *19* (1-2), 55-68; (e) Vo-Dinh, T.; Tromberg, B.; Griffin, G.; Ambrose, K.; Sepaniak, M.; Gardenhire, E., Antibody-based fiberoptics biosensor for the carcinogen benzo(a)pyrene. *Applied Spectroscopy* **1987,** *41* (5), 735-738.

2. Vo-Dinh, T.; Cullum, B., Biosensors and biochips: advances in biological and medical diagnostics. *Fresenius Journal of Analytical Chemistry* **2000,** *366* (6-7), 540-551.

3. (a) Bardea, A.; Patolsky, F.; Dagan, A.; Willner, I., Sensing and amplification of oligonucleotide-DNA interactions by means of impedance spectroscopy: a route to a Tay-Sachs sensor. *Chemical Communications* **1999,** (1), 21-22; (b) Piehler, J.; Brecht, A.; Gauglitz, G.; Zerlin, M.; Maul, C.; Thiericke, R.; Grabley, S., Label-free monitoring of DNA-ligand interactions. *Analytical Biochemistry* **1997,** *249* (1), 94-102; (c) Wang, J.; Rivas, G.; Fernandes, J.; Paz, J.; Jiang, M.; Waymire, R., Indicator-free electrochemical DNA hybridization biosensor. *Analytica Chimica Acta* **1998,** *375* (3), 197-203.

4. T. Vo-Dinh, B.G. Tromberg, G.D. Griffin, K.R. Ambrose, M.J. Sepaniak, and E.M. Gardenhire. *Suppl. Spectrosc* **1987,** 41, 735-738.

5. (a) Huber, A.; Demartis, S.; Neri, D., The use of biosensor technology for the engineering of antibodies and enzymes. *Journal of Molecular Recognition* **1999,** *12* (3), 198-216; (b) Van Regenmortel, M.; Altschuh, D.; Chatellier, J.; Christensen, L.; Rauffer-Bruyere, N.; Richalet-Secordel, P.; Witz, J.; Zeder-Lutz, G., Measurement of antigen-antibody interactions with biosensors. *Journal of Molecular Recognition* **1998,** *11* (1-6), 163-167; (c) VO-DINH, T.; Alarie, J.; Johnson, R.; Sepaniak, M.; Santella, R., Evaluation of the fiberoptic antibody-based fluoroimmunosensor for dna adducts in human placenta samples. *Clinical Chemistry* **1991,** *37* (4), 532-535.

6. (a) Polster, J.; Prestel, G.; Wollenweber, M.; Kraus, G.; Gauglitz, G., Simultaneous determination of penicillin and ampicillin by spectral fibre-optical enzyme optodes and multivariate data analysis based on transient signals obtained by flow injection analysis. *Talanta* **1995,** *42* (12), 2065-2072; (b) Rosenzweig, Z.; Kopelman, R., Analytical properties and sensor size effects of a micrometer-sized optical fiber glucose biosensor. *Analytical Chemistry* **1996,** *68* (8), 1408-1413.

7. (a) Erdem, A.; Kerman, K.; Meric, B.; Akarca, U.; Ozsoz, M., DNA electrochemical biosensor for the detection of short DNA sequences related to the hepatitis B virus. *Electroanalysis* **1999,** *11* (8), 586-588; (b) Wang, J.; Cai, X.; Rivas, G.; Shiraishi, H.; Farias, P.; Dontha, N., DNA electrochemical biosensor for the detection of short DNA sequences related to the human immunodeficiency virus. *Analytical Chemistry* **1996,** *68* (15), 2629-2634.

8. (a) Franchina, J.; Lackowski, W.; Dermody, D.; Crooks, R.; Bergbreiter, D.; Sirkar, K.; Russell, R.; Pishko, M., Electrostatic immobilization of glucose oxidase in a weak acid, polyelectrolyte hyperbranched ultrathin film on gold: Fabrication, characterization, and enzymatic activity. *Analytical Chemistry* **1999,** *71* (15), 3133-3139; (b) Heim, S.; Schnieder, I.; Binz, D.; Vogel, A.; Bilitewski, U., Development of an automated microbial sensor system. *Biosensors & Bioelectronics* **1999,** *14* (2), 187-193; (c) Schuler, R.; Wittkampf, M.; Chemnitius, G., Modified gas-permeable silicone rubber membranes for covalent immobilisation of enzymes and their use in biosensor development. *Analyst* **1999,** *124* (8), 1181-1184.

9. (a) Cornell, B.; BraachMaksvytis, V.; King, L.; Osman, P.; Raguse, B.; Wieczorek, L.; Pace, R., A biosensor that uses ion-channel switches. *Nature* **1997,** *387* (6633), 580-583; (b) Cotton, G.; Ayers, B.; Xu, R.; Muir, T., Insertion of a synthetic peptide into a recombinant protein framework: A protein biosensor. *Journal of the American Chemical Society* **1999,** *121* (5), 1100-1101; (c) Ramstrom, O.; Ansell, R., Molecular imprinting technology: Challenges and prospects for the future. *Chirality* **1998,** *10* (3), 195-209; (d) Song, X.; Swanson, B., Direct, ultrasensitive, and selective optical detection of protein toxins using multivalent interactions. *Analytical Chemistry* **1999,** *71* (11), 2097-2107.

10. (a) Davis, J.; Glidle, A.; Cass, A.; Zhang, J.; Cooper, J., Spectroscopic evaluation of protein affinity binding at polymeric biosensor films. *Journal of the American Chemical Society* **1999,** *121* (17), 4302-4303; (b) Liljeblad, M.; Lundblad, A.; Ohlson, S.; Pahlsson, P., Detection of low-molecular-weight heparin oligosaccharides (Fragmin (TM)) using surface plasmon resonance. *Journal of Molecular Recognition* **1998,** *11* (1-6), 191-193; (c) Mayes, A.; Blyth, J.; Kyrolainen-Reay, M.; Millington, R.; Lowe, C., A holographic alcohol sensor. *Analytical Chemistry* **1999,** *71* (16), 3390-3396.

11. (a) Karyakin, A.; Vuki, M.; Lukachova, L.; Karyakina, E.; Orlov, A.; Karpachova, G.; Wang, J., Processible polyaniline as an advanced potentiometric pH transducer. Application to biosensors. *Analytical Chemistry* **1999,** *71* (13), 2534-2540; (b) Rao, T.; Yagi, I.; Miwa, T.; Tryk, D.; Fujishima, A., Electrochemical oxidation of NADH at highly boron-doped diamond electrodes. *Analytical Chemistry* **1999,** *71* (13), 2506-2511; (c) Sarkar, P.; Tothill, I.; Setford, S.; Turner, A., Screen-printed amperometric biosensors for the rapid measurement of L- and D-amino acids. *Analyst* **1999,** *124* (6), 865-870; (d) Zhang, J.; Li, B.; Xu, G.; Cheng, G.; Dong, S., Self-gelatinizable graft copolymer of poly(vinyl alcohol) with 4-vinylpyridine as an immobilization matrix for the construction of a tyrosinase-based amperometric biosensor. *Analyst* **1999,** *124* (5), 699-703.

12. (a) Chan, C.; Lehmann, M.; Tag, K.; Lung, M.; Kunze, G.; Riedel, K.; Gruendig, B.; Renneberg, R., Measurement of biodegradable substances using the salt-tolerant yeast Arxula adeninivorans for a microbial sensor immobilized with poly(carbamoyl) sulfonate (PCS) part I: Construction and characterization of the microbial sensor. *Biosensors & Bioelectronics* **1999,** *14* (2), 131-138; (b) Wessa, T.; Rapp, M.; Ache, H., New immobilization method for SAW-biosensors: covalent attachment of antibodies via CNBr. *Biosensors & Bioelectronics* **1999,** *14* (1), 93-98.

13. Peng, L.; You, M.; Yuan, Q.; Wu, C.; Han, D.; Chen, Y.; Zhong, Z.; Xue, J.; Tan, W., Macroscopic Volume Change of Dynamic Hydrogels Induced by Reversible DNA Hybridization. *Journal of the American Chemical Society* **2012,** *134* (29), 12302-12307.

14. (a) Antonio, T.; Cabral, M.; Cesarino, I.; Machado, S.; Pedrosa, V., Toward pH-controllable bioelectrocatalysis for hydrogen peroxide based on polymer brushes. *Electrochemistry Communications* **2013,** *29*, 41-44; (b) Bayley, H., Self-assembling biomolecular materials in medicine. *Journal of Cellular Biochemistry* **1994,** *56* (2), 168-170; (c) Moreira, F.; Sharma, S.; Dutra, R.; Noronha, J.; Cass, A.; Sales, M., Smart plastic antibody material (SPAM) tailored on disposable screen printed electrodes for protein recognition: Application to myoglobin detection. *Biosensors & Bioelectronics* **2013,** *45*, 237-244; (d) Zhao, J.; Chen, G.; Zhu, L.; Li, G., Graphene quantum dots-based platform for the fabrication of electrochemical biosensors. *Electrochemistry Communications* **2011,** *13* (1), 31-33.

15. (a) Luo, Z.; Cai, K.; Zhang, B.; Duan, L.; Liu, A.; Gong, D., Application of Mesoporous Silica Nanoreservoir in Smart Drug Controlled Release Systems. *Progress in Chemistry* **2011,** *23* (11), 2326-2338; (b) Vallet-Regi, M.; Ruiz-Hernandez, E.; Gonzalez, B.; Baeza, A., Design of Smart Nanomaterials for Drug and Gene Delivery. *Journal of Biomaterials and Tissue Engineering* **2011,** *1* (1), 6-29.

16. Wichterle, O.; Lim, D., Hydrophilic gels for biological use. *Nature* **1960,** *185* (4706), 117-118.

17. (a) Cushing, M.; Anseth, K., Hydrogel cell cultures. *Science* **2007,** *316* (5828), 1133-1134; (b) Tsang, V.; Bhatia, S., Three-dimensional tissue fabrication. *Advanced Drug Delivery Reviews* **2004,** *56* (11), 1635-1647.

18. Guiseppi-Elie, A.; Lei, C.; Baughman, R., Direct electron transfer of glucose oxidase on carbon nanotubes. *Nanotechnology* **2002,** *13* (5), 559-564.

19. (a) Ibrahim, A.; Safi-Harb, S.; Swank, J.; Parke, W.; Zane, S.; Turolla, R., Discovery of cyclotron resonance features in the Soft Gamma Repeater SGR 1806-20. *Astrophysical Journal* **2002,** *574* (1), L51-L55; (b) Ulijn, R.; Bibi, N.; Jayawarna, V.; Thornton, P.; Todd, S.; Mart, R.; Smith, A.; Gough, J., Bioresponsive hydrogels. *Materials Today* **2007,** *10* (4), 40-48.

20. Jobst, G.; Moser, I.; Urban, G., Numerical simulation of multi-layered enzymatic sensors. *Biosensors & Bioelectronics* **1996,** *11* (1-2), 111-117.

21. Hjerten, S.; Liao, J.; Nakazato, K.; Wang, Y.; Zamaratskaia, G.; Zhang, H., Gels mimicking antibodies in their selective recognition of proteins. *Chromatographia* **1997,** *44* (5-6), 227-234.

22. (a) Cumbo, A.; Lorber, B.; Corvini, P.; Meier, W.; Shahgaldian, P., A synthetic nanomaterial for virus recognition produced by surface imprinting. *Nature Communications* **2013,** *4*; (b) Dickert, F.; Hayden, O., Bioimprinting of polymers and sol-gel phases. Selective detection of yeasts with imprinted polymers. *Analytical Chemistry* **2002,** *74* (6), 1302-1306; (c) Hellner, G.; Boros, Z.; Tomin, A.; Poppe, L., Novel Sol-Gel Lipases by Designed Bioimprinting for Continuous-Flow Kinetic Resolutions. *Advanced Synthesis & Catalysis* **2011,** *353* (13), 2481-2491; (d) Nishino, H.; Huang, C.; Shea, K., Selective protein capture by epitope imprinting. *Angewandte Chemie-International Edition* **2006,** *45* (15), 2392-2396; (e) Stephenson, C.; Carro, W.; Yehl, M.; Shimizu, K., POLY 130-Virus imprinting and reuptake in polymer films. *Abstracts of Papers of the American Chemical Society* **2006,** *232*; (f) Yang, J.; Liu, L.; Cao, X., Combination of bioimprinting and silane precursor alkyls improved the activity of sol-gel-encapsulated lipase. *Enzyme and Microbial Technology* **2010,** *46* (3-4), 257-261; (g) Zhou, X.; Li, W.; He, X.; Chen, L.; Zhang, Y., Recent advances in the study of protein imprinting. *Separation and Purification Reviews* **2007,** *36* (3-4), 257-283.

23. Miyata, T.; Jige, M.; Nakaminami, T.; Uragami, T., Tumor marker-responsive behavior of gels prepared by biomolecular imprinting. *Proceedings of the National Academy of Sciences of the United States of America* **2006,** *103* (5), 1190-1193.

24. (a) Araki, K.; Maruyama, T.; Kamiya, N.; Goto, M., Metal ion-selective membrane prepared by surface molecular imprinting. *Journal of Chromatography B-Analytical Technologies in the Biomedical and Life Sciences* **2005,** *818* (2), 141-145; (b) Deng, H.; Gao, L.; Zhang, S.; Yuan, J., Preparation of a Copper Ion Selective Membrane by Surface-Modified Molecular Imprinting. *Industrial & Engineering Chemistry Research* **2012,** *51* (43), 14018-14025; (c) Gupta, G.; Singh, P.; Boopathi, M.; Kamboj, D.; Singh, B.; Vijayaraghavan, R., Molecularly imprinted polymer for the recognition of biological warfare agent staphylococcal enterotoxin B based on Surface Plasmon Resonance. *Thin Solid Films* **2010,** *519* (3), 1115-1121; (d) Harvey, S., Molecularly imprinted polymers for selective analysis of chemical warfare surrogate and nuclear signature compounds in complex matrices. *Journal of Separation Science* **2005,** *28* (11), 1221-1230; (e) Liu, J.; Wulff, G., Functional mimicry of the active site of carboxypeptidase A by a molecular imprinting strategy: Cooperativity of an amidinium and a copper ion in a transition-state imprinted cavity giving rise to high catalytic activity. *Journal of the American Chemical Society* **2004,** *126* (24), 7452-7453; (f) Pavel, D.; Lagowski, J.; Lepage, C., Computationally designed monomers for molecular imprinting of chemical warfare agents - Part V. *Polymer* **2006,** *47* (25), 8389-8399.

25. (a) Ellington, A.; Szostak, J., Invitro selection of rna molecules that bind specific ligands. *Nature* **1990,** *346* (6287), 818-822; (b) Tuerk, C.; Gold, L., Systematic evolution of ligands by exponential enrichment - rna ligands to bacteriophage-t4 dna-polymerase. *Science* **1990,** *249* (4968), 505-510.

26. (a) Cho, E.; Lee, J.; Ellington, A., Applications of Aptamers as Sensors. *Annual Review of Analytical Chemistry* **2009,** *2*, 241-264; (b) Hoppe-Seyler, F.; Butz, K., Peptide aptamers: powerful new tools for molecular medicine. *Journal of Molecular Medicine-Jmm* **2000,** *78* (8), 426-430.

27. Scrimin, P.; Prins, L., Sensing through signal amplification. *Chemical Society Reviews* **2011,** *40* (9), 4488-4505.

28. (a) Cheong, W. J.; Ali, F.; Choi, J. H.; Lee, J. O.; Sung, K. Y., Recent applications of molecular imprinted polymers for enantio-selective recognition. *Talanta* **2013,** *106*, 45-59; (b) Cheong, W. J.; Yang, S. H.; Ali, F., Molecular imprinted polymers for separation science: A review of reviews. *Journal of Separation Science* **2013,** *36* (3), 609-628; (c) Sharma, P. S.; Pietrzyk-Le, A.; D'Souza, F.; Kutner, W., Electrochemically synthesized polymers in molecular imprinting for chemical sensing. *Analytical and Bioanalytical Chemistry* **2012,** *402* (10), 3177-3204; (d) Shen, X.; Zhu, L.; Wang, N.; Ye, L.; Tang, H., Molecular imprinting for removing highly toxic organic pollutants. *Chemical Communications* **2012,** *48* (6), 788-798; (e) Volkert, A. A.; Haes, A. J., Advancements in nanosensors using plastic antibodies. *Analyst* **2014,** *139* (1), 21-31; (f) Wu, X., Molecular imprinting for anion recognition in aqueous media. *Microchimica Acta* **2012,** *176* (1-2), 23-47; (g) Wulff, G.; Liu, J., Design of Biomimetic Catalysts by Molecular Imprinting in Synthetic Polymers: The Role of Transition State Stabilization. *Accounts of Chemical Research* **2012,** *45* (2), 239-247.

29. (a) Du, J., Molecular Imprinting-Based Chemiluminescence Techniques in Pharmaceutical Analysis. *Current Pharmaceutical Analysis* **2010,** *6* (1), 30-38; (b) Verheyen, E.; Schillemans, J. P.; van Wijk, M.; Demeniex, M.-A.; Hennink, W. E.; van Nostrum, C. F., Challenges for the effective molecular imprinting of proteins. *Biomaterials* **2011,** *32* (11), 3008-3020.

30. (a) Haralabatos, I. C.; Ciocca, V.; Panettieri, R. A.; Atkins, P. C., Thrombin activation in asthma. *Journal of Allergy and Clinical Immunology* **1998,** *101* (1), S114-S114; (b) Lambrecht, B. N.; Hammad, H., Asthma and coagulation. *The New England journal of medicine* **2013,** *369* (20), 1964-6.

31. (a) Citartan, M.; Gopinath, S. C. B.; Tominaga, J.; Tan, S.-C.; Tang, T.-H., Assays for aptamer-based platforms. *Biosensors & Bioelectronics* **2012,** *34* (1), 1-11; (b) Gui, G.; Zhuo, Y.; Chai, Y.-Q.; Liao, N.; Zhao, M.; Han, J.; Zhu, Q.; Yuan, R.; Xiang, Y., Supersandwich-type electrochemiluminescenct aptasensor based on Ru(phen)(3)(2+) functionalized hollow gold nanoparticles as signal-amplifying tags. *Biosensors & Bioelectronics* **2013,** *47*, 524-529; (c) Wang, L.; Li, L.; Xu, Y.; Cheng, G.; He, P.; Fang, Y., Simultaneously fluorescence detecting thrombin and lysozyme based on magnetic nanoparticle condensation. *Talanta* **2009,** *79* (3), 557-561.

32. (a) Hansen, D. E., Recent developments in the molecular imprinting of proteins. *Biomaterials* **2007,** *28* (29), 4178-4191; (b) Takeuchi, T.; Hishiya, T., Molecular imprinting of proteins emerging as a tool for protein recognition. *Organic & Biomolecular Chemistry* **2008,** *6* (14), 2459-2467.

33. (a) Chen, H.-M.; Huang, T.-H.; Tsai, R.-M., A biotin-hydrogel-coated quartz crystal microbalance biosensor and applications in immunoassay and peptide-displaying cell detection. *Analytical Biochemistry* **2009,** *392* (1), 1-7; (b) Endo, T.; Ikeda, R.; Yanagida, Y.; Hatsuzawa, T., Stimuli-responsive hydrogel-silver nanoparticles composite for development of localized surface plasmon resonance-based optical biosensor. *Analytica Chimica Acta* **2008,** *611* (2), 205-211; (c) Jang, E.; Son, K. J.; Kim, B.; Koh, W.-G., Phenol biosensor based on hydrogel microarrays entrapping tyrosinase and quantum dots. *Analyst* **2010,** *135* (11), 2871-2878; (d) Meiring, J. E.; Lee, S.; Costner, E. A.; Schmid, M. J.; Michaelson, T. B.; Willson, C. G.; Grayson, S. M., Pattern recognition of shape-encoded hydrogel biosensor arrays. *Optical Engineering* **2009,** *48* (3); (e) Tang, Z.; Gao, L.; Wu, Y.; Su, T.; Wu, Q.; Liu, X.; Li, W.; Wang, Q., BSA-rGO nanocomposite hydrogel formed by UV polymerization and in situ reduction applied as biosensor electrode. *Journal of Materials Chemistry B* **2013,** *1* (40), 5393-5397; (f) Zhang, Q.; Wang, Y.; Mateescu, A.; Sergelen, K.; Kibrom, A.; Jonas, U.; Wei, T.; Dostalek, J., Biosensor based on hydrogel optical waveguide spectroscopy for the detection of 17 beta-estradiol. *Talanta* **2013,** *104*, 149-154.

34. (a) Ellington, A.; Szostak, J., Invitro Selection of rna molecules that bind specific ligands. *Nature* **1990,** *346* (6287), 818-822; (b) Tuerk, C.; Gold, L., Systematic evolution of ligands by exponential enrichment - rna ligands to bacteriophage-t4 dna-polymerase. *Science* **1990,** *249* (4968), 505-510.

35. (a) Bock, L. C.; Griffin, L. C.; Latham, J. A.; Vermaas, E. H.; Toole, J. J., Selection of single-stranded-dna molecules that bind and inhibit human thrombin. *Nature* **1992,** *355* (6360), 564-566; (b) Green, L. S.; Jellinek, D.; Jenison, R.; Ostman, A.; Heldin, C. H.; Janjic, N., Inhibitory DNA ligands to platelet-derived growth factor B-chain. *Biochemistry* **1996,** *35* (45), 14413-14424; (c) Macaya, R. F.; Schultze, P.; Smith, F. W.; Roe, J. A.; Feigon, J., Thrombin-binding dna aptamer forms a unimolecular quadruplex structure in solution. *Proceedings of the National Academy of Sciences of the United States of America* **1993,** *90* (8), 3745-3749; (d) Tasset, D. M.; Kubik, M. F.; Steiner, W., Oligonucleotide inhibitors of human thrombin that bind distinct epitopes. *Journal of Molecular Biology* **1997,** *272* (5), 688-698.

36. Bai, W.; Gariano, N. A.; Spivak, D. A., Macromolecular Amplification of Binding Response in Superaptamer Hydrogels. *Journal of the American Chemical Society* **2013,** *135* (18), 6977-6984.

37. Marques, M. R. C.; Loebenberg, R.; Almukainzi, M., Simulated Biological Fluids with Possible Application in Dissolution Testing. *Dissolution Technologies* **2011,** *18* (3), 15-28.

38. Zaki, A.; Dave, N.; Liu, J., Amplifying the Macromolecular Crowding Effect Using Nanoparticles. *Journal of the American Chemical Society* **2012,** *134* (1), 35-38.

39. Miyata, T.; Jige, M.; Nakaminami, T.; Uragami, T., Tumor marker-responsive behavior of gels prepared by biomolecular imprinting. *Proceedings of the National Academy of Sciences of the United States of America* **2006,** *103* (5), 1190-1193.

40. Peng, L.; You, M.; Yuan, Q.; Wu, C.; Han, D.; Chen, Y.; Zhong, Z.; Xue, J.; Tan, W., Macroscopic Volume Change of Dynamic Hydrogels Induced by Reversible DNA Hybridization. *Journal of the American Chemical Society* **2012,** *134* (29), 12302-12307.

41. (a) Hoshino, Y.; Shea, K. J., The evolution of plastic antibodies. *Journal of Materials Chemistry* **2011**, *21* (11), 3517-3521; (b) Migonney, V.; Souirti, A.; PavonDjavid, G.; Ravion, O.; Pfluger, F.; Jozefowicz, M., Biospecific polymers: Recognition of phosphorylated polystyrene derivatives by anti-DNA antibodies. *Journal of Biomaterials Science-Polymer Edition* **1997**, *8* (7), 533-544.

42. Miyata, T.; Jige, M.; Nakaminami, T.; Uragami, T., Tumor marker-responsive behavior of gels prepared by biomolecular imprinting. *Proceedings of the National Academy of Sciences of the United States of America* **2006**, *103* (5), 1190-1193.

43. (a) Miyata, T., Preparation of smart soft materials using molecular complexes. *Polymer Journal* **2010**, *42* (4), 277-289; (b) Miyata, T.; Hayashi, T.; Kuriu, Y.; Uragami, T., Responsive behavior of tumor-marker-imprinted hydrogels using macromolecular cross-linkers. *Journal of Molecular Recognition* **2012**, *25* (6), 336-343.

44. Tauer, K.; Gau, D.; Schulze, S.; Voelkel, A.; Dimova, R., Thermal property changes of poly(N-isopropylacrylamide) microgel particles and block copolymers. *Colloid and Polymer Science* **2009**, *287* (3), 299-312.

45. (a) Akhavan, B.; Jarvis, K.; Majewski, P., Tuning the hydrophobicity of plasma polymer coated silica particles. *Powder Technology* **2013**, *249*, 403-411; (b) Liu, B.-Y.; Chen, L.-J., Role of Surface Hydrophobicity in Pretilt Angle Control of Polymer-Stabilized Liquid Crystal Alignment Systems. *Journal of Physical Chemistry C* **2013**, *117* (26), 13474-13478; (c) Sunshine, J. C.; Akanda, M. I.; Li, D.; Kozielski, K. L.; Green, J. J., Effects of Base Polymer Hydrophobicity and End-Group Modification on Polymeric Gene Delivery. *Biomacromolecules* **2011**, *12* (10), 3592-3600.

46. (a) Bowerman, C. J.; Ryan, D. M.; Nissan, D. A.; Nilsson, B. L., The effect of increasing hydrophobicity on the self-assembly of amphipathic beta-sheet peptides. *Molecular Biosystems* **2009**, *5* (9), 1058-1069; (b) Lins, L.; Brasseur, R., The hydrophobic effect in protein-folding. *Faseb Journal* **1995**, *9* (7), 535-540; (c) Spolar, R. S.; Ha, J. H.; Record, M. T., Hydrophobic effect in protein folding and other noncovalent processes involving proteins. *Proceedings of the National Academy of Sciences of the United States of America* **1989**, *86* (21), 8382-8385.

47. Tauer, K. ; Gau, D.; Schulze S.; Völkel A.; Dimova, R., Thermal property changes of poly(N-isopropylacrylamide) microgel particles and block copolymers. *Colloid Polym Sci* **2009**, *287*, 299–312.

48. (a) Negi, A.; Rana, T.; Kumar, Y.; Ram, R.; Hallan, V.; Zaidi, A. A., Analysis of the Coat Protein Gene of Indian Strain of Apple Stem Grooving Virus. *Journal of Plant Biochemistry and Biotechnology* **2010,** *19* (1), 91-94; (b) Pupola, N.; Morocko-Bicevska, I.; Kale, A.; Zeltins, A., Occurrence and Diversity of Pome Fruit Viruses in Apple and Pear Orchards in Latvia. *Journal of Phytopathology* **2011,** *159* (9), 597-605; (c) Wu, Z. B.; Ku, H. M.; Su, C. C.; Chen, I. Z.; Jan, F. J., Molecular and biological characterization of an isolate of apple stem pitting virus causing pear vein yellows disease in taiwan. *Journal of Plant Pathology* **2010,** *92* (3), 721-728.

49. (a) Cella, L. N.; Blackstock, D.; Yates, M. A.; Mulchandani, A.; Chen, W., Detection of RNA Viruses: Current Technologies and Future Perspectives. *Critical Reviews in Eukaryotic Gene Expression* **2013,** *23* (2), 125-137; (b) Cheng, M. S.; Toh, C.-S., Novel biosensing methodologies for ultrasensitive detection of viruses. *Analyst* **2013,** *138* (21), 6219-6229; (c) Mehle, N.; Ravnikar, M., Plant viruses in aqueous environment - Survival, water mediated transmission and detection. *Water Research* **2012,** *46* (16), 4902-4917; (d) Park, J.-W.; Lee, S. J.; Choi, E.-J.; Kim, J.; Song, J.-Y.; Gu, M. B., An ultra-sensitive detection of a whole virus using dual aptamers developed by immobilization-free screening. *Biosensors & Bioelectronics* **2014,** *51*, 324-329; (e) Pazienza, V.; Niro, G. A.; Fontana, R.; Vinciguerra, M.; Andriulli, A., Advance in molecular diagnostic tools for hepatitis B virus detection. *Clinical Chemistry and Laboratory Medicine* **2013,** *51* (9), 1707-1717; (f) Takei, F.; Tani, H.; Matsuura, Y.; Nakatani, K., Detection of hepatitis C virus by single-step hairpin primer RT-PCR. *Bioorganic & Medicinal Chemistry Letters* **2014,** *24* (1), 394-396.

50. (a) Jelkmann, W.; Keim-Konrad, R., Immuno-capture polymerase chain reaction and plate-trapped ELISA for the detection of apple stem pitting virus. *Journal of Phytopathology-Phytopathologische Zeitschrift* **1997,** *145* (11-12), 499-503; (b) Klerks, M. M.; Leone, G.; Lindner, J. L.; Schoen, C. D.; van den Heuvel, J., Rapid and sensitive detection of Apple stem pitting virus in apple trees through RNA amplification and probing with fluorescent molecular beacons. *Phytopathology* **2001,** *91* (11), 1085-1091; (c) Komorowska, B.; Malinowski, T.; Michalczuk, L., Evaluation of several RT-PCR primer pairs for the detection of Apple stem pitting virus. *Journal of Virological Methods* **2010,** *168* (1-2), 242-247.

51. Lautner, G.; Balogh, Z.; Bardoczy, V.; Meszaros, T.; Gyurcsanyi, R. E., Aptamer-based biochips for label-free detection of plant virus coat proteins by SPR imaging. *Analyst* **2010,** *135* (5), 918-926.

52. Balogh, Z.; Lautner, G.; Bardoczy, V.; Komorowska, B.; Gyurcsanyi, R. E.; Meszaros, T., Selection and versatile application of virus-specific aptamers. *Faseb Journal* **2010,** *24* (11), 4187-4195.

53. (a) Gong, Y.-N.; Lu, T.-B., Fast detection of oxygen by the naked eye using a stable metal-organic framework containing methyl viologen cations. *Chemical Communications* **2013,** *49* (70), 7711-7713; (b) Lin, C.; Zhang, Y.; Zhou, X.; Yao, B.; Fang, Q., Naked-eye detection of nucleic acids through rolling circle amplification and magnetic particle mediated aggregation. *Biosensors & Bioelectronics* **2013,** *47*, 515-519;

53. (c) Liu, D.; Wang, Z.; Jin, A.; Huang, X.; Sun, X.; Wang, F.; Yan, Q.; Ge, S.; Xia, N.; Niu, G.; Liu, G.; Walker, A. R. H.; Chen, X., Acetylcholinesterase-Catalyzed Hydrolysis Allows Ultrasensitive Detection of Pathogens with the Naked Eye. *Angewandte Chemie-International Edition* **2013,** *52* (52), 14065-14069; (d) Safavieh, M.; Ahmed, M. U.; Sokullu, E.; Ng, A.; Braescuac, L.; Zourob, M., A simple cassette as point-of-care diagnostic device for naked-eye colorimetric bacteria detection. *Analyst* **2014,** *139* (2), 482-487; (e) Zhou, W.; Su, J.; Chai, Y.; Yuan, R.; Xiang, Y., Naked eye detection of trace cancer biomarkers based on biobarcode and enzyme-assisted DNA recycling hybrid amplifications. *Biosensors & bioelectronics* **2014,** *53*, 494-8.

54. (a) Bailey, R. C.; Hupp, J. T., Micropatterned polymeric gratings as chemoresponsive volatile organic compound sensors: Implications for analyte detection and identification via diffraction-based sensor arrays. *Analytical Chemistry* **2003,** *75* (10), 2392-2398; (b) Bailey, R. C.; Nam, J. M.; Mirkin, C. A.; Hupp, J. T., Real-time multicolor DNA detection with chemoresponsive diffraction gratings and nanoparticle probes. *Journal of the American Chemical Society* **2003,** *125* (44), 13541-13547; (c) St John, P. M.; Davis, R.; Cady, N.; Czajka, J.; Batt, C. A.; Craighead, H. G., Diffraction-based cell detection using a microcontact printed antibody grating. *Analytical Chemistry* **1998,** *70* (6), 1108-1111.

55. (a) Ye, G.; Wang, X., Polymer diffraction gratings on stimuli-responsive hydrogel surfaces: Soft-lithographic fabrication and optical sensing properties. *Sensors and Actuators B-Chemical* **2010,** *147* (2), 707-713; (b) Ye, G.; Yang, C.; Wang, X., Sensing Diffraction Gratings of Antigen-Responsive Hydrogel for Human Immunoglobulin-G Detection. *Macromolecular Rapid Communications* **2010,** *31* (15), 1332-1336.

56. (a) Chen, J.-K.; Zhou, G.-Y.; Chang, C.-J., Real-time multicolor antigen detection with chemoresponsive diffraction gratings of silicon oxide nanopillar arrays. *Sensors and Actuators B-Chemical* **2013,** *186*, 802-810; (b) Mao, D.; Liu, P.; Dong, L., Multichannel Detection Using Transmissive Diffraction Grating Sensor. *Journal of Polymer Science Part B-Polymer Physics* **2011,** *49* (23), 1645-1650; (c) Wang, X.; Wang, X., Aptamer-functionalized hydrogel diffraction gratings for the human thrombin detection. *Chemical Communications* **2013,** *49* (53), 5957-5959.

VITA

Wei Bai was born in Hefei, China and earned his bachelor's degrees in applied chemistry at Anhui University of Technology in 2004 and a master's degree in polymer science and engineering at University of Science and Technology of China in 2007.

In the fall of 2008 he was admitted to graduate school at Louisiana State University and joined the research group of Dr. David Spivak in the next semester. He worked on developing naked-eye biosensors based on novel bio-imprinted hydrogels for recognition and visual detection of specific biomarkers like proteins and virus. During that time he published 9 papers on peer-reviewed journals, including 4 first-author papers and 3 second-author papers with a total Impact Factor of 54.84. He also participated in several national and international conferences like (MIP Conferences and ACS Conferences) to present his work.

He was also awarded TA scholar award (2011), Timethy S. Evenson Award for Excellence in Macromolecular Science (2012), Outstanding Seminar Speaker of Macromolecular Seminar (2013), 2nd prize in 3MT® competition (2014) and two Coates travel awards. He was elected as vice president of the macromolecular studies graduate student association in 2011. Wei Bai will be receiving the degree of Doctor of Philosophy on May 16, 2014 at the LSU spring commencement.